Guidelines for Electrical Transmission Line Structural Loading

THIRD EDITION

ASCE Manuals and Reports on Engineering Practice No. 74

ASCE

SEL
Structural Engineering Institute
of the American Society of Civil Engineers

Guidelines for Electrical Transmission Line Structural Loading

Third Edition

Prepared by
the Task Committee on Structural Loadings of
the Committee on Electrical Transmission Structures
of the Structural Engineering Institute of
the American Society of Civil Engineers

Edited by
C. Jerry Wong
Michael D. Miller

ASCE American Society of Civil Engineers

SEL Structural Engineering Institute
of the American Society of Civil Engineers

MANUALS AND REPORTS
ON ENGINEERING PRACTICE

(As developed by the ASCE Technical Procedures Committee, July 1930, and revised March 1935, February 1962, and April 1982)

A manual or report in this series consists of an orderly presentation of facts on a particular subject, supplemented by an analysis of limitations and applications of these facts. It contains information useful to the average engineer in his or her everyday work, rather than findings that may be useful only occasionally or rarely. It is not in any sense a "standard," however; nor is it so elementary or so conclusive as to provide a "rule of thumb" for nonengineers.

Furthermore, material in this series, in distinction from a paper (which expresses only one person's observations or opinions), is the work of a committee or group selected to assemble and express information on a specific topic. As often as practicable, the committee is under the direction of one or more of the Technical Divisions and Councils, and the product evolved has been subjected to review by the Executive Committee of the Division or Council. As a step in the process of this review, proposed manuscripts are often brought before the members of the Technical Divisions and Councils for comment, which may serve as the basis for improvement. When published, each work shows the names of the committees by which it was compiled and indicates clearly the several processes through which it has passed in review, in order that its merit may be definitely understood.

In February 1962 (and revised in April 1982) the Board of Direction voted to establish a series entitled "Manuals and Reports on Engineering Practice," to include the Manuals published and authorized to date, future Manuals of Professional Practice, and Reports on Engineering Practice. All such Manual or Report material of the Society would have been refereed in a manner approved by the Board Committee on Publications and would be bound, with applicable discussion, in books similar to past Manuals. Numbering would be consecutive and would be a continuation of present Manual numbers. In some cases of reports of joint committees, bypassing of Journal publications may be authorized.

MANUALS AND REPORTS
ON ENGINEERING PRACTICE
CURRENTLY AVAILABLE

PREFACE

Since the original publication of Manual 74 in 1991, and the preceding "Guidelines for Transmission Line Structural Loading" in 1984, the understanding of structural loadings on transmission line structures has broadened significantly. However, improvements in computational capability have enabled the transmission line engineer to more easily determine structural loadings without properly understanding the parameters that affect these loads. Many seasoned professionals have expressed concern for the apparent lack of recent information on the topic of structural loadings as new engineers enter this industry. The Committee on Electrical Transmission Structures is charged with the responsibility to report, evaluate, and provide loading requirements of transmission structures. This task committee was therefore formed to update and revise the 1991 manual.

The recommendations presented herein are the consensus opinion of the task committee members. Although the subject matter of this guide has been thoroughly researched, it should be applied only in the context of sound engineering judgment.

The committee wishes to thank the Peer Review Committee members for their assistance and contributions to this document: Anthony M. DiGioia (Chair), Mark Allen, Alan G. Davenport, Elias Ghannoun, John W. Harrison, and Robert Morris. Also, the committee is grateful for the comments and guidance of Leon Kempner Jr. and Dan Jackman.

It is with much appreciation that we acknowledge the contributions of Task Committee member Jerome G. Hanson and Peer Review Committee member John W. Harrison, who are no longer with us.

Respectfully submitted,
Task Committee on Structural Loadings

Frank W. Agnew   Harry V. Durden   John D. Mozer
Richard F. Aichinger   William Y. Ford   Robert E. Nickerson
Jim Andersen   Bruce Freimark   Wesley J. Oliphant
Carl W. Austin   Jim Hogan   Mark Ostendorp
Terry G. Burley   Magdi Ishac   Alain Peyrot
Ronald J. Carrington   Kathy Jones   Larry Shan
Michael S. Cheung   James M. McGuire   David Tennent
Habib J. Dagher   Kishor C. Mehta   George T. Watson
Nicholas J. DeSantis   Michael D. Miller   C. Jerry Wong (Chair)

CONTENTS

FOREWORD

BACKGROUND

This new edition of *Guidelines for Electrical Transmission Line Structural Loading* (Manual 74) has been prompted by the need to introduce several major changes to the most recent Manual 74 (1991), as well as to have an opportunity to better define or refine some of the minor issues addressed in the previous document.

The previous editions (1984, 1991) have been well received and found wide use as practical guides to supplement the mandatory specifics prescribed by the National Electrical Safety Code (NESC) or other state requirements, which are intended to be legal minimums to set safety standards for the public. Experience and a better knowledge of weather loads have led to the finding that the legal minimums are inadequate to represent the plurality or complexity of performance demands imposed on a typical high voltage transmission line throughout its lifetime. These deficiencies have been the justification for this and subsequent editions of Manual 74 where loads over and above the legal requirements are discussed.

This edition presents once more the detailed guidelines and procedures for developing transmission line structure loads and provides explanations that might illuminate the issues. Although intended as a guide for lines 69 kV and above, the application of the concepts in this document might be justified at lower voltages.

MANUAL IMPLEMENTATION AND USE

This manual is intended to provide the most relevant and up-to-date information related to transmission line structural loading. It is not

intended to be a step-by-step manual or a prescriptive code for direct implementation by a utility. Rather, it is intended to be a resource that can readily be absorbed into a loading policy. Much of the information contained within this document can be simplified for a particular utility's use once regional or local climatic data and relative reliability levels are determined.

WEATHER-RELATED LOADS

A new combined ice and wind map has been compiled by a subcommittee of ANSI/ASCE 7. This map shows the 50-year return period (RP_{50}) extreme radial ice thicknesses combined with 3-sec wind velocities. This map is statistically based and is a significant improvement over the map in the 1991 edition of Manual 74. The ice load requirements from this new map are different from those of the previous edition. It should be noted that this map does not include information on in-cloud icing and sticky snow. Appendix H should be appraised before attempting to use the data shown on the ice and wind map.

There are some discussions but no firm recommendations regarding the influence that physical length of exposure of a line has on the estimation of the risk of storm events. This spatial problem is valid and exists, but requires more research and discussion before more than general guidance can be offered.

Of equal significance is the new extreme wind map showing RP_{50} winds of 3-sec duration—the newly accepted time period for gathering and processing wind data. This change from the fastest-mile to a 3-sec gust basis has required changes to the gust response factors (G_{RF}) and the data in other tables.

The 1991 edition of Manual 74 proposed G_{RF} values based on Davenport's model and neglected the resonance component for structures and wires. This assumption was based on the hypothesis that the peak vibration response on the conductors, ground wires, and structures will typically be out of phase with one another. In addition, damping will significantly reduce their resonant response relative to the quasi-static background response.

Surveys by the International Council on Large Electric Systems (CIGRE), such as Brochure 109, have confirmed that frequent permanent structural outages of transmission lines can result from high-intensity, narrow-front winds such as tornados, downbursts, and microbursts that accompany major thermal events. These events do not cause many structure failures per incident unless cascading failures also occur, but the total number of events can be quite high. From an economic standpoint, these high-intensity wind events have previously been deemed to be beyond our efforts to resist. The 1991 manual provided some discussion on this issue.

This edition highlights some of the techniques that have been applied to try to mitigate the impact of high-intensity wind events. Several major utilities have revised design load criteria in attempts to better withstand these high-intensity wind events on a cost-effective basis.

APPROACH TO RELIABILITY-BASED DESIGN

Another change is in the application of the basic concepts of reliability-based design (RBD). This revision to Manual 74 uses a relative reliability factor and acknowledges the difficulty in accurately calculating the probability of failure of a line. The approximate levels of inputs and transfer functions needed to convert weather data into loads do not justify the complex procedures presented in the previous edition, and several very useful parts of the RBD concept were being lost in the general confusion about the subject. In this edition of Manual 74, an attempt is made to identify and articulate these most useful portions in Chapter 1 and Appendix B. This change in emphasis on RBD may appear innocuous but represents a major step in clarifying what can effectively be accomplished with both weather and strength data in transmission line work.

The two key elements of the RBD method demonstrated are (1) those for adjusting the relative reliability level of a line design with respect to ice or wind loads, and (2) the very simple techniques for ensuring that foundations and the structures have appropriate strength levels relative to each other. These two items are the only two statistically sensitive issues in this document, but they are fundamental in attempts to maintain control over the behavior of a line under more than the extreme design conditions.

A summary of the issues associated with the full application of RBD theory can be found in Appendix B and ASCE Manual 111, *Reliability-Based Design of Utility Pole Structures* (ASCE 2006).

ADDITIONAL LOAD CONSIDERATIONS

Chapter 3 of this manual presents detailed discussion of loading specifics applied to prevent cascading types of failure, failure containment, and loads to protect against damage and injury during construction and maintenance. There is also some general nonquantitative discussion about load effects from galloping wires, and mention of problems of vibration of tower members and seismic effects.

Because this manual is intended as a loading document, it contains almost no discussion of strengths except in most general terms and to note the differentiation between limit states and damage limits when discussing the problems of the application of RBD concepts.

This page intentionally left blank

CHAPTER 1

OVERVIEW OF LOAD CRITERIA

1.0 INTRODUCTION

This manual addresses a number of issues that must be considered to provide cost-effective and reliable designs for transmission line structures. Key issues that must be considered include the following:

1. Uniform procedures and definitions across the industry for the calculation of loads. This will facilitate communication between people involved in transmission line design; the accumulation of meaningful databases for further refinement of the procedures; and comparisons of the effectiveness of different design procedures.
2. Design procedures that provide for an acceptable minimum reliability for all lines, as well as a means for increasing this reliability whenever needed or justified. An essential line should be more reliable than a less important line.
3. Procedures for computing design loads and load factors that are independent of the materials of the supporting structures. Load criteria should reflect uncertainties in the loads and the accepted risk that these loads will be exceeded.
4. Adjustment of the load criteria on some of the critical structures or components of a line to ensure that an initial failure does not trigger the cascading failure of multiple structures (domino effect).
5. Incentives for developing better local databases for weather-related phenomena such as wind and ice. A designer with access to climatic data should be allowed to adjust the design loads to local conditions.
6. Legislated loads, which are intended to provide *minimum* levels for public safety, are always to be considered.

Load and resistance factor design (LRFD) methodologies based on reliability theory are being used in all facets of structural engineering (AISC 2001; ASCE 2005; ACI 2002). Some of these methods have been assessed and the pertinent parts have been used in this manual. Improved techniques for quantifying weather-related load data are now available. This revision to Manual 74 incorporates the use of relative reliability in development of loads.

1.1 PRINCIPAL SYSTEMS OF A TRANSMISSION LINE

A transmission line (TL) consists of two separate structural systems, the structural support system and the wire system. They are usually considered separately, even though it is evident that they act as one larger system. The structural support system, comprising towers, poles, and foundations, has the primary task of supporting the load from the wire, insulators, hardware, and wire accessories, including accumulated ice. It also provides restraint to the wind on the wire system. The structural support system, or structure, is certainly an essential element of a line, but much of the unusual behavior and most of the problems of a line start on or are generated by the wire system. The wire system consists of the conductors and ground wires and includes all components such as dead-end insulators and hardware in series with the wires. The wire system affects all major angle and dead-end structures.

The major loads of a transmission line are generated on or by the wire system, except for high-intensity-type winds such as tornados, which load the structures themselves. We should first turn to the wire systems when we want to understand what happens to transmission lines. This is especially true with regard to behavior in an ice storm event. Although the support system can support very heavy vertical loads at relatively low cost, this same support system can prove to be inadequate when unusual or unexpected things happen to the wire system. A simple break in the wire system may promote a difficult-to-control cascade.

For these reasons, among others, the design of the components of the wire system is usually based on conservative strength factors. Generally, the foundations should be designed to be more reliable than the supported structures. The strength levels of the structures and foundations of the support system can be adjusted relative to each other. The strength levels of important angle and dead-end structures can also be adjusted upward from those of tangent structures to increase their reliability.

1.2 LOADS AND RELATIVE RELIABILITY

When describing loads in a transmission line system, it is convenient to distinguish between the events that produce the loads and the resulting loads in the line components. The load events can be classified as weather-related, construction and maintenance (C&M), and what have at times been described as secondary load events, resulting from initial damage to or the failure of some component of the line. The latter can be caused by an overload of ice and/or wind or some other event, but the implications are that if a component breaks, a cascading of many structures may result. Thus, these trigger events place demands on the structural system that falls within the designation of failure containment (FC).

1.2.1 Weather-Related Events

Weather-related events of interest are extreme winds, extreme ice with accompanying wind, and high-intensity winds such as tornados and microbursts that are a significant problem in many areas of this country and the world. Representative temperatures associated with these loading events should be developed when determining the loads. It is customary to associate extreme values of these events with some selected return period (RP_N). For $N = 50$ years (designated as RP_{50}), the prediction is that, on average, that level of extreme event would be reached or exceeded with a probability of 1/50 or 2% every year. However, because return period events are not evenly spaced over time, there will be some 50-year periods with no RP_{50} events. whereas other periods will have two or more events equaling or exceeding RP_{50} values. Table 1-1 shows the probabilities of one or more RP_N events during a span of 50 years. For RP_{50}, the probability that the designated load will be exceeded at least once in 50 years is $[1 - (1 - 0.02)^{50}] = 0.64$. It is instructive to note that there is an almost 1 in 4 probability of a 200-year event occurring once in 50 years $[1 - (1 - 0.005)^{50}] = 0.22$; this point that has implications when failure containment is discussed in Section 1.2.2.1.

1.2.1.1 Return Period Adjustments. It is possible to adjust the relative probability of failure of two designs by changing the return period of the design load. The higher the return period of the design load, the more reliable the design. If the nominal or characteristic design strength of two components is consistently defined [for example, if both components have a 5% lower exclusion limit (LEL) characteristic strength], then the relative probability of failure of the two components is approximately inversely proportional to the design load return period (Peyrot and Dagher 1984). Hence, doubling the return period of the design load

Table 1-1. Load Factors, γ_w, to Adjust Relative Reliability from 50-Year RP Extreme Wind Load Design

Relative Reliability Factor (RRF)	Load Return Period, RP (years)	Probability that the Load Is Exceeded in 50 Years $= 1 - (1 - 1/RP)^{50}$	Wind Load Factor, γ_w
0.5	25	0.87	0.85
1	50	0.64	1.00
2	100	0.39	1.15
4	200	0.22	1.30
8	400	0.12	1.45

reduces the relative probability of failure by approximately a factor of 2. It is convenient to define the relative reliability factor (RRF) as:

$$RRF \cong \frac{\text{Probability of failure of component or structure for a design load of 50 years}}{\text{Probability of failure of component or structure for a design load of RP years}} \qquad (1\text{-}1)$$

The RRF is given in Tables 1-1 and 1-2 as a function of load return period, and, alternatively, as a function of the load factors applied to the 50-year RP values. A line designed for 50-year return period loads has an RRF = 1 and represents a baseline design. A more reliable line designed for 200-year RP loads has an RRF = 4 [in other words, has a relative probability of failure that is approximately four times less than the baseline (50-year) design].

Extreme value distributions can be used to determine the extreme wind loads or extreme uniform radial ice thicknesses that can be expected in an N-year return period. The Gumbel and generalized Pareto extreme value distributions are briefly discussed in Appendix B, Section B.8.

If local ice and wind data are not available for a long period of record, then the 50-year return period values shown on the wind map, Fig. 1-1, and the ice and concurrent wind maps of Figs. 2-13 through 2-18 in Chapter 2, should be used. The loads derived from these maps can be adjusted to other return periods using the factors γ_w or γ_i, of Tables 1-1 and 1-2. The selection of the relative reliability factor should be based on the importance of the line. The factors in Table 1-1, which are applied to the wind load, were derived from the Gumbel distribution based on wind data with a dispersion of 18%, in the mid-range of typical annual extreme wind data.

Table 1-2. Factors γ_i and Corresponding γ_w to Adjust Relative
Reliability from 50-Year Extreme Uniform Ice Thickness and
Concurrent Wind Load Design

Relative Reliability Factor (RRF)	Load Return Period, RP (years)	Ice Thickness Factor, γ_i	Concurrent Wind Load Factor, γ_w
0.5	25	0.80	1.0
1	50	1.00	1.0
2	100	1.25	1.0
4	200	1.50	1.0
8	400	1.85	1.0

It is possible to adjust the relative reliabilities for line designs by select-ing RP_{25}, RP_{100}, RP_{200}, or even RP_{400} values. The factors in Table 1-1 show that increasing the design wind load by 15% approximately doubles the relative reliability factor, and increasing it by 30% quadruples it. The factors in Table 1-2 show that the uniform ice thickness for a 50-year return period must be increased by 25% to approximately double the rela-tive reliability factor, and by 50% to quadruple it. The concurrent wind speed shown in Figs. 2-13 through 2-18 that is applied with the extreme uniform ice thickness is not adjusted for return period.

The relative reliability factor is used as a tool to *approximately* adjust design reliability because it is currently very difficult to accurately calcu-late the probability of failure of a line. Powerful mathematical tools to calculate the line reliability are available, but we do not have all the data necessary to accurately carry out such an analysis. Specifically, predicted probabilities of failure are in error if the uncertainties in the probability laws of climatic events, structure strengths, component strengths, and transfer functions converting the data of climatic events into loads are not taken into account. To illustrate the point, consider, for example, the uncertainty in predicting the force coefficients as illustrated in Figs. H-1 and H-2 in Appendix H. The discretionary range of the force coefficients may be more than 100%, which exceeds the total range of load factors in Table 1-1. Until more information becomes available to resolve the force coefficient and other load and strength data issues, it is recommended that the RRF be used as an admittedly approximate tool to adjust struc-tural reliability.

1.2.1.2 Spatial Influences on Weather-Related Events. The original data for the maps of extreme wind and ice thickness values of Figs. 1-1 and 2-13 through 2-18 were collected at points. Projections of point data
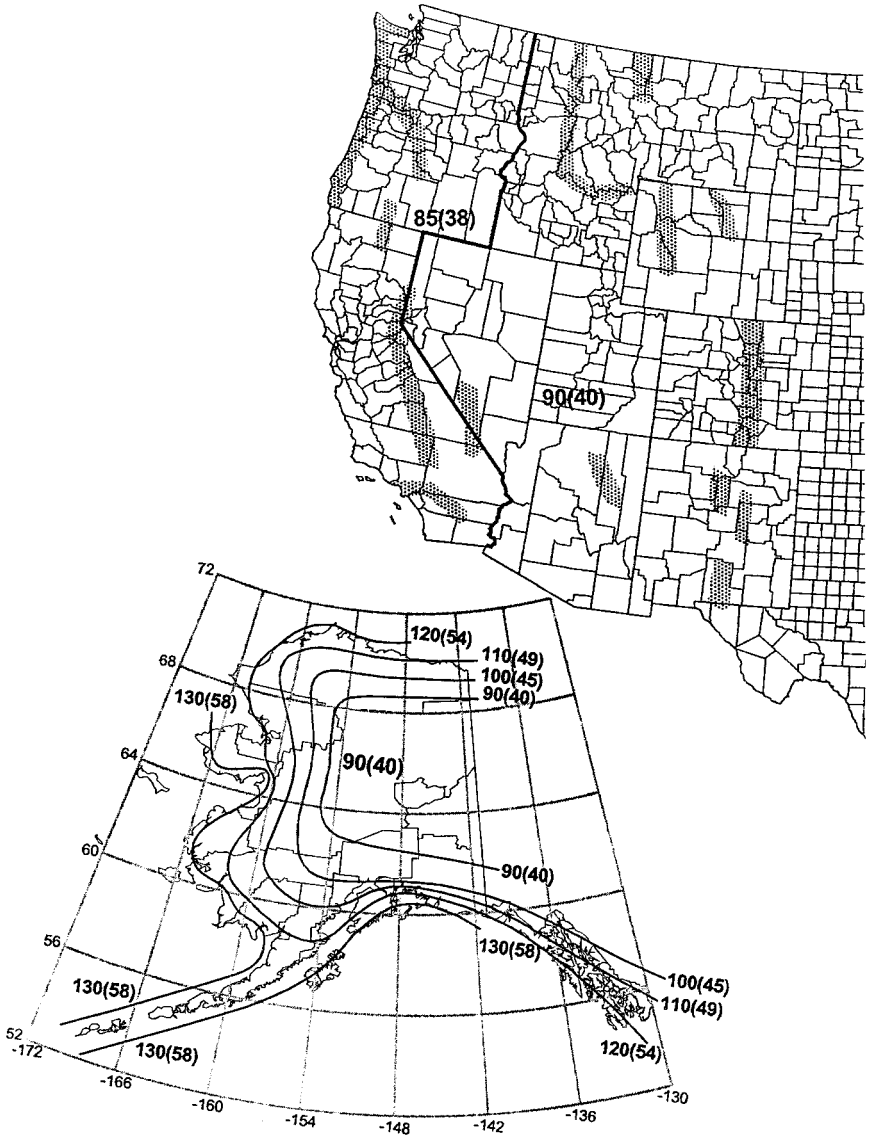
Figure 1-1. Basic wind speed. Source: ASCE (2005).

by Gumbel to determine RP_N values will produce event values appropriate for the design of point structures such as telecommunication towers, radio masts, or the structures of a switchyard. However, a transmission line has length and is exposed to a larger number of extreme events than is any single point structure. Therefore, its likelihood of experiencing a
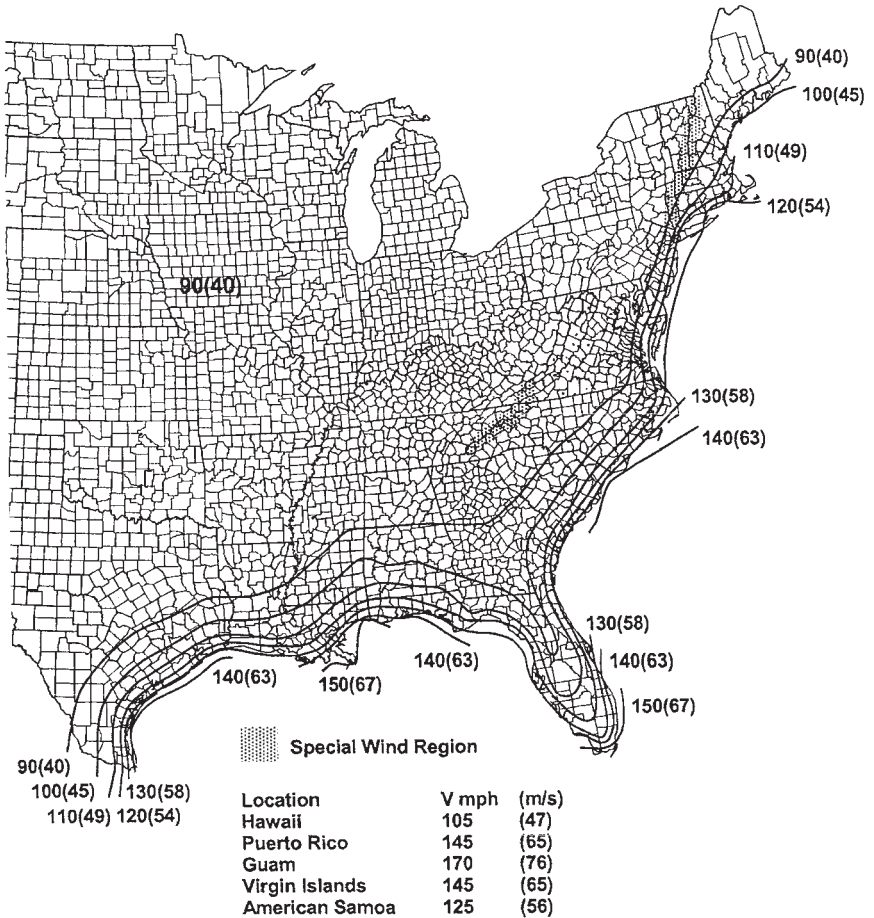
Notes:
1. Values are nominal design 3-second gust wind speeds in miles per hour (m/s) at 33 ft (10 m) above ground for Exposure C category.
2. Linear interpolation between wind contours is permitted.
3. Islands and coastal areas outside the last contour shall use the last wind speed contour of the coastal area.
4. Mountainous terrain, gorges, ocean promontories, and special wind regions shall be examined for unusual wind conditions.

Figure 1-1. Continued.

failure is a function of line length and is greater than that of a point structure. Also, weak components within a line are more likely to be exposed or "found" by an extreme event in a larger population.

Having noted these points, it also becomes evident that it is difficult to select the load criteria based on the length of a given line or line section. The result could be structures and components suitable for a line of given

length and not appropriate if they are to be used on another line of different length. Further discussion on spatial effects using point data for wind and ice loads for transmission line loading is provided in Appendix B, Section B.6. This aspect of defining weather-related load criteria was theoretically demonstrated in Dagher et al. (1993), illustrated by Laflamme (1993) in field test experiments, and used in development of actual line loading criteria by Ghannoum (1983) and Behncke et al. (1998).

1.2.1.3 Alternate Sources of Weather-Related Loads.   In this manual the nominal events and derived loads will be the RP_N winds or ice values. These can be the RP_{50} values from the maps of Figs. 1-1 and 2-13 through 2-18, or the same values adjusted to another return period N using the factors in Tables 1-1 and 1-2 if greater or lesser reliability is deemed justified. A spatial factor may then be applied to adjust for the length of the line, as in Dagher (1993). The effect of the wind direction relative to the line for both extreme wind events and extreme icing events may also be considered.

1.2.2 Additional Load Considerations

The loads derived from the weather conditions to be expected along the line route must be supplemented by the loads created during C&M operations, and those deemed necessary to contain and limit damage after some component fails.

1.2.2.1 Failure Containment.   Even though the line may be designed to very high levels of reliability regarding weather-related loads, there will always remain the risk of casual or accidental events or greater than expected weather-related events that are beyond the control of the line designer.

Failures of components due to fatigue or wear may be avoided by rigid inspection procedures. Destruction of a structure or damage to key components of a transmission line system caused by impacts of vehicles or planes, sabotage, landslides, floods, and any of dozens of other damaging events may not be foreseeable. Obviously, design procedures cannot control the occurrence of all of these events, but an attempt can be made to limit the consequences to the immediate impact zone. If a failure is triggered by an accidental event or by a localized extreme wind or ice event, it should not propagate without control into a multi-structure cascade continuing far beyond the initial failure zone. This containment can be accomplished by designing all structures with longitudinal strength, by inserting anti-cascade structures at intervals, or by load-limiting devices. This subject is discussed further in Chapter 3, Section 3.3 (Longitudinal Loads) and in Appendix I.

1.2.2.2 Construction and Maintenance. Some line components, structure components, or entire structures may be subjected to critical loads during C&M operations. During this time the risk of injuries is greatest because personnel are on the structures or under the wire assemblies. Therefore, loads resulting from all C&M operations must be multiplied by suitable load factors to provide an adequate margin of safety. Details of these loads and suggested factors can be found in Chapter 3, Section 3.1 (Construction and Maintenance Loads). National regulations and local codes of practice must also be followed.

1.2.3 Loads and Load Effects

Loads on a transmission line are the forces that are applied to the wires and to the structures. The loads that are applied to the wires are subsequently transmitted to the structures. The loads applied to the wires or structures should include appropriate load factors. The resultant forces, stresses, and displacements in the components of the transmission line system caused by these applied loads are called the load effects.

Legislated loads, such as those of the National Electrical Safety Code (NESC), have their own load factors. The load factors for extreme wind and extreme ice concurrent with wind are recommended in Tables 1-1 and 1-2. The load factor of 1.0 as applied in this document assumes the weather-related loads have a return period of 50 years. Due to life-safety concerns, the load factors for C&M loads are generally 1.5 or greater and are discussed further in Chapter 3, Section 3.1 (Construction and Maintenance Loads).

1.3 WIRE SYSTEMS

Although this manual is a loading document, it is necessary to understand how tensions are generated in the wire systems and how resulting loads are imposed on the support systems. Therefore, Chapter 4 provides information regarding (1) the effects of creep and heavy loads on wire tensions; (2) the need to keep wire tensions within certain limits; and (3) simplifications and assumptions that may be used for determining wire tensions and resulting loads at the structure attachment.

1.4 LIMIT STATES DESIGN

This section discusses coordination of loads and strengths within the overall concept of the behavior of a line as a system. It is important to recognize two limit states for components:

1. The *failure limit* at which point the component can no longer sustain the load, which may lead to the failure of the line.
2. The *damage limit* at which point the component and the line will still function, possibly at a reduced level, but permanent damage has been done and serviceability and possibly the future performance of the line has been compromised. Examples include overstressed conductors that may need to be resagged, or hardware fittings that may be distorted to the point where maintenance is difficult. Insulators that have been loaded beyond their recognized safe working values, and guys overstressed and in need of re-tensioning, are also typical examples. Because almost all of these components are within the wire system, conventional practice is to ensure that under weather-related loads and during C&M operations the use of these components is limited to their damage limits, which is defined as a percentage of their rated or nominal strengths. To accomplish this, it is important to understand how the nominal or rated strength is defined by the manufacturer. A meaningful definition of the nominal strength should include the exclusion limit that corresponds to the rated strength.

Under failure containment conditions, the acceptable load limits for hardware, insulators, and guys are set closer to ultimate or rated strength limits because a failure has already occurred. Damaged material must be replaced or repaired, and resagging of a few extra spans or re-tensioning of a few guy wires may be needed. These problems are relatively small compared to the complete loss of a line. These components are prone to deterioration over time, with wear and fatigue caused by galloping, vibration, and simple wind motions. This further justifies limiting the allowable capacities of all the components of the wire system.

1.4.1 Component Strength

A component is usually selected so that its nominal strength exceeds the maximum load effect determined from all the different loading conditions for which the line is being designed. The actual strength of a given component is a random variable that has an average or mean value and a coefficient of variation, COV (COV is the standard deviation/mean value). In design, the strength of a manufactured component is identified by a unique value called its nominal strength. This is usually calculated with equations described in design manuals and design standards (AISC 2005; ASCE 1988; ASCE 1990a; PCI 1983; ASCE 2000a; ANSI 2002). The nominal strength may also be provided by the manufacturer in the form

of a minimum or guaranteed strength (i.e., catalog strength), or as a percentage of an estimated breaking load. For example, the nominal strength in compression of a steel angle in a latticed tower is given by a compression formula in ASCE Standard 10-97 (ASCE 2000a). Such a nominal value actually represents an e% exclusion limit of strength if it has an e% probability of not being reached.

For a Gaussian or normal distribution, the probability density functions with low and high COVs are depicted in Fig. 1-2. The manufactured components of wires, line hardware, and insulators will have very small COVs and their distributions will look like curve A, whereas natural components such as wood poles and foundations will have distributions more like curve B.

To obtain relatively consistent reliabilities for different types of components that have different COVs (steel angles, wood poles, concrete poles, steel poles, foundations, etc.), it is important that their nominal strengths correspond to the same LEL. Therefore, it is recommended that strength design guides publish nominal strength values corresponding to a 5th percentile (or 5% LEL; a 5% exclusion limit strength means that 95% of all the population of this component will meet or exceed this limit). This is currently not always the case because strength guides have evolved separately and at different times. The selection of a
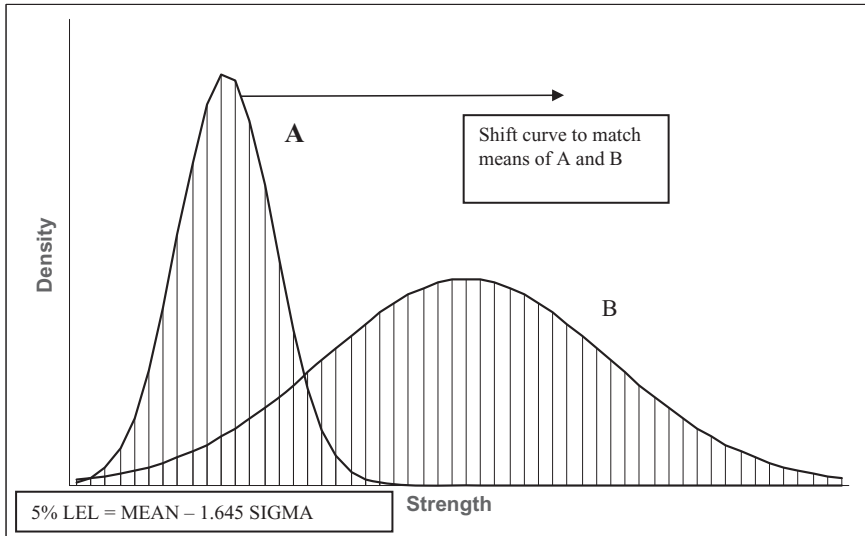
Figure 1-2. *Two Gaussian distributions for material.*

strength exclusion limit is intended to identify a strength value that is usually met with a high probability. The value for e%, such as 5% or 10%, provides a confidence level of 95% or 90%, respectively, that the characteristic strength will be met. Further discussion on this topic can be found in ASCE (2006).

1.4.2 Relative Reliability of Components and Failure Containment

There is a natural and well-founded desire to exercise some control over the sequence of failure of the different line components. An event that cannot be avoided or a weather-related load exceeding the RP_N load can, if not controlled (by using, for example, anti-cascading measures), lead to unnecessary and excessive damage. For many reasons, it is not possible to precisely delineate the desired sequence of failure of the many different components, among the first being the large scatter of use factors (ratios of design load effect to the factored strength) of many of the components. Furthermore, although the conductors and the ground wires can be selected with small steps in strength and can be installed to even finer gradations, the insulators and hardware that are in series with the wires are manufactured in standard strength ratings (i.e., at 15,000, 25,000, 36,000, and 50,000 lbs).

Many components of the wire system are typically designed to a lower percentage of their nominal strength than are other components of the line. The extra reserve of strength should ensure that, even with normal deterioration with aging, they should remain more reliable than the major components of the support system. This "extra reserve of strength" is especially important under extreme loading events because a component failure in the wire system puts critical demands on the failure containment capabilities of the support system.

The components of the support system do require some attention regarding their relative strengths. It is general practice to design foundations for a higher degree of reliability than the structures they support. An exception to this may be for direct-embedded pole structures where the foundation may rotate without leading to a pole failure. The rigorous approach to arranging this relative relationship would require knowledge of the dispersion characteristics or COVs of these two major line components. Additional information and discussion on relative reliability of components can be found in ASCE (2006).

1.4.3 Considerations for Special Structures

Crossing structures, long span structures, and some heavy angle and dead-end structures whose potential failure could cause severe consequences deserve special consideration. Failure of a heavy angle or

dead-end structure could introduce excessive slack into the line and could trigger a cascade. The failure of a crossing structure would likely result in damage to other facilities and disruption of services, and could present a greater risk to the public. Increasing the loading applied to the wire and support systems by 10% to 15% is one approach commonly used to minimize these risks.

1.4.4 Load and Resistance Factor Design

Although this is a loading manual and not a design document, the following presentation of LRFD is given to suggest load factors that can be used with the loads on transmission lines.

1.4.4.1 Load and Resistance Factor Equations. LRFD design describes one way of assessing behavior at various limit states. The following set of LRFD design equations provide an alternative approach for the design of components in a transmission line.

Weather-Related Loads. Equation 1-2a or 1-2b is the design equation that controls reliability for weather-related events. The limit state considered is damage of a component caused by the occurrence of extreme wind or combinations of ice and wind.

$$\phi R_n > \text{effect of } [DL \text{ and } \gamma Q_{50}] \tag{1-2a}$$

or

$$\phi R_n > \text{effect of } [DL \text{ and } Q_{RP}] \tag{1-2b}$$

where
ϕ = strength factor (Table 1-3)
γ = factor for wind force γ_w (Table 1-1) used in the extreme wind design, or factor for ice thickness γ_i and factor for wind γ_w (Table 1-2) used in combined ice and wind design. These factors are used to adjust the relative reliability with respect to a design with 50-year RP loads. The factor for the ice thickness, γ_i, is applied to the thickness of ice on the conductor, structure, or component prior to calculating the associated load (weight, transverse wind force, etc.). The wind force load factor, γ_w, is then applied to the calculated wind load on the bare or on the ice-covered component, depending on the load case. The ice weight load factor, if any, is applied to the resulting weight of ice, including the ice thickness load factor.

R_n = nominal strength of the component
DL = dead loads (not including weight of ice)
Q_{50} = wind or combined ice and wind loads based on 50-year RP
Q_{RP} = loads similar to Q_{50}, based on return period, RP

Failure Containment Loads. Equation 1-3 provides for the security of the line. Ideally, the limit state considered in Eq. 1-2 should be an ultimate or failure limit state. The purpose of the equation is not to prevent localized damage, but to prevent failure propagation. However, for simplicity, it may be assumed that damage and ultimate limit states are identical. With that conservative assumption, the same R_n can be used in all of the design equations.

$$\phi R_n > \text{effect of } [DL \text{ and } FC] \tag{1-3}$$

where
ϕ = strength factor (Table 1-3)
R_n = nominal strength of the component
DL = dead loads
FC = failure containment loads

Construction and Maintenance Loads. Table 1-4 considers the damage limit state of a component from C&M loads.

$$\phi R_n > \text{effect of } [DL \text{ and } \gamma_{CM}(C\&M)] \tag{1-4}$$

where
ϕ = strength factor (Table 1-3)
R_n = nominal strength of the component
γ_{CM} = load factor applied to the C&M load
DL = dead loads
$C\&M$ = loads produced by construction and maintenance operations

Legislated Loads. Equation 1-5 is included to emphasize that requirements from governing codes should always be considered.

$$\phi_{LL} R_n > \text{effect of } [LL] \tag{1-5}$$

where
ϕ_{LL} = legislated load strength factor
R_n = nominal strength of the component
LL = legislated loads

Table 1-3. Strength Factor ϕ to Convert to a 5% LEL with 10% COV_R[a]

Lower Exclusion Limit, (e%), of the Nominal Strength Value Used in the Design	Strength Factor, ϕ for COV_R =		
	0.05	0.1	0.2
0.1	1.00	1.16	1.48
1	0.97	1.07	1.27
2	0.95	1.04	1.21
5[b]	**0.93**	**1.00**	**1.12**
10	0.92	0.96	1.04
20	0.90	0.92	0.95
50	0.86	0.85	0.81
Mean	0.86	0.85	0.79

[a] Assumes lognormal strength property; the purpose is to achieve reliability levels equivalent to those for a component with a 5th percentile strength and a 10% COV_R. Different strength factors should be used if lognormal distribution is not representative.
[b] The entire table would collapse to this 5% LEL row if the nominal strength used in all design guides is a 5th percentile value.
LEL, lower exclusion limit; COV_R, coefficient of variation of component strength.

Table 1-4. Load Conditions that May Be Considered in Design

Equation	Load Case Description
1-2a or 1-2b Weather Loads	Extreme wind from any direction. Extreme ice with reduced wind (combined ice and wind). Unbalanced ice without wind (where applicable). Substantial wind on reduced ice (where applicable).
1-3 Failure Containment Loads	Failure containment criterion or loading (for example, broken conductor load).
1-4 Construction & Maintenance Loads	Structure erection loads. Stringing loads. Worker load.
1-5 Legislated Loads	Legislated loads (such as the NESC)

NESC, National Electrical Safety Code.

A load factor of 1.0 is used on the dead loads in all the above equations. If there is some uncertainty in structure dead loads, a conservative load factor value should be used.

The load factor γ in Eq. 1-2a (or the return period RP in Eq. 1-2b) allows a designer to modify the reliability of a line. The absence of load factor in Eq. 1-3 emphasizes the fact that the design loads that provide the security level of a line cannot be described statistically. However, simply increasing the nominal loads can increase the security of a line. Suggested minimum FC loads are presented in Chapter 3.

The strength and load factors to use with Eq. 1-2a (or strength factor and return period to use with Eq. 1-2b) could be developed by a number of different techniques. They could be chosen by consensus to represent current or projected practice. Preferably, they can be selected to control the relative reliability (or probability of failure) of the components of the line. That selection process is commonly referred to as reliability-based LRFD.

1.4.4.2 Design Load Combinations.   Equations 1-2 through 1-4 are generic equations to satisfy the basic requirements of relatively consistent reliability, providing for failure containment, and designing for C&M loads. Equation 1-5 represents design requirements for legislated loads. In practice, several load cases are considered in each of the categories of loads covered by the equations. Table 1-4 describes load cases normally considered in design.

Design loads on supporting structures are generally obtained by applying the selected load conditions to assumed maximum vertical span, wind span, and line angle. However, actual spans, line angles, and combinations of loads less than the maximum loads may be critical in some cases. The designer should be aware of conditions where the lesser values result in higher stresses in some components of the structures. An example of such a case is the foundation uplift loads that are due to the minimum weight span.

1.4.4.3 Selection of Load Factors.   The variability of loads and strengths can be formally considered in design through applications of probability theory. A probability-based design procedure is one that considers the probability of occurrence of a given limit state over a fixed period of time, usually 1 year or the planned lifetime of the system. The procedure should address two essential points: (1) how the probability of occurrence of the limit state is to be estimated; and (2) how small should the probability of occurrence be.

The ultimate goal of relative-reliability-based design is to control the reliability of the line system. Line reliability is directly affected by the reliability of each component in each subsystem.

Because accurate control of a line system's reliability is beyond the current state of the art, the approach adopted in this document is to control the relative failure probability of different lines or of different structure types or different components within a line, through the relative reliability factor (RRF, Eq. 1-1). Line RRF is approximately increased or decreased by a given factor by simply increasing or decreasing the return period, RP, of the load used in designing the line. In most applications, Tables 1-1 and 1-2 may be used for this purpose. A larger design load factor results in a more reliable line. It is important to note that the factor γ is applied to the wind force and to the ice thickness.

Techniques for calculating the loads Q_{50}, Q_{RP}, FC, and $C\&M$ in Eqs. 1-2 through 1-4 are described throughout this manual. The load factor γ in Eq. 1.-2a (or the return period RP in Eq.1-2b) that corresponds to a given relative reliability factor can be obtained from Tables 1-1 and 1-2. The RRF was defined in Eq. 1-1. The factored load γQ_{50} (with γ from Tables 1-1 or 1-2) is an approximation of the load Q_{RP}.

For wind loadings only, it is interesting to observe that every time the wind load factor γ is increased by increments of 0.15 (see 0.85, 1.00, 1.15, 1.30, 1.45 in Table 1-1), the return period of the wind load is doubled (25, 50, 100, 200, and 400 years). This also results in approximately reducing the probability of failure against wind by a factor of 2. This observation does not apply to ice concurrent with wind.

If statistical data on weather-related events are available, the use of Eq. 1-2b (using Q_{RP}) is recommended over that of Eq. 1-2a (using γQ_{50}). In addition to considering minimum values corresponding to historical or utility practice, selection of an appropriate RRF should be based on the importance of the line and its location and length. A higher or lower reliability may be selected for a portion of a line.

The reliability of a long line is less than that of a short one, all design parameters being the same. The primary reason for the reduced reliability is that a long line is exposed to a larger number of severe events and therefore its likelihood of experiencing some kind of failure is greater. Also, weak components are more likely to be exposed in a larger population. Therefore, the line designer may want to consider increasing the RRF for long lines due to these considerations.

Design for loads with a return period of 50 years (i.e., RRF = 1) are considered the basis for transmission line work. For temporary construction, an RRF < 1 may be acceptable (i.e., a design with RP < 50 years may be used, as shown in Tables 1-1 and 1-2).

1.4.4.4 Selection of Strength Factors.   The purpose of the strength factor, ϕ, in Eqs. 1.-2 through 1-4 is to account for the nonuniformity of the exclusion limits that currently exist in published formulas for nominal strength, R_n, and for differences in strength coefficients of variation, COV_R.

The values of the strength factor, ϕ, can be obtained from Table 1-3. The factors indicated assume a log-normal distribution of strength, which is considered more realistic than the normal distribution.

The use of Table 1-3 requires knowledge of the lower exclusion limit (LEL) corresponding to the nominal strength R_n of a component, as well as the COV_R of the component strength. Both numbers will vary from one type of component to another (for example, steel versus wood pole) and will depend on the strength design guide or method used to calculate nominal strength (ASCE 2006).

The strength factors of Table 1-3 are to be applied to the nominal strength. These values are based on a log-normal strength distribution and have been derived so as to result in relatively equivalent reliabilities (i.e., approximately equivalent probability of failure) when subjected to extreme wind events, independent of material (i.e., COV_R). As a result, these factors do not directly correspond to the simple calculation of $(1 - 1.645 \times COV_R)$, which may otherwise be used to obtain a "strength reduction factor" for applying to a mean strength, assuming a normal strength distribution, and without regard to the failure rates for different materials.

Typical values of the LEL and COV_R for different components used in transmission and distribution line are:

1. *Steel Components and Prestressed Concrete Poles.* For components of steel towers and steel or prestressed concrete pole structures designed according to the ASCE and Precast/Prestressed Concrete Institute (PCI) publications (ASCE 1988; ASCE 1990a; PCI 1997), it can be assumed that R_n (or R_e) has an exclusion limit in the range of 5% to 10% and COV_R is in the range of 10% to 20%. Therefore, from Table 1-3, ϕ is in the range of 0.96 to 1.12, or, typically, $\phi = 1.0$.

2. *Reinforced Concrete.* For reinforced (non-prestressed) concrete components designed according to the ACI-318 procedures (ACI 2002), the ACI strength reduction factors can be used in lieu of the ϕ factors given in Table 1-3 because the ACI factors already contain strength-derating effects for the various concrete components.

3. *Wood Poles.* For wood pole structures, the statistical data in ANSI O5.1 (ANSI 2002) can be used to determine a value for R_n at the 5% LEL. The corresponding strength factor can then be obtained from Table 1-3. Alternatively, the COV_R and 5% LEL may be computed from actual data and the corresponding strength factor obtained from Table 1-3, for $e = 5\%$.

4. *Foundations.* For foundations for which statistical data are available, Table 1-3 can be used. For foundations for which statistical data are not available, nominal strengths and strength factors based on established practice can be used. In such cases, however, the

reliability of the foundation relative to that of the supported structure is unknown.

5. *Conductors and Ground Wires.* The LRFD format described herein is also applicable to the mechanical design of conductors or ground wires. If the nominal strength for a conductor is defined as its rated ultimate strength, then a strength factor of 0.60 to 0.80 is recommended. Using a strength factor of 0.60 to 0.80 should prevent damage to the conductor and reduces the possibility of its rupture. These suggestions are not reliability-based but represent current practice.

A summary of the LRFD procedure is given in Table 1-5.

Table 1-5. Summary of LRFD Design Procedure

I. Select Relative Reliability Factor (RRF) or Minimum Design Load Return Period, Depending on Type of Line (Table 1-1)

II. Obtain Factors, γ, from Tables 1-1 and 1-2

III. Determine Design Load Effect, Q_D, in Each Component

Weather	Q_D = Effect of [DL and $\gamma\, Q_{50}$]	Eq. 1-2a
or	Q_D = Effect of [DL and Q_{RP}]	Eq. 1-2b
Failure Containment	Q_D = Effect of [DL and FC]	Eq. 1-3
Construction & Maintenance		
	Q_D = Effect of [DL and γ_{CM} (C&M)]	Eq. 1-4
Legislated Loads	Q_D = Effect of [LL]	Eq. 1-5

IV. Obtain Strength Factor, ϕ, From Table 1-3

V. Design Component for Nominal Strength, R_n, Such That:

$$\phi\, R_n > Q_D$$

DL, dead loads from weights of components; Q_{50}, weather-related load with a 50-year return period; Q_{RP}, weather-related load with an RP-year return period; FC, failure containment loads; LL, legislated loads.

This page intentionally left blank

CHAPTER 2

WEATHER-RELATED LOADS

2.0 INTRODUCTION

This chapter discusses weather-related loads on transmission structures. These are loads associated with wind, ice, or a combination of wind and ice. Temperature, atmospheric pressure, and local topography influence the magnitude of weather-related loads. These influences should be considered when appropriate.

A standard wind pressure formula applicable to transmission lines is presented. The wind pressures recommended in this chapter are primarily based on the provisions of ASCE Standard 7-05 (ASCE 2000b, ASCE 2005). The wind equations presented in this manual are developed from information currently available; however, due to the spatial extent of transmission lines and the different types of storms they experience, accurate wind load prediction is difficult. Therefore, it is hoped that in future editions of this manual the wind equations can be simplified.

Ice loads and combined ice and wind loads are also described. The manual provides a basis for estimating the thickness of ice on conductors and ground wires, and the wind speeds to be considered in combination with ice.

Supplemental information on wind speed averaging time, force coefficients, gust response factors, and ice loading is given in Appendices C through H.

2.1 EXTREME WIND

2.1.1 Wind Force

The wind force acting on the surface of transmission line components can be determined by using the wind force formula, shown in Eqs. 2-1a

and 2-1b. Equation 2-1b is used when specific return period wind speeds are known other than for 50 years.

$$F = \gamma_w Q K_z K_{zt} (V_{50})^2 GC_f A \qquad (2\text{-}1a)$$

or

$$F = Q K_z K_{zt} (V_{RP})^2 GC_f A \qquad (2\text{-}1b)$$

where

F = the wind force in the direction of wind unless otherwise specified, in pounds

γ_w = the load factor from Table 1-1 or 1-2 to adjust the force, F, to the desired return period

V_{50} = basic wind speed, 50-year return period, 3-sec gust, in mph (m/s), which can be obtained from the map in Fig. 1-1 in Chapter 1.

V_{RP} = the 3-sec gust design wind speed, in mph, associated with the RP-year return period

K_z = the velocity pressure exposure coefficient, which modifies the basic wind speed for various heights above ground and for different exposure categories (the values are to be obtained from Eq. 2-3 or Table 2-2).

K_{zt} = the topographic factor obtained from Eq. 2-14 below

Q = numerical constant defined in Section 2.1.2

G = the gust response factor for conductors, ground wires, and structures as specified in Section 2.1.5

C_f = the force coefficient values as recommended in Section 2.1.6

A = the area projected on a plane normal to the wind direction, in ft^2 (m^2)

The wind force calculated from Eq. 2-1a or 2-1b is based on the selection of appropriate values of wind speed, velocity pressure exposure coefficient, gust response factor, force coefficient, and load factor based on the selected wind return period. These parameters are discussed in subsequent sections. The wire tension corresponding to the wind loading should be calculated using the temperature that is most likely to occur at the time of the extreme wind loading event.

2.1.2 Numerical Constant, Q

The numerical constant, Q, converts the kinetic energy of moving air into the potential energy of pressure. For wind speed in mph (m/s) and pressure in psf (Pa), the recommended value is:

$$Q = 0.00256 \text{ customary units (0.613 metric units)} \qquad (2\text{-}2)$$

The value of Q reflects the mass density of air for the standard atmosphere [i.e., temperature of 59 °F (15 °C) and sea level pressure of 29.92 in. of mercury (101.325 kPa)]. For some cases, the effects of temperature on the air density factor and elevation on the value of Q may be considered. Sufficient weather data should be provided to justify a different value of the constant for a specific design application. Variations of this factor for other temperatures and elevations are given in Appendix C.

2.1.3 Basic Wind Speed

In the United States, the basic wind speed is the 3-sec gust wind speed at 33 ft (10 m) above ground in flat and open country terrain (Exposure C as defined in Section 2.1.4.1) and associated with a 50-year return period.

The National Weather Service (NWS) has redefined the basic wind speed as the peak gust that is recorded and archived for most NWS weather stations. Given the response characteristics of the instrumentation used, the peak gust is associated with an average time of approximately 3 seconds.

2.1.3.1 Basic Wind Speed from ASCE Standard 7-05. ASCE Standard 7-05 gives basic wind speeds in the form of a map, as shown in Fig. 1-1 in Chapter 1. The methodology for developing the maps is described in the commentary of ASCE 7. The wind speed values shown on the maps are normalized to 33 ft (10 m) above ground, flat and open terrain (Exposure C as defined in Section 2.1.4.1), and a 50-year return period.

In certain regions in the country, such as mountainous terrain, topographical characteristics (discussed in Section 2.1.7) may cause significant variations of wind speed over short distances. These variations of wind speed cannot be shown on a map of small scale. In addition, special wind regions designated on the map (Fig. 1-1) caution the designer that the wind speeds may vary significantly in these regions from those shown on the map. The designers should consult local meteorological data in these cases to establish design wind speed.

2.1.3.2 Use of Local Wind Data. It is possible to determine the basic wind speed using regional wind data for a specific location. ASCE Standard 7-05 provides provisions for the use of regional weather-related data. One possible conversion procedure to obtain 3-sec gust wind speeds from wind speeds of different averaging times is given in Appendix D.

2.1.4 Velocity Pressure Exposure Coefficient

The velocity pressure exposure coefficient, K_z, used in Eqs. 2-1a and 2-1b and defined by Eq. 2-3 (below) modifies the basic wind speed to account for terrain and height effects. It is recognized that wind speed varies with height because of ground friction and that the amount of friction varies with ground roughness. The ground roughness is characterized by the various exposure categories described here.

2.1.4.1 Exposure Categories. The following terrain roughness or exposure categories are recommended for use with this document and are specified in ASCE Standard 7-05.

Exposure B. This exposure is classified as urban and suburban areas, well-wooded areas, or terrain with numerous, closely spaced obstructions having the size of single-family dwellings or larger. A typical view of terrain representative of Exposure B is shown in Fig. 2-1. Use of Exposure B shall be limited to those areas for which terrain representative of Exposure B exists (in the direction from which the wind is blowing) for a distance of at least 1,500 ft (460 m) or 10 times the height of the transmission structure, whichever is greater.

In the use of Exposure B, a question arises as to what is the longest distance of flat, unobstructed terrain located in the middle of a suburban area permitted before the Exposure C category must be used. A guideline is 600 ft (180 m) or 10 times the height of the structure, whichever is smaller, as the size of intermediate flat, open country allowed for continued use of the Exposure B category.

Figure 2-1. Typical terrain representative of Exposure B.

Exposure C. This exposure is defined as open terrain with scattered obstructions having heights generally less than 30 ft (9.1 m). This category includes flat, open country, farms, grasslands, and shorelines in hurricane-prone regions. A typical view of terrain representative of Exposure C is shown in Fig. 2-2. This exposure category should be used whenever terrain does not fit the descriptions of the other exposure categories. It should also be noted that this exposure is representative of airport terrain, where most wind speed measurements are recorded.

Exposure D. This exposure is described as flat, unobstructed areas directly exposed to wind flowing over open water (excluding shorelines in hurricane-prone regions, Fig. 2-3) for a distance of at least 1 mile (1.6 km). Shorelines in Exposure D include inland waterways, the Great Lakes, and coastal areas of California, Oregon, Washington, and Alaska. The Exposure D category applies to structures directly exposed to bodies of water and coastal beaches. Exposure D extends inland from the shoreline a distance of 1,500 feet or 10 times the height of the structure, whichever is greater.

2.1.4.2 Equations. Values of the velocity pressure exposure coefficient, K_z are given by Eq. 2-3.

$$K_z = 2.01\left(\frac{z_h}{z_g}\right)^{\frac{2}{\alpha}} \quad \text{for } 33 \leq z_h \leq z_g \tag{2-3}$$

The velocity pressure exposure coefficient, as defined in Eq. 2-3, is dependent on effective height, z_h; the gradient height, z_g; and the power

Figure 2-2. Typical terrain representative of Exposure C.

Figure 2-3. Typical terrain representative of Exposure D.

law exponent, α. The effective height is discussed in Section 2.1.4.3. The gradient height defines the thickness of atmospheric boundary layer. Above this elevation, the wind speed is assumed to be constant. The power law exponent accounts for the wind profile with respect to height. Values for the power law exponent and corresponding gradient heights are given in Table 2-1 for the different exposure categories.

Effects of the velocity pressure exposure coefficient on wind force for the different terrain exposure categories are significant. It is essential that the appropriate exposure category be selected after careful review of the surrounding terrain. It is recommended that Exposure C be used unless the designer has absolutely determined that Exposure B or Exposure D is more appropriate. The transfer of the basic wind speed between exposure categories should only be used with good engineering judgment.

For Exposure Categories B, C, and D, heights up to 200 ft (60 m) aboveground and for use with 3-sec wind, Table 2-2 can be used to determine K_z.

2.1.4.3 Effective Height.   The effective height, z_h, is theoretically the height above the ground to the center of pressure of the wind load. The effective height is used for selection of a velocity pressure exposure coefficient, K_z (Table 2-2), and gust response factors, G_w or G_t (Eq. 2-4 or 2-5 below).

Table 2-1. Power Law Exponent

Exposure Category	α	z_g (ft)
B	7.0	1,200
C	9.5	900
D	11.5	700

Table 2-2. Velocity Pressure Exposure Coefficient, K_z

Effective Height z_h (ft)[a]	Exposure B	Exposure C	Exposure D
0–33	0.72	1.00	1.18
40	0.76	1.04	1.22
50	0.81	1.09	1.27
60	0.85	1.13	1.31
70	0.89	1.17	1.34
80	0.93	1.21	1.38
90	0.96	1.24	1.40
100	0.99	1.26	1.43
120	1.04	1.31	1.48
140	1.09	1.36	1.52
160	1.13	1.39	1.55
180	1.17	1.43	1.58
200	1.20	1.46	1.61

[a] Linear interpolation for intermediate values of height z_h is acceptable.

   The effective height of a conductor and ground wire subjected to wind and wind plus ice is influenced by the blow-out swing of the wire and insulators. However, for structural design purposes, the effective heights of all the wires can be approximated as the average height above ground of all of the wire attachment points to the structure.
   The velocity pressure coefficient varies over the structure height. Structures should be divided into sections, and the effective height, z_h, is the height to the center of each section. For some structures, a second or simpler alternative for structure heights 200 ft (60 m) or less is to assume one section and use two-thirds of the total structure height for the effective height. This alternative will provide a uniform wind pressure on the structure.

2.1.5 Gust Response Factor

The gust response factor accounts for the dynamic effects and lack of correlation of gusts on the wind response of transmission line components. It has been recognized that gusts generally do not envelop the entire span between transmission structures, and that some reduction reflecting the spatial extent of gusts should be included in the calculation of wind load. Both the dynamic effects and lack of correlation have been incorporated in the original gust response equations developed by Davenport (1979). A brief discussion of these equations can be found in Appendix F.

It should be noted that the gust response factor is different from the gust factor, which is used by some electric utilities in their wind loading criteria. The *gust factor* is the ratio of the gust wind speed at a specified short duration (e.g., 3 seconds) to some mean wind speed measured over a specified averaging time (e.g., 10 minutes). The *gust response factor*, on the other hand, is the ratio of the peak load effect on the structure or wires to the mean load effect corresponding to the design wind speed. Therefore, the gust factor is a multiplier of the mean wind speed to obtain the gust wind speed, whereas the gust response factor is a multiplier of the design wind load to obtain the peak load effect. The gust response factors specified in this manual take the place of the traditional gust factors.

The original Davenport gust response factors were multipliers of the mean wind loading corresponding to the 10-min average wind speed. Because the wind loading formula (Eq. 2-1a or 2-1b) in this manual is based on the 3-sec gust wind speed, a correction factor has been applied to the Davenport gust response factors for use in this formula. This correction factor can be determined from the wind speed versus averaging time curve by Durst (1960) presented in Appendix D.

2.1.5.1 Equations and Notation. The wire (conductor and ground wire) and structure gust response factors, G_w and G_t, respectively, may be determined from the following equations:

$$G_w = \frac{1 + 2.7 E \sqrt{B_w}}{K_v^{\,2}} \tag{2-4}$$

$$G_t = \frac{1 + 2.7 E \sqrt{B_t}}{K_v^{\,2}} \tag{2-5}$$

in which

$$E = 4.9 \sqrt{\kappa} \left(\frac{33}{z_h} \right)^{\frac{1}{\alpha_{FM}}} \tag{2-6}$$

$$B_w = \frac{1}{1 + \dfrac{0.8S}{L_s}} \tag{2-7}$$

$$B_t = \frac{1}{1 + \dfrac{0.56z_h}{L_s}} \tag{2-8}$$

where

z_h = effective height of the wire for the calculation of G_w, in ft, as defined in Section 2.1.4.3

z_h = two-thirds of the total height of the structure for the calculation of G_t, in ft

S = design wind span, in ft, of the wires (conductors and ground wires)

K_v = 1.43, the ratio of the 3-sec gust wind speed to the 10-min average wind speed (Appendix D)

α_{FM}, κ, and L_s are wind parameters given in Table 2-3.

The derivation of these equations is given in Appendix F.

2.1.5.2 Wire Gust Response Factor. The wire gust response factor, G_w, is used in Eq. 2-1a or 2-1b for computing the peak dynamic wind loads acting on conductors and overhead ground wires. It is given by Eq. 2-4. G_w is a function of exposure category (defined in Section 2.1.4.1), design wind span between structures, and the effective height, z_h.

Equation 2-4 and the curves for G_w in Figs. 2-4 through 2-7 were developed from the Davenport equations given in Appendix F, neglecting the resonant response of the wires to wind gusts. Wire resonance usually has a small effect on G_w, and this simplification is appropriate.

2.1.5.3 Structure Gust Response Factor. The structure gust response factor, G_t, is used in Eq. 2-1a or 2-1b for computing the wind loads acting on transmission structures and on the insulator and hardware assemblies

Table 2-3. Exposure Category Constants

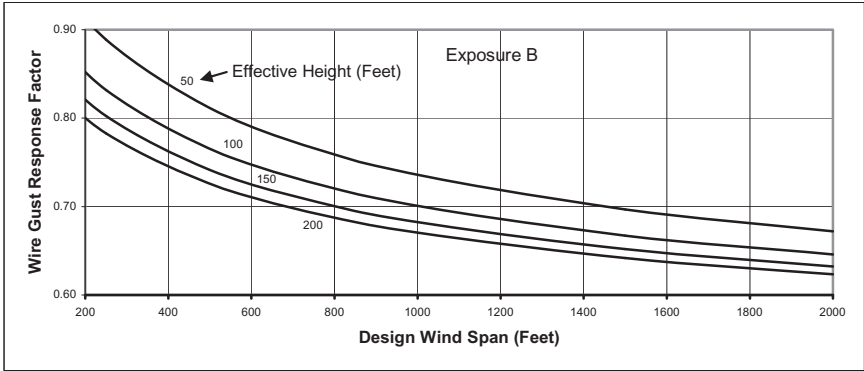| Exposure Category	Power Law Exponent, Sustained Wind, α_{FM}	Surface Drag Coefficient, κ	Turbulence Scale, L_s (ft)
B	4.5	0.010	170
C	7.0	0.005	220
D	10.0	0.003	250

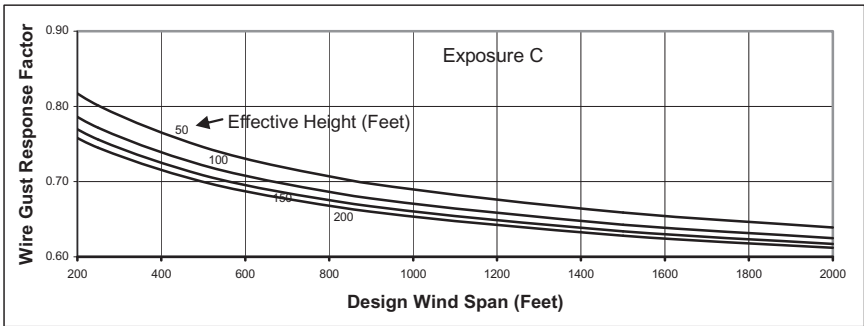Figure 2-4. Wire gust response factor, Exposure B.

Figure 2-5. Wire gust response factor, Exposure C.
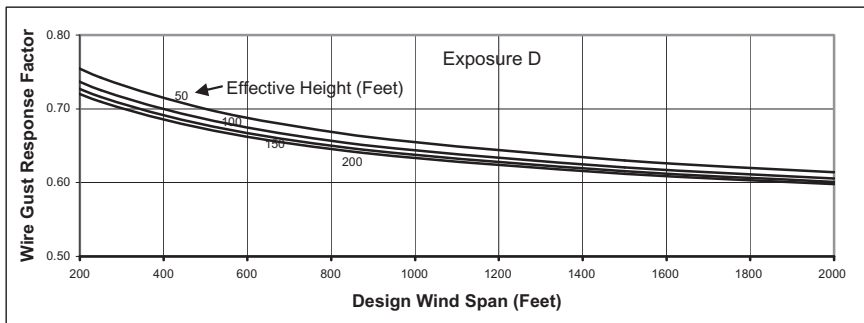
Figure 2-6. Wire gust response factor, Exposure D.
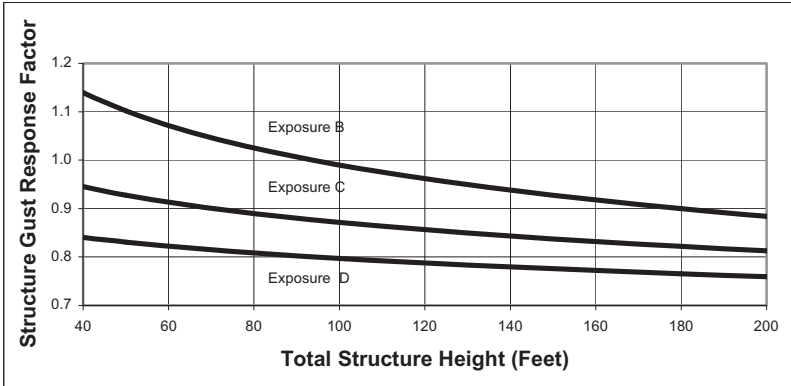
Figure 2-7. Structure gust response factor.

attached to the structures. G_t, given by Eq. 2-5, is a function of the exposure category (defined in Section 2.1.4.1) and the effective height, z_h.

Equation 2-5 for G_t was also developed from the Davenport equations by neglecting the resonant response terms for the structure, and the curves for these equations are shown in Fig. 2-7. With the elimination of the resonance terms, the equation yields identical values for all structure types, that is, for self-supporting latticed towers, guyed towers, monopole structures, H-frame structures, and so on. This simplified equation is applicable for most practical transmission structure types.

2.1.6 Force Coefficient

The force coefficient, C_f (frequently referred to as the drag coefficient) in the wind force formula, Eq. 2-1a or 2-1b, accounts for the effects of a member's characteristics (shape, size, orientation with respect to the wind, solidity, shielding, and surface roughness) on the resultant force. The force coefficient is the ratio of the resulting force per unit area in the direction of the wind to the applied wind pressure. It is also referred to as a drag coefficient, pressure coefficient, or shape factor.

2.1.6.1 Factors Influencing Force Coefficients.   This section discusses some of the important factors in the determination of force coefficient for a member or assembly of members. Additional theoretical background can be found in Hoerner (1958), Sachs (1978), and Mehta and Lou (1983).

2.1.6.1.1 Shape and Size.   Shapes fall into two general classifications: bluff and streamlined. The forces due to wind on a bluff structure can be attributed primarily to the pressure distribution around the shape. For

streamlined shapes, such as airplane wings, friction accounts for the majority of the drag force. Most buildings and engineering structures are bluff bodies (MacDonald 1975).

Within the bluff body classification there are two subdivisions. Members with sharp corners, such as rolled structural shapes, are referred to as blunt, whereas shapes with radiused corners are considered to be semi-aerodynamic. The pressure distribution around blunt shapes remains relatively constant for a given shape regardless of size or wind speed. A single force coefficient is given for such shapes.

With semi-aerodynamic shapes, the pressure distribution varies with wind speed. Above a particular (critical) wind speed, the negative pressure on the leeward side of the shape decreases in magnitude, causing a reduction in the overall force coefficient. The wind speed at which this change occurs in wind tunnel tests is dependent on the Reynolds number, a dimensionless ratio that relates the wind's inertia force (pressure) to its viscous force (friction). The equation for the Reynolds number is given as:

$$R = 9,350\left(\sqrt{K_Z}V\right)s \tag{2-9}$$

where
R = the Reynolds number, referenced at 59 °F at sea level
K_z = the terrain factor at height z above ground (Table 2-2)
V = the basic design wind speed, in mph (Section 2.1)
s = the diameter of the conductor or ground wire or the width of the structural shape normal to the wind direction, in ft

The buildup of ice on wires and structural members changes the force coefficient on these components; refer to Section 2.3.5.2 and Appendix G.

2.1.6.1.2 Aspect Ratio.   The ratio of a member's length to its diameter (or width) is known as the aspect ratio. Short members have lower force coefficients than do long members of the same shape. The force coefficients given in Section 2.1.6.2 are applicable to members with aspect ratios greater than 40, which is typical of most transmission line structures. Correction factors for aspect ratios less than 40 are given in Appendix G.

2.1.6.1.3 Yawed Wind.   The term yawed wind is used to describe winds whose angle of incidence with a shape is other than perpendicular. The angle of yaw is designated by Ψ and is measured in a horizontal plane. Figure 2-8 shows an example of yawed wind and the resultant force directions. Force coefficients for yawed wind on conductors, ground wires, and structures are presented in Section 2.1.6.2.
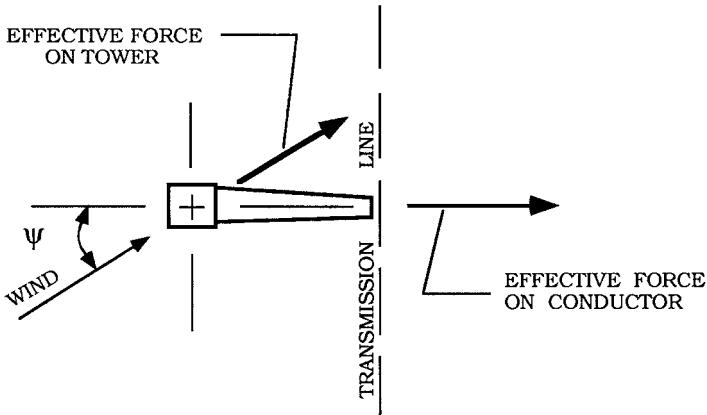
Figure 2-8. Illustration of yawed wind on a transmission line.

2.1.6.1.4 Solidity. An important factor that influences the force coefficient for lattice truss structures is the solidity of the frame. The force coefficient for the total structure is dependent on the airflow resistance of individual members and on the airflow patterns around the members. The force coefficients shown in Section 2.1.6.2 are a function of the solidity ratio, Φ, defined as:

$$\Phi = \frac{A_{\mathrm{m}}}{A_{\mathrm{o}}} \tag{2-10}$$

where
A_{m} = the area of all members in the windward face of the structure
A_{o} = the area of the outline of the windward face of the structure

The solidity ratio of each discrete panel in the transverse and longitudinal faces should be used for determination of the wind loads. For latticed structures that are less than 200 ft (60 m) in height, the solidity ratios for the various tower panels over the height of the transverse and longitudinal faces may be averaged to simplify the wind load calculation.

2.1.6.1.5 Shielding. When two members are placed in line with the wind, such as in a latticed tower structure, the leeward frame is partially shielded by the windward frame. The shielding factor is defined as the ratio of force coefficient for a shielded frame to the force coefficient for an unshielded frame. The shielding is influenced by the solidity ratio, spacing between frames, and yaw angle.

2.1.6.2 Recommended Force Coefficients. The following sections give the force coefficients recommended by this manual for various components of a transmission system. Other force coefficients can be used where justified by experimental data. Additional background information on force coefficients can be found in Appendix G.

2.1.6.2.1 Conductors and Ground Wires. Many designers currently use a force coefficient of 1.0 for conductors and ground wires, as indicated in NESC Rule 252 (NESC 2007). Wind tunnel test values, shown in Appendix G, range from 0.7 to 1.35. These data exhibit large variations in the wire force coefficient over a wide range in the Reynolds number. Unless more definitive field data based on wind force measurements are available (such as from wind tunnel testing), a constant force coefficient value of

$$C_f = 1.0 \qquad (2\text{-}11)$$

is recommended for single and bundled conductors and for ground wires. Smaller wire sizes typically have a higher force coefficient (see Appendix G). Note: If a reduced value of C_f is used on bare wires based upon wind tunnel testing, for wind loadings on ice-covered conductors the C_f should revert to a value of 1.0.

Equation 2-1a or 2-1b may be modified by $\cos^2 \Psi$ to account for yawed wind on conductors and ground wires, in which Ψ is the yaw angle. The $\cos^2 \Psi$ term accounts for yawed wind acting on wires that are not perpendicular to the wind. The designer must recognize that for all angles of yaw, the effective force calculated by Eq. 2-12 is perpendicular to the conductor or ground wire.

$$F = \gamma_w Q K_z K_{zt} V^2 G_w \cos^2 \Psi C_f A \qquad (2\text{-}12)$$

2.1.6.2.2 Latticed Truss Structures. This manual recommends that force coefficients for square-section and triangular-section latticed truss structures be determined from ASCE Standard 7-05 unless other requirements dictate the design. These force coefficients account for both the windward and leeward faces, including shielding of the leeward face by members in the windward face. The force coefficients, therefore, are multiplied by the projected area of one tower face.

The ASCE Standard 7-05 force coefficients for square-section and triangular-section latticed truss structures having flat-sided members are given in Table 2-4. The force coefficients given in this table for square-section structures can also be used for rectangular-section structures. For towers with round-section member shapes, the force coefficients are determined by multiplying the value from Table 2-4 by the correction

Table 2-4. Force Coefficients, C_f, for Normal Wind on Latticed Truss Structures Having Flat-Sided Members

Solidity Ratio, Φ	Force Coefficient, C_f[a]	
	Square-Section Structures	Triangular-Section Structures
<0.025	4.0	3.6
0.025–0.44	$4.1 - 5.2\Phi$	$3.7 - 4.5\Phi$
0.45–0.69	1.8	1.7
0.70–1.00	$1.3 + 0.7\Phi$	$1.0 + \Phi$

Source: "Minimum design loads for buildings and other structures." ASCE 7-88 (revision of ANSI A58. 1-1982).
[a] C_f values account for both the windward and leeward faces, including shielding of the leeward face.

Table 2-5. Correction Factors for Normal Wind on Round-Section Members in Latticed Truss Structures

Solidity Ratio, Φ	Correction Factor
<0.30	0.67
0.30–0.79	$0.67\Phi + 0.47$
0.80–1.00	1.00

Source: "Guide for design of steel transmission towers." (ASCE 1988).

factors given in Table 2-5. For latticed truss structures without a well-defined square or triangular cross section, the second method of 2.1.6.2.3 (below) can be used.

2.1.6.2.3 Latticed Truss Structures—Yawed Wind. For yawed wind, one of the following two methods can be used to determine the wind load on a latticed tower. The first alternative is to determine the loads in the transverse and longitudinal directions of the tower independently by applying the following equations:

$$F_t = \gamma_w Q K_z K_{zt} V^2 G_t \cos \Psi C_{ft} A_{mt} \qquad (2\text{-}13a)$$

$$F_l = \gamma_w Q K_z K_{zt} V^2 G_t \sin \Psi C_{fl} A_{ml} \qquad (2\text{-}13b)$$

where
$F_{t,l}$ = the force in the transverse or longitudinal direction
Ψ = the yaw angle measured in a horizontal plane
A_{mt} = the area of all members in the face of the structure that is parallel to the line, in ft^2

A_{ml} = the area of all members in the face of the structure that is perpendicular to the line, in ft^2

C_{ft} = the force coefficient associated with face of the structure that is parallel to the line

C_{fl} = the force coefficient associated with face of the structure that is perpendicular to the line

For the definition of the other variables, see Eq. 2-1a or 2-1b. Additional information on the force coefficients of latticed truss structures can be found in Appendix G.

The second alternative method is to determine the wind force on each member independently (neglecting shielding) based on the geometrical relationship between the wind velocity vector and the axis of the member. The force is in the plane formed by the wind velocity vector and the member axis, and it is perpendicular to the member. Its magnitude is based on Eq. 2-12, where K_z is calculated at the average height of the member; G_w is replaced by G_t; the incidence angle Ψ is determined from 3-D geometry from the direction of the wind velocity vector to the normal to the member axis in the plane formed by the wind velocity vector and the member axis; and the drag coefficient is equal to 1.6 for an angle member and 1.0 for a round member. The advantage of this alternative is that it is universal (applicable to towers of any conceivable geometry) because it is based on fluid mechanics principles. If this alternative method is selected for yawed winds, it could also be used for winds perpendicular to the faces as a replacement for the method described in Section 2.1.6.2.2.

2.1.6.2.4 Pole Structures.   The total face-on or yawed wind force on single-shaft and H-frame structures is the sum of the wind forces on the individual members within the structure. Typically, transmission pole shafts and closed cross-sectional structural shapes exceed one foot in diameter, which results in a Reynolds number in excess of $6.0 \times (10)^5$ based on the wind speeds shown in Fig. 1-1 in Chapter 1. They can be considered infinitely long, with wind along the longitudinal axis of the member. The ratio of the corner radius to the overall radius of the member is generally in the range of 0.05 to 0.15.

Surface roughness (e.g., rough for wood, smooth for steel) will influence the force coefficients for these shapes. Attachments on pole structures, such as steps, ladders, arms, and brackets, will also influence the force coefficients. The effects of attachments and surface conditions can be significant on highly streamlined shapes, such as circular members.

Table 2-6 lists recommended force coefficients for structural shapes commonly used in transmission pole structures. These coefficients are based on the research by James (1976) and on values given in ASCE Standard 7-05.

Table 2-6. Member Force Coefficients

Member Shape	Force Coefficient, C_f	Adapted From
Circular	0.9	ASCE Standard 7-05 (ASCE 2005)
16-sided polygonal	0.9	James (1976)
12-sided polygonal	1.0	James (1976)
8-sided polygonal	1.4	ASCE Standard 7-05 (ASCE 2005), James (1976)
6-sided polygonal	1.4	ASCE Standard 7-05 (ASCE 2005)
Square, rectangle	2.0	ASCE Standard 7-05 (ASCE 2005)

The recommended force coefficients include the effect of typical surface roughness and attachments, such as steps, ladders, and brackets. For example, the force coefficient for a circular member is based on ASCE Standard 7-05 assuming a rough surface. This accounts for the surface condition of a wood pole or typical steel pole attachments. For 12-sided and 16-sided polygonal shapes, the corner radius ratio term from James (1976) has been omitted to account for the effects of typical attachments.

In certain cases, it may be appropriate to select force coefficients other than those given in Table 2-6. Appendix G provides additional force coefficients for various shapes. The use of these or other values should be based on design experience and/or research results.

2.1.6.2.5 Other Members.   Appendix G also lists force coefficients for structural shapes based on Reynolds number, corner radius, and yaw angle. The effects of steps, ladders, arms, brackets, and other projections are not included in the values shown in Appendix G.

2.1.7 Topographic Effects

Topography can significantly influence wind speeds the transmission line structures may experience. Some guidelines on the effects of hills and ridges on wind speeds are available (for example, ASCE Standard 7-05). In addition, extensive field programs and research have been devoted to the subject of boundary-layer flow over hills and complex terrain (Taylor et al. 1987; Walmsley et al. 1986). Topographical influences that have some affect are (1) funneling of winds; (2) mountains and hills; (3) canyons and valleys.

Specific recommendations on some of these effects are beyond the scope of this document. The designer may benefit from the advice of a meteorologist in situations where these topographical effects may be severe.

2.1.7.1 Funneling of Winds.   This effect occurs where there is a natural flow of air from an unrestricted area through a restricted area, such as a mountain pass. As air is funneled into the canyons, it accelerates by the Venturi effect. This type of wind is often called a local canyon wind. The wind velocity through a canyon may be as much as double that in the unrestricted areas on each side. If this condition should exist along the right-of-way, the design loads should be adjusted accordingly.

Buildings may create the same kind of funneling effect as mountains. Generally speaking, buildings would not be a major influence on a transmission line. They could, however, alter the wind loadings on one or two structures and the designer should be aware that wind funneling generated by adjacent buildings could be present in a few locations along the line.

2.1.7.2 Mountains.   Wind tunnel tests (Arya et al. 1987, Britter et al. 1981, Finnigan et al. 1990, Gong and Ibbotson 1989, Snyder and Britter 1987) and field experiments (Coppin et al. 1994) suggest that wind speed can increase in localized areas of mountains on the windward side as well as on the leeward side (Armitt et al. 1975). When the wind is blowing normal to a mountain ridge, the air compresses as it moves up the windward side of the hill. With any opening in the ridge, the compressed air is released and accelerates as in the case of local canyon winds.

With the appropriate combination of pressure and temperature, the wind going over a mountain ridge accelerates on the leeward side of the ridge. Accelerated winds of this type are sometimes called Santa Ana, chinook, standing wave, or downslope winds. Several areas in the United States experience downslope winds because of their proximity to mountain ridges.

2.1.7.3 Wind Speed-Up over Hills, Ridges, and Escarpments.   ASCE Standard 7-05 provides special provisions to address wind speed-up over hills and escarpments. These provisions apply to isolated hills or escarpments located in exposure categories B, C, or D. The topographic feature (two-dimensional ridge or escarpment, or three-dimensional axis-symmetrical hill) is described by two parameters, H and L_h, Fig. 2-9. H is the height of the hill or difference in elevation between the crest and that of the upwind terrain. L_h is the distance upwind of the crest to where the ground elevation is equal to half the height of the hill.

The topographic effects may be considered in the design and location where the upwind terrain is free of such topographic features for a distance equal to $100H$ or 2 miles, whichever is smaller. The effect of wind speed-up need not to be considered when $H/L_h < 0.2$, or when $H < 15$ ft (4.5 m) for Exposure C and D, or <60 ft (18 m) for Exposure B.

Topographic Factor, K_{zt}

ESCARPMENT   2-D RIDGE OR 3-D AXISYMMETRICAL HILL

Topographic Multipliers for Exposure C										
	K_1 Multiplier				K_2 Multiplier			K_3 Multiplier		
H/L_h	2-D Ridge	2-D Escarp.	3-D Axisym. Hill	x/L_h	2-D Escarp.	All Other Cases	z/L_h	2-D Ridge	2-D Escarp.	3-D Axisym. Hill
0.20	0.29	0.17	0.21	0.00	1.00	1.00	0.00	1.00	1.00	1.00
0.25	0.36	0.21	0.26	0.50	0.88	0.67	0.10	0.74	0.78	0.67
0.30	0.43	0.26	0.32	1.00	0.75	0.33	0.20	0.55	0.61	0.45
0.35	0.51	0.30	0.37	1.50	0.63	0.00	0.30	0.41	0.47	0.30
0.40	0.58	0.34	0.42	2.00	0.50	0.00	0.40	0.30	0.37	0.20
0.45	0.65	0.38	0.47	2.50	0.38	0.00	0.50	0.22	0.29	0.14
0.50	0.72	0.43	0.53	3.00	0.25	0.00	0.60	0.17	0.22	0.09
				3.50	0.13	0.00	0.70	0.12	0.17	0.06
				4.00	0.00	0.00	0.80	0.09	0.14	0.04
							0.90	0.07	0.11	0.03
							1.00	0.05	0.08	0.02
							1.50	0.01	0.02	0.00
							2.00	0.00	0.00	0.00

Notes:
1. For values of H/L_h, x/L_h and z/L_h other than those shown, linear interpolation is permitted.
2. For $H/L_h > 0.5$, assume $H/L_h = 0.5$ for evaluating K_1 and substitute $2H$ for L_h for evaluating K_2 and K_3.
3. Multipliers are based on the assumption that wind approaches the hill or escarpment along the direction of maximum slope.
4. Notation:
   H: Height of hill or escarpment relative to the upwind terrain, in feet (meters).
   L_h: Distance upwind of crest to where the difference in ground elevation is half the height of hill or escarpment, in feet (meters).
   K_1: Factor to account for shape of topographic feature and maximum speed-up effect.
   K_2: Factor to account for reduction in speed-up with distance upwind or downwind of crest.
   K_3: Factor to account for reduction in speed-up with height above local terrain.
   x: Distance (upwind or downwind) from the crest to the building site, in feet (meters).
   z: Height above local ground level, in feet (meters).
   μ: Horizontal attenuation factor.
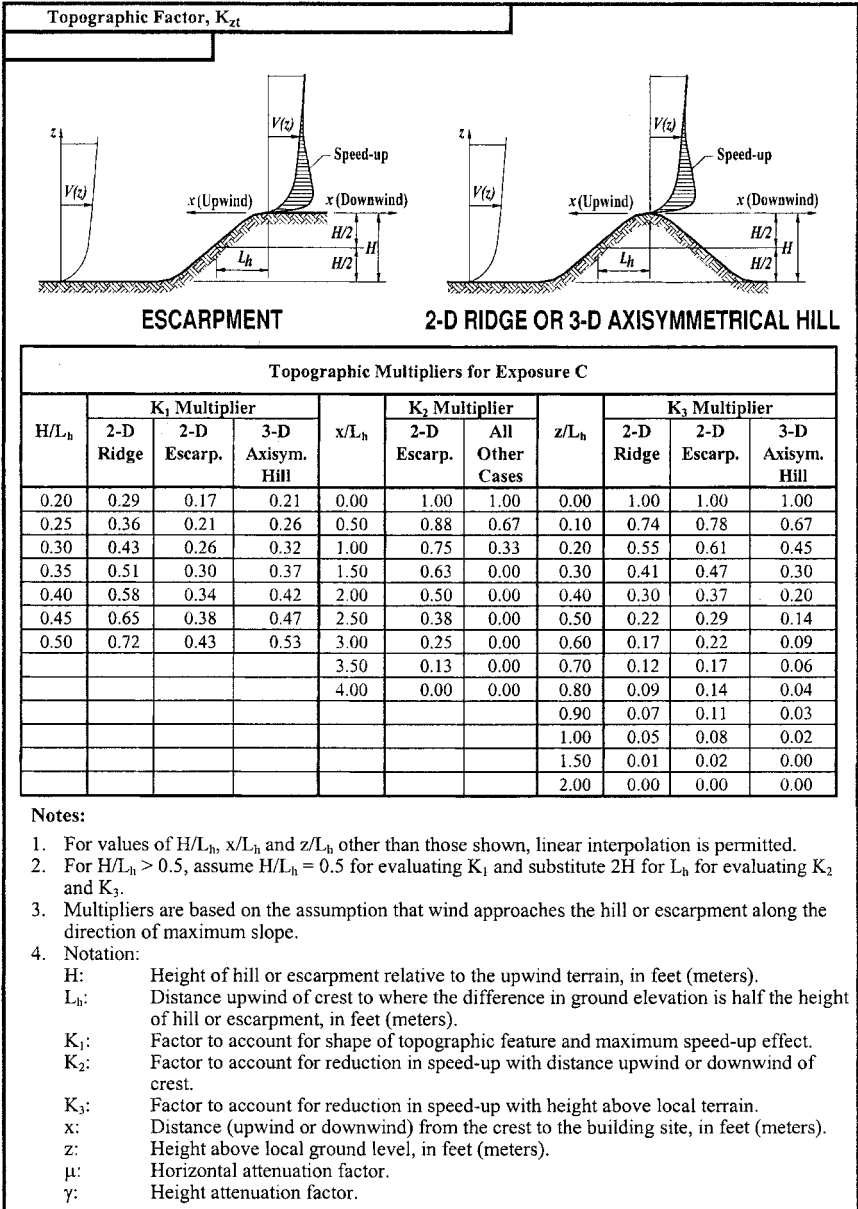   γ: Height attenuation factor.

Figure 2-9. Topographic factor for terrain effect. Source: ASCE (2005)

Topographic Factor, K_{zt} – Method 2

Equations:

$$K_{zt} = (1 + K_1 K_2 K_3)^2$$

K_1 determined from table below

$$K_2 = (1 - \frac{|x|}{\mu L_h})$$

$$K_3 = e^{-\gamma z/L_h}$$

Parameters for Speed-Up Over Hills and Escarpments						
Hill Shape	**$K_1/(H/L_h)$**			**γ**	**μ**	
	Exposure				**Upwind of Crest**	**Downwind of Crest**
	B	**C**	**D**			
2-dimensional ridges (or valleys with negative H in $K_1/(H/L_h)$	1.30	1.45	1.55	3	1.5	1.5
2-dimensional escarpments	0.75	0.85	0.95	2.5	1.5	4
3-dimensional axisym. hill	0.95	1.05	1.15	4	1.5	1.5

Figure 2-9. Continued.

To account for the wind speed-up over isolated hills and escarpments that constitute abrupt changes in the general topography, a topographic factor, K_{zt}, may be applied to the transmission structures sited on the upper half of the hills and ridges or near the edges of escarpments:

$$K_{zt} = (1 + K_1 K_2 K_3)^2 \qquad (2\text{-}14)$$

Definitions of the multipliers K_1, K_2, K_3 are given in Fig. 2-9. These multipliers are based on the assumption that the wind approaches the hill along the direction of maximum slope, causing the greatest speed-up near the crest. The value of K_{zt} should not be less than 1.0.

It is not the intent of this section to address the general case of wind flow over hilly or complex terrain for which engineering judgment, expert advice, or wind tunnel tests may be required.

2.1.7.4 Canyons and Valleys. Transmission lines may be subject to high winds coming from canyons, from cool air masses spilling over a ridge, or from general winds moving through the valley. Air masses spilling over into a valley can be several miles in width and may reach velocities in excess of 100 mph (160 kph). This kind of event can occur several miles away from a mountain range.

2.1.8   Wind Load Applications on Latticed Towers

There is no standard procedure for the application of the wind forces determined from Eq. 2-1a or 2-1b, or 2-13a or 2-13b to the panel points of the latticed tower. Typically, the structure designer will follow the procedures specified by the individual utility. For example, some utilities may distribute the wind forces to the windward panel points, whereas others may distribute the wind forces to all panel points at an elevation. However, all utilities generally distribute wind forces to the respective member connecting joints as concentrated vector loads. It is important to mention a few key points that should be considered when applying the calculated wind forces.

The wind forces determined by Eq. 2-1a or 2-1b, or 2-13a or 2-13b, using the recommended force coefficients of this manual have accounted for both the windward and leeward tower faces, including shielding. Therefore, the wind forces calculated on a complete latticed truss system, such as a self-supporting structure body, can be distributed to the panel points of the structure without further consideration. Where the latticed truss systems in a structure are separated, such as the case of a single circuit structure with a large opening to accommodate the middle phase of a "delta" or "horizontal" phase configuration, the second method of Section 2.1.6.2.3 can be used. This method is also applicable to guyed Vs and other guyed structures (ASCE 1997a).

For separated latticed truss systems and individual tubular shaft members of an H-frame structure, the windward faces should be considered as each being individually exposed to the calculated wind force determined from Eq. 2-1a or 2-1b with the appropriate force coefficients. The wind forces can then be distributed to the structure panel points according to the criteria specified by the utility. Other locations on a structure may need to be reviewed where physically separated latticed truss systems or tubular shaft members are used.

Longitudinal winds may also produce significant structure loadings. This case should be considered in the structure design.

2.2 HIGH-INTENSITY WINDS

Tornados, microbursts, and downbursts are the high-intensity winds (HIWs) discussed in this section. HIWs are generally the result of intense, localized thermal activity that frequently accompanies a thunderstorm or squall line. These HIWs are commonly narrow-front winds with speeds greater than the sustained, broad-front, systemic winds described in Section 2.1. HIWs do not follow the pattern and characteristics of extreme winds from which the mathematics of gust response factors in Section 2.1 were developed. Some data from HIWs were included in the development of the basic extreme wind maps of Fig. 1-1 in Chapter 1.

Analyses of line failures in several countries have identified HIW events as the leading cause of transmission line failures, with some located far from the usual centers of tornado activity. It is possible to apply rational and economic measures to a transmission line design to defend against the majority of these HIWs in the absence of windborne debris.

The following sections illustrate the steps that could be taken to mitigate the effects of these HIW events. Understanding the past wind engineering history of these extreme events and the evaluation of the regional wind climate are the first steps to a rational and economic mitigation plan. HIW, similar to the extreme wind, is affected by local topography.

The economy of including HIW load cases in the structure designs will depend on the other local loads. Structures designed for light winds and little ice might not be made to withstand HIW economically, but structures already designed for high wind or heavy ice might require just a small cost increase to include HIW loads.

2.2.1 Tornados

The usual perception of a tornado is of an overwhelming event destroying all in its path and defying resistance. Although most tornados are capable of causing severe damage to houses, mobile homes, and automobiles, most engineered structures often survive without major damage.

The majority of tornados contain wind speeds well within the capabilities of engineered structures. Transmission line structures can be designed to resist the HIW of most tornados. However, occasional tornados are more severe and these can be expected to cause damage to engineered structures. For these severe types of tornados, the line designer's focus changes from resisting the HIW to one of failure containment.

Tornados occur in most subtropical and temperate landmasses around the world. Fortunately, most tornados do not carry overwhelming winds and therefore cause limited structural damage to engineered structures. On average, 800 to 1,000 tornados occur each year in the contiguous United States, and the activity zone extends well up into Canada. The total number of reported tornados in 1-degree squares of latitude and longitude for a 30-year period (1950 to 1980) is shown in Fig. 2-10. A 1-degree square contains about 4,000 sq. mi (10,000 km²).

Fujita and Pearson (1973) have developed a rating (the FPP scale) to categorize tornados by their intensity and size. This method assigns a numerical value of the FPP scale to each tornado based on the appearance and extent of damage. The FPP scale and associated wind speed, path length, and path width ranges are shown in Table 2-7. The wind speeds given in this table are assigned from qualitative assessments of observed tornado damage. They are equivalent to the fastest quarter-mile wind speeds assumed at 16 to 33 ft (5 to 10 m) above ground level.

It is common practice to refer to a tornado by one scale only (e.g., F2, to indicate a gust wind speed of 113 to 157 mph), although the total classification might be an FPP of 213, indicating a gust wind speed of 113 to 157 mph, a path length of 1.0 to 3.1 miles, and a width of 531 to 1670 feet. There are documented tornados of FPP 135 and other extreme combinations; however, for the purposes of transmission line design it may be reasonable to assume that the FPP scales are equal (i.e., tornados are FPP of 222 or 111). Justification for this assumption and further discussion can be found in Schaefer et al. (1985).

The probability of a tornado strike at a given point is very small (McDonald 1983), even in areas of tornado prevalence. However, the probability of a transmission line being crossed by a tornado is significant (Twisdale 1982). The fact that the width of path is very narrow for most tornados, however, makes it possible to improve transmission line resistance to most tornados at reasonable cost. Almost all tornados can engulf a house or small structure, but very few have a width of path of the most extreme winds that will load the full span of a transmission line.

All tornados that were observed in a 63-year period and categorized by F scale are shown in Table 2-8. 86% of the tornados are assigned to the scale of F2 or smaller; the F2 rating corresponds to a wind speed of 157 mph or less. Of equal importance is the observation that the width of path of the extreme winds will usually be less than 530 ft (160 m).
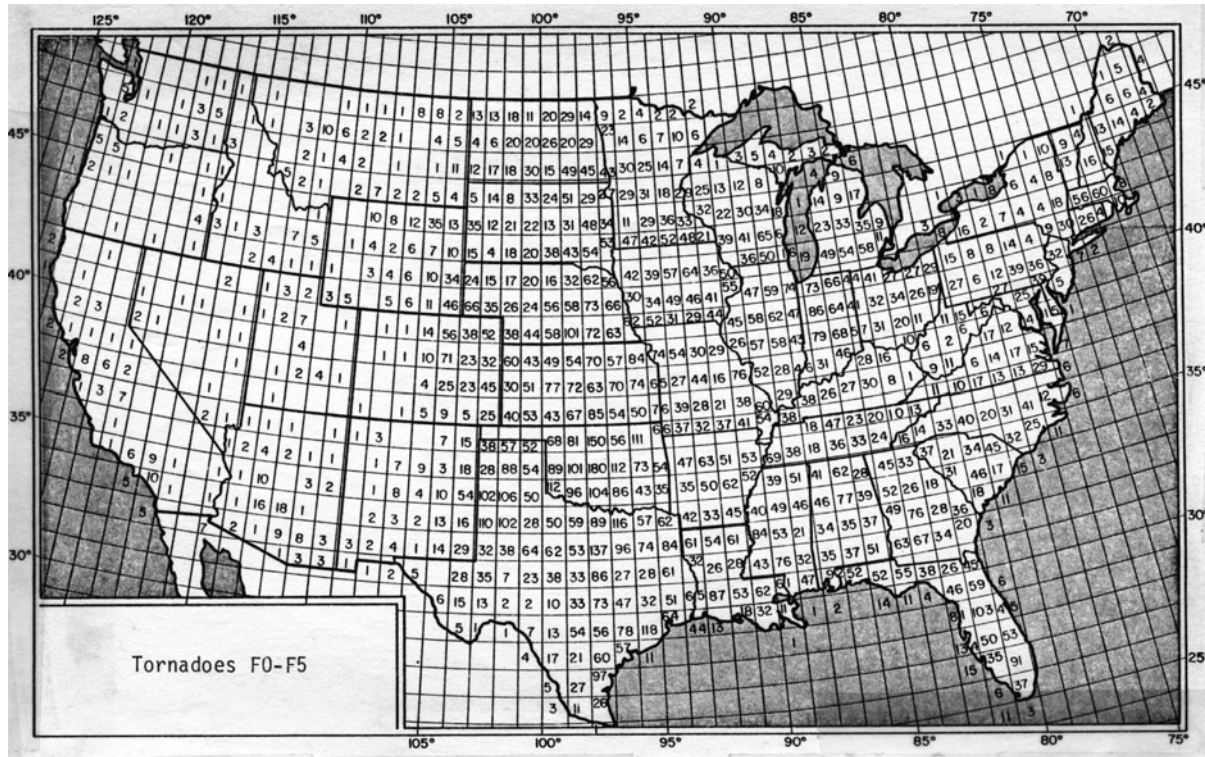
Figure 2-10. Total number of reported tornados during a 30-year period. Source: Tescon et al. (1979).

Table 2-7. Ranges of Tornado Wind Speed, Path Length,
and Path Width for FPP Scale[a]

Scale	Tornado Wind Speed, F (mph)	Path Length, P (miles)	Path Width, P (ft)
0	≤72	<1.0	≤50
1	73–112	1.0–3.1	51–170
2	113–157	3.2–9.9	171–530
3	158–206	10–31	531–1,670
4	207–260	32–99	1,671–4,750
5	261–318	100–315	4,751–6,000

[a] FPP, Fujita-Pearson tornado scale. The EF (Enhanced Fujita) scale contains new information on wind speed classifications and damage indicators.

Table 2-8. Tornado Frequencies and F-Scale Classifications for
1916–1978 in the United States

F-Scale (Gust Wind Speed Range)	Number of Tornados	Percentage	Cumulative Percentage
F0 (40–72 mph)	5,718	22.9	22.9
Fl (73–112 mph)	8,645	34.7	57.6
F2 (113–157 mph)	7,102	28.5	86.1
F3 (158–206 mph)	2,665	10.7	96.8
F4 (207–260 mph)	673	2.7	99.5
F5 (261–318 mph)	127	0.5	100.0
Total	24,930	100.0	

Source: Tecson et al. (1979).

The wind pattern within a tornado is composed of circular wind combined with a translation motion, the highest velocities being where the rotary and translation components add together (Abbey 1976; Mehta et al. 1976; Minor et al. 1977; Wen and Chu 1973). A hypothetical pattern of tornado wind velocities and directions is shown in Fig. 2-11. The figure shows the vector sum of the two major velocity components, with the direction being a function of the ratio of the two components. The maximum rotary wind will be at a distance from the center of the tornado and, at this circular annular path, very large vertical winds may be sufficient to lift conductors and reverse vertical crossarm loads. Radial winds will also be produced as air moves into the uplift areas.

The data in Tables 2-7 and 2-8 indicate that it is not practical to design a transmission line to withstand all tornados. The fact that 86% of
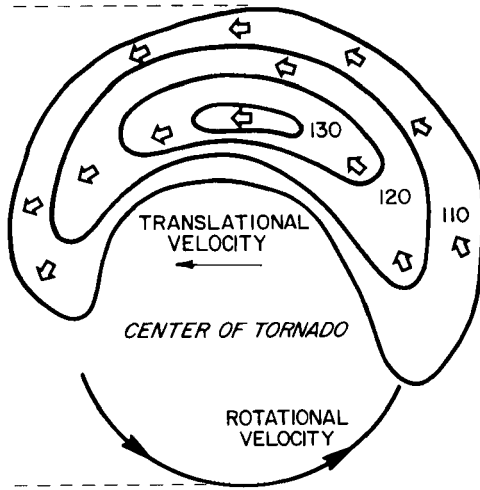
Figure 2-11. Hypothetical pattern of tornado wind velocities and directions.

categorized tornados are rated at F2 or less indicates the possibilities of economical designs that might resist most tornados. Many, but not all, of the tornados of F2 or less are characterized by intense winds acting over a small width of path. This width may be sufficient to create very large loads acting on the structure, but the conductor loads on the full span will be much smaller.

The extreme wind loads described in Section 2.1 of this document, or those of the NESC or other codes, are typically applied concurrently to the wire systems and to the structures, and are derived from the same wind speed. For medium- to long-span construction, this usually produces total wind on conductor loads many times greater than the wind on structure loads. The center of pressure of the total transverse loading is close to the level of the conductor loads. Some design practices employ span factors or gust factors that have the effect of slightly reducing the ratio of conductor to structure loads, but the center of pressure remains close to the conductor support points.

One possible "tornado" loading is a wind loading corresponding to a moderate tornado (scale Fl or F2) applied only to the transmission structure over the full structure height from any direction. It can be assumed that "tornado" loading applied to the wires is neglected because of the small tornado path widths [e.g., 200 to 500 ft (60 to 150 m)] and the complexity of the wind force mechanism applied to the wires. Coincident with the "tornado" wind loading should be a wire vertical load of zero. This is of particular importance for lines with V-string insulator assemblies.

Because the tornado wind speeds are gust wind speeds, the gust response factor (G) and velocity pressure exposure coefficient (K_z) should be considered equal to 1.0 for calculating the wind force of Eq. 2-1a or 2-1b. The selection of the "tornado" wind could be the scale F2 value (113 to 157 mph) or any other target value consistent with costs and expected improvement in resistance. Because tornado loading is considered to be an extreme loading condition, it is appropriate to use a load factor of 1.0 for this case.

Latticed transmission towers may be susceptible to windborne debris from HIWs. Metal roof panels that become entangled in the tower will create large wind loads that the tower cannot withstand due to local buckling of truss members.

2.2.2 Downbursts

Downbursts are usually associated with the more severe thunderstorm cells and seldom reach the intensity levels or wind speeds of F2-class tornados, but they can have relatively wide gust fronts so that two or three spans may be affected. Downbursts are usually evidenced by elliptical damage patterns to vegetation.

The normal procedure for providing protection or defense against downburst effects is either the application of tornado-type narrow-front loading described above, or simply relying on the extreme wind loadings of Section 2.1 with a gust response factors closer to 1.0.

2.2.3 Microbursts

Microbursts are more focused than downbursts; they can reach the intensity levels or wind speeds of F2-class tornados and have narrow frontal widths that can engulf a structure and a section of conductors. Normal gust width can be expected to be 330 to 660 ft (100 to 200 m). Microbursts are also usually evidenced by elliptical and strip damage patterns to vegetation.

The normal procedure for providing protection against microburst effects is the application of tornado-type narrow-front wind loading described above to supplement the normal extreme wind loads.

2.2.4 Risk Assessment for High-Intensity Winds

In the design of major transmission lines or in the review of security of existing lines, the transmission line owner might consider a detailed wind engineering risk assessment study. This study should provide the probability of downburst and/or tornado winds that can be expected in a given time frame over a stated length of line. It is also important to understand the special interactions between HIW and line structures. This

information can then be used to assess the costs of modifying designs to accept certain expected wind levels.

Such a study may take the form of an initial assessment of the meteorological data to determine the type, intensity, and predominant directionality characteristics of HIW events that occur throughout the line route in question. This is then followed by a sectionalized review of the line route with consideration given to route direction, topographical features, exposed sites, and recognized historical storm track paths or corridors. A risk modeling methodology is then adopted and applied to each of the finite line elements and to the whole line length to provide wind velocity/ return period predictions for all line route elements. From these values the designer can make a selection of the appropriate design velocity.

Schwarzkopf and Rosso (1993) assessed the risk of tornados and downbursts intercepting a particular transmission line. Their results were presented in chart form similar to Fig. 2-12. The annual risks associated with tornados and downburst winds were calculated with appropriate confidence limits for the total line length. This result was presented to the line designers to form the basis for selection of their HIW loads.
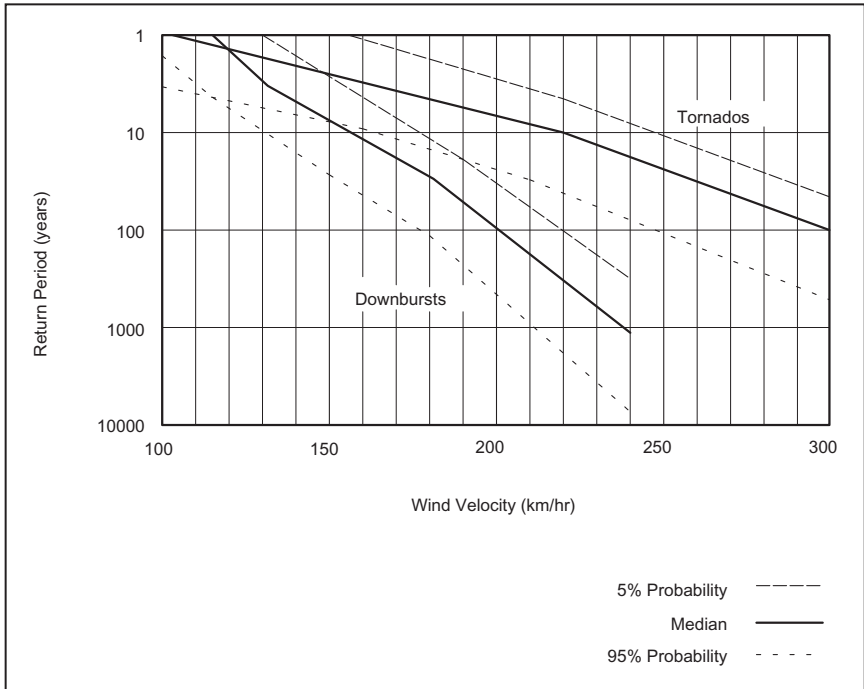
Figure 2-12. Return period of wind speeds traversing a 650-km line section. Source: Adapted from Schwarzkopf and Rosso (1993).

Other examples include utilities in South Africa (Behncke et al. 1994) and in Canada (Ishac and White 1995). These utilities have already established the costs of including the effects of F2 tornado winds in the design of high voltage transmission lines. The noticeable effects on structure designs are a lowering of the load center on rigid latticed structures, which results in the need to reinforce the internal shear bracing in the body of lattice framework. Both studies of the costs of meeting the calculated forces of F2 tornados with narrow-fronted winds of about 160 mph (71 m/sec) indicated small increases in structure weights.

Failure rate predictions are already extremely difficult for typical extreme winds because of the problems associated with conversion of wind speed data to wind loads. These problems even more pronounced with HIW. The design exercise of checking for the calculated loads of the selected HIW will possibly disclose very small and limited areas of the structures that need to be reinforced and that might cost little compared to the benefits.

2.3 ICE AND WIND LOADING

2.3.1 Introduction

Ice accretion on a transmission line is often a governing loading criterion in structure design. In addition to imposing substantial vertical loads on the structural system, the ice buildup on the conductors presents a greater projected area exposed to the wind, and it affects the force coefficient. In addition to the direct effect these loads have on the structural system, their resultant load on the wires causes significantly higher wire tensions compared to bare conductor conditions. Meteorological data suggest, and a survey of utility practice (ASCE 1982) confirms, that ice and concurrent wind loadings should be included in the load criteria of transmission structure designs throughout most of the United States.

The following discussion provides general guidance for the selection of ice and wind-on-ice loads. Where more detailed icing data have been compiled for a service area, that data should take precedence over the information in this manual. Electric utilities are urged to develop ice and concurrent wind loading criteria established specifically for their service regions based on historical data.

2.3.2 Categories of Icing

Ice can be classified by either its method of formation or its physical characteristics. Precipitation icing from freezing rain or freezing drizzle is the most common icing mechanism. The glaze ice that forms in these conditions is usually clear, but may also be translucent because of included

air bubbles. In-cloud icing is caused by supercooled cloud droplets, carried by the wind, colliding with a surface. The ice that forms ranges from hard, clear glaze to softer, lower-density white rime ice containing entrapped air. In-cloud icing may occur in regions with level terrain, but is more frequently associated with mountainous areas, occurring both on exposed summits and upslopes. Snow, both wet and dry, may adhere to wires by capillary forces, freezing and sintering, and forming a cylindrical sleeve around the wire. The density of accreted snow depends on the wind speed and the wetness of the snow. Hoarfrost is an accumulation of ice crystals formed by the direct deposition of water vapor from the air onto a structure. The amount of ice accreted by vapor deposition does not impose significant loads on structures.

It is important that the transmission line engineer be aware of the icing conditions (i.e., freezing precipitation, in-cloud icing, or sticky snow) that may occur along the route of a proposed transmission line. Ice accretions produced by freezing rain rarely exceed a thickness of a few inches, whereas lower-density accretions due to in-cloud icing and sticky snow can build to thicknesses of a foot or more. Furthermore, in-cloud icing can produce significant unbalanced loadings between adjacent spans with different wind exposures. The designer would benefit from the advice of a meteorologist in regions where in-cloud icing may be severe.

Appendix H, Section H.1 provides additional information on the meteorological conditions that are associated with the various types of icing and properties of the ice accretions.

2.3.3 Design Assumptions for Ice Loading

The four categories of icing (glaze, in-cloud, snow, and hoarfrost) cover the spectrum of the icing phenomenon. The distinctions made by definition of each category may not be identifiable in practice. There can be an overlap of more than one type of icing condition, such as snow and freezing rain or in-cloud icing and freezing drizzle. In specifying ice loadings, the accretion density should be noted and is typically assumed to be uniform with thickness.

For simplicity, the design ice thickness is specified as an equivalent uniform radial thickness over the length of the wire. However, natural ice accretions may be uniform, elliptical, crescent-shaped, pennant-shaped, or have icicles attached.

2.3.4 Ice Loading on Wires Due to Freezing Rain

2.3.4.1 Using Historical Ice Data. Because weather stations do not collect ice thickness data, ice accretion models are often used to estimate ice thicknesses using meteorological data. Where modeled or actual ice

thickness and concurrent wind speed data are available, the design ice thickness is I (which is I_{RP} or $\gamma_I I_{50}$). The concurrent wind speed is used to determine the transverse wind-on-ice load that is combined with the vertical load due to the weight of the ice.

2.3.4.2 Using Ice Maps. In areas where local historical icing data are not available, the ice map given in Figs. 2-13 through 2-18 can be used with some limitations. This map shows 50-year point ice thicknesses due to freezing precipitation with concurrent 3-sec wind speeds V_I at 33 ft (10 m) above ground for the continental United States and Alaska. The values in Figs. 2-13 through 2-18 do not include in-cloud icing or sticky snow accretions, which are caused by meteorological conditions that may produce significantly different loading patterns (see Appendix H, Section H.5).

Multipliers to determine ice thicknesses and concurrent wind speeds from I_{50} and V_I for 25-, 100-, 200- and 400-year return periods are presented in Table 1-2 in Chapter 1. The mapped ice thicknesses and wind speeds are based on wind Exposure C, but should also be used for wind Exposures B and D.

The amount of ice that accretes on a wire depends on the wind speed at the wire height. Design thicknesses of ice I_z for heights z above ground can be obtained from:

$$I_z = I\left(\frac{z}{33}\right)^{0.10} \quad 0 \text{ ft} < z < 900 \text{ ft}$$

$$I_z = I\left(\frac{z}{10}\right)^{0.10} \quad 0 \text{ m} < z < 275 \text{ m}$$

(2-15)

where
I = nominal ice thickness (I_{RP} or γI_{50})
I_z = design ice thickness
z = height above ground

This is an average ice thickness profile assuming a 1/7 power law for the wind speed profile. At sites that tend to be windy or where the wind speed increases rapidly with height, the ice thickness gradient will be more pronounced than is indicated by Eq. 2-15. The concurrent wind speed is also increased with height above ground using Eq. 2-3. Ice thicknesses on a ridge, hill, or escarpment will be greater than those in level terrain because of wind speed-up effects. The topographic factor for the ice thickness on isolated ridges, hills, or escarpments is $K_{zt}^{0.35}$, where K_{zt}

is obtained from Eq. 2-14. However, while ice thickness and concurrent wind are affected by height above the ground and topography, the uncertainties associated with quantifying those effects might not justify the detailed calculations above.

For areas not covered by Figs. 2-13 through 2-18 and areas where in-cloud icing or sticky snow is the most severe icing mechanism,

Notes:
1. Ice thicknesses on structures in exposed locations at elevations higher than the surrounding terrain and in valleys and gorges may exceed the mapped values.
2. In the mountain west, indicated by the shading, ice thicknesses may exceed the mapped values in the foothills and passes. However, at elevations above 5,000 ft, freezing rain is unlikely.
3. In the Appalachian Mountains, indicated by the shading, ice thicknesses may vary significantly over short distances.

Figure 2-13. Extreme radial glaze ice thickness (in.), western United States (except Pacific Northwest); 50-year return period with concurrent 3-sec wind speeds. Source: ASCE (2005).

other sources of information must be consulted to determine design ice thicknesses; refer to Appendix H, Sections H.4 and H.5 for additional information. Figures 2-13 through 2-18 represent ice thickness values at single points, and do not include spatial effects (refer to Appendix B, Section B.6).

2.3.4.3 Combined Wind and Ice Loads. The ice thicknesses due to freezing rain described in Sections 2.3.4.1 and 2.3.4.2 are equivalent
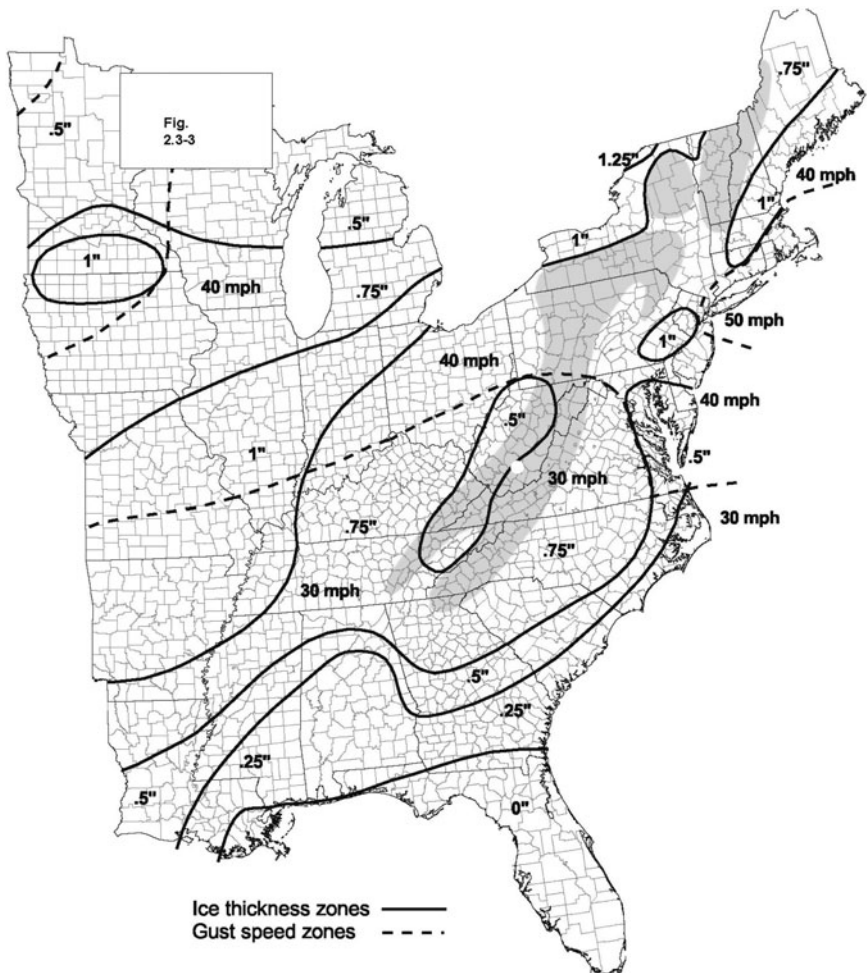
Figure 2-14. Extreme radial glaze ice thickness (in.), eastern United States; 50-year return period with concurrent 3-sec wind speed. Source: ASCE (2005).
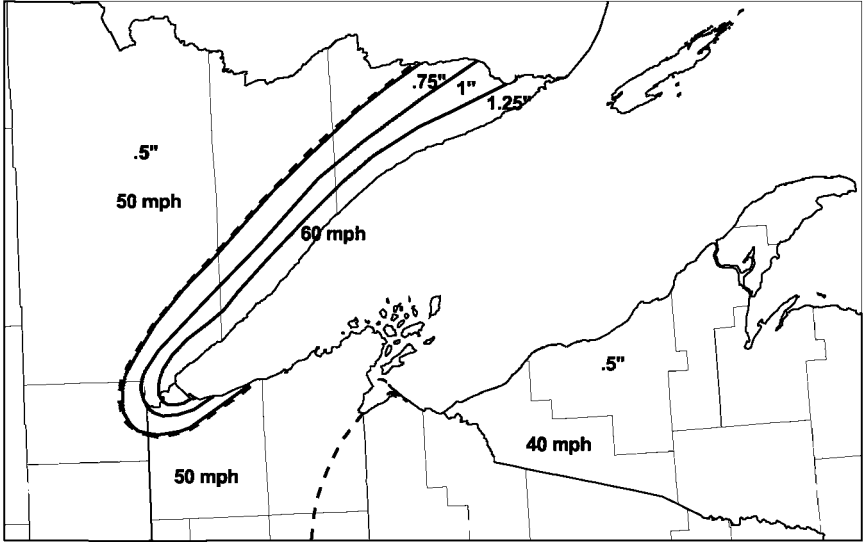
Figure 2-15. Extreme radial glaze ice thickness (in.), Lake Superior detail; 50-year return period with concurrent 3-sec wind speeds. Source: ASCE (2005).
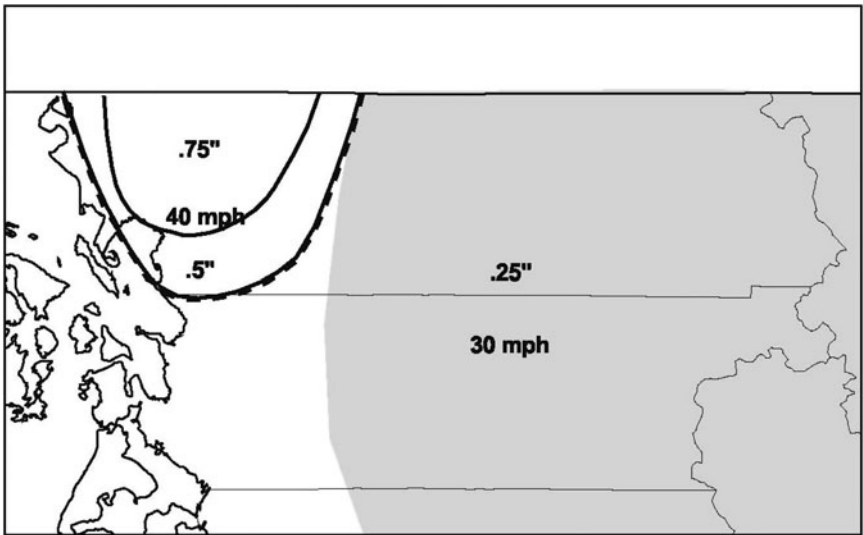
Figure 2-16. Extreme radial glaze ice thickness (in.), Fraser Valley detail; 50-year return period with concurrent 3-sec wind speed. Source: ASCE (2005).
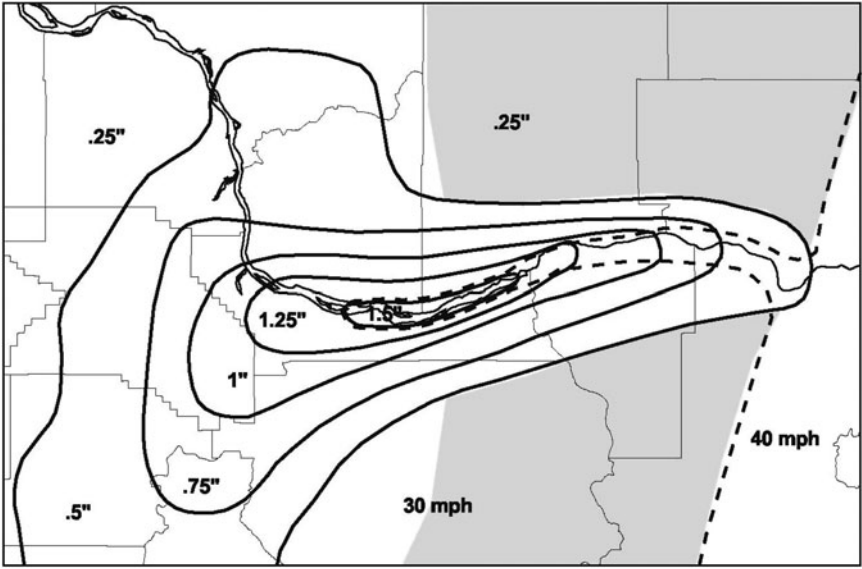
Figure 2-17. Extreme radial glaze ice thickness (in.), Columbia River Gorge detail; 50-year return period with concurrent 3-sec wind speed. Source: ASCE (2005).

Ice thickness zones ———
Gust speed zones – – –
Weather stations •

Note:
Ice thicknesses in exposed locations at elevations higher than the surrounding terrain and in valleys and gorges may exceed the mapped values
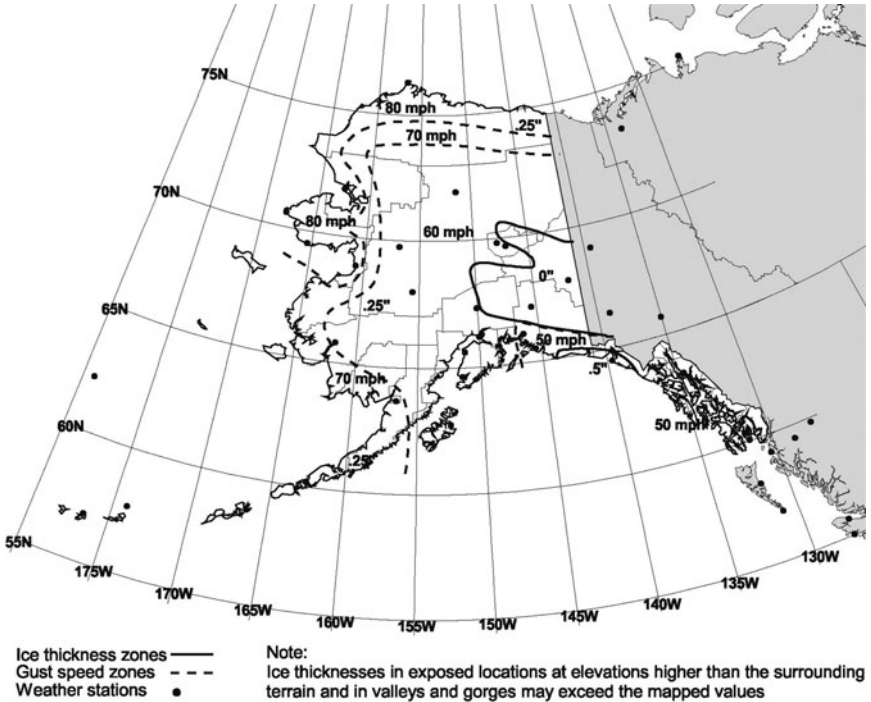
Figure 2-18. Extreme radial glaze ice thickness (in.), Alaska; 50-year return period with concurrent 3-sec wind speed. Source: ASCE (2005).

uniform radial thicknesses. Using a specific gravity of approximately 0.9 (57 lb/ft³) for glaze ice, the linear ice load on a wire is calculated from:

$$Wi = 1.24(d + I_z)I_z \qquad (2\text{-}16a)$$

where
Wi = weight of glaze ice (lb/ft)
d = bare diameter of wire (in.)
I_Z = design ice thickness (in.)

In SI units, use:

$$Wi = 0.0282(d + I_Z)I_Z \qquad (2\text{-}16b)$$

where
Wi = weight of glaze ice (N/m)
d = bare diameter of wire (mm)
I_Z = design ice thickness (mm)

Ice buildup on a wire can substantially increase its projected area. The transverse load due to wind pressure acting on ice-covered wires acts concurrently with the vertical load due to the weight of the ice. The 3-sec gust speeds provided in Figs. 2-13 through 2-18 should be used with I_z to compute the wind-on-ice load using the methodology presented in Section 2.1. When calculating forces due to wind on ice-covered wires, the force coefficient is dependent on the shape of ice buildup (McComber et al. 1982). However, typical force coefficients of ice-covered wires are not known. Some organizations recommend using force coefficients of from 1.0 to 1.4 for wires covered with glaze ice [IEC 2003; ISO Standard 12494 (ISO 1999)].

2.3.5 Ice Buildup on Structural Members

2.3.5.1 Vertical Loads.   Ice accretion on the structural members themselves is typically not included directly in the design. For the design of bracing members of latticed structures and crossarms, the construction and maintenance loads recommended in Chapter 3, Section 3.1 will generally impose design stresses greater than the bending stresses resulting from the vertical weight of ice-coated members. For vertical supports (e.g., pole shaft or leg angle), the additional axial load due to ice on the member does not add significantly to the member stress.

2.3.5.2 Concurrent Wind Loads.   Ice buildup on the structure may increase the projected area of the structure exposed to wind. For

broad-profile structural members (e.g., pole sections), the fractional increase in overall projected area due to ice is small. For angle members, the increased area may be partially offset by a reduction in the force coefficient due to the ice coating's streamlining effect on the relatively bluff angle member. Thus, for transmission line structures it is usually not necessary to design for the increase in the structure's projected area due to ice buildup on its members.

2.3.6 Unbalanced Ice Loading

Although the principal design loading combination is for the same ice thickness applied to all spans, unequal ice loading should also be considered in design. Ice thicknesses and concurrent wind speeds may differ from one span to the next, typically when the exposure of a transmission line changes as it goes over a hill or ridge. Generally, tangent structures with suspension insulator strings will not experience significant longitudinal conductor loads due to unbalanced ice loads; however, shield wire attachments with short hardware assemblies may transfer most of the imbalance to the structure. Refer to Section 3.3 and Appendix I of this manual.

This page intentionally left blank

CHAPTER 3

ADDITIONAL LOAD CONSIDERATIONS

3.0 INTRODUCTION

Transmission line design should consider loadings from many sources in addition to the more common weather-related events described in Chapter 2. This chapter on special loads addresses other loadings that transmission structures may encounter. The section is not all-inclusive; conditions requiring special investigation and design, such as landslides, ice flow, frost heave, flooding, and many other possible load-producing events, are not addressed.

3.1 CONSTRUCTION AND MAINTENANCE LOADS

3.1.1 General

Construction and maintenance (C&M) loads, unlike weather-related loads, are controllable to a large extent and are directly related to construction methods. Personnel safety should be a paramount factor when establishing C&M loads.

3.1.2 Construction Loads

Construction loads are those loads that act upon the structures due to the assembly and erection of the structures, and due to the installation of ground wires, insulators, conductors, and line hardware.

3.1.2.1 Structure Erection.   Special erection methods, such as lifting a structure, may produce critical loads in some structure members. Erection loads result from supporting the weight of the structure in a different manner from how the weight is supported on an in-service structure. These loads may be simple, such as lifting wood, concrete, or steel poles, or they may be significantly more complex, as in the case of truss actions developed by tilting up a ground-assembled latticed tower or from picking up large sections of a latticed tower for crane or helicopter erection.

During erection and maintenance, some structure members are loaded in flexure by the vertical weight of the workers. This loading should be treated as an independent vertical load equivalent to 250 lbs, the approximate weight of a lineman and tools, etc. used with minimum suggested load factor of 1.5 acting on horizontal or near-horizontal members.

3.1.2.2 Ground Wire and Conductor Installation.   Ground wires and conductors should be installed using IEEE Standard 524-03, "IEEE Guide to the Installation of Overhead Transmission Line Conductors" (IEEE 2003). Ground-wire and conductor installation loads can be in different directions, different locations, and larger magnitudes than those applied to the in-service transmission line. Examples of installation loads include:

1. At the ends of a wire pull, the wire passes over the stringing blocks and then downward to the pulling or tensioning equipment at ground level. A tension load is produced at the location where the stringing blocks are mounted to the structure. This tension load is predominantly vertical with a horizontal component that is a function of the angles made by the wire entering and leaving the stringing blocks, and the horizontal alignment of the tensioning equipment. A pulling line slope of three horizontal to one vertical is considered good practice.

   When long lengths of conductor are strung, the tension on the pulling end will exceed the tension at the opposite end of the conductor by a significant amount. This increase in tension is caused by differences in elevation of supporting structures, number of travelers, efficiency of travelers, and length of conductor.

2. Wires may be transferred from tensioning equipment to temporary anchors so that additional wires may be pulled in the same spans; consequently, there may be several loads acting simultaneously on a structure. As stringing progresses, it may be desirable or necessary to transfer wire tensions from the tensioning equipment or temporary anchors to the structure. These wire installation loads can be

calculated on the basis of stringing tensions and prescribed limits of stringing equipment locations. An example of these calculations can be found in IEEE Standard 524-03.

3. Guys may be used to make temporary dead-end connections to self-supporting suspension structures or to crossarm support points. These guys increase vertical loads on the structures. The guys and structures should be analyzed to ensure design capacities are not exceeded.

4. For lines designed for no ice or very little ice, the maximum loads on some structures and components may be reached during stringing or sagging-in operations. The "initial" wire tensions will increase when pulling up a slope. The tension in the wire will increase by the unit weight times the elevation change, while the wire is in the sheaves and before clipping-in and offsets are applied. This can severely increase the vertical load on the uphill structures.

5. The sagging-in process usually requires an iterative process of over-tensioning and then backing off in order to pull up the spans at the far end of the pull. This can cause a problem in hilly terrain or when pulling through angle structures.

6. During tension-stringing operations, the running board may sometimes jam in the block; structures have been pulled over when there was inadequate control to quickly stop the pull. Although a few utilities have designed suspension structures to resist such possible loads, a more practical solution is to control the stringing operation in accordance with IEEE Standard 524-03.

3.1.2.3 Recommended Minimum Loads for Installing Ground Wires and Conductors.

1. For transverse and vertical loads, use a 3-psf (0.144-kPa) wind (35 mph, 15.6 m/s) and no ice on the wires and structure. Use the lowest temperature that can be expected to occur during stringing operations.

2. For transverse wind loads, use the maximum design wind span with a load factor of 1.5.

3. For transverse and longitudinal components of wire tension, use tensions based on initial wire conditions at the lowest temperature that can be expected to occur during stringing operations with a load factor of 1.5.

4. For vertical loads, use the higher of the following conditions:
   a. For dead-end conditions with pulling or tensioning equipment at ground level, use the vertical component of the pulling line,

     the maximum single vertical span, and a load factor of 1.5. If the pulling line slope is not known, use a 3/1 ratio (horizontal/vertical).
  b. For intact conditions (ahead and back spans are attached to the structure), use the maximum design low-point distance and a load factor of 2.0.

3.1.3 Maintenance Loads

Maintenance loads are those loads that act on the structures as a result of scheduled or emergency inspection and/or replacement of all or part of a structure or all or part of the ground wire, insulator, conductor, and conductor hardware system. An appropriate load factor should be applied when designing for maintenance loads. Structure maintenance loads consist of the effects of workers on the structure and of load effects on adjacent structures due to temporary modifications, such as guying, to permit the repair or replacement of the structure being maintained.

The most common maintenance performed on a transmission line includes adjusting or replacing ground wires, conductors, insulators, and hardware. At times it is necessary to remove the wires from their supports and either lower them to the ground or transfer them to a temporary structure or some temporary alternate location on the structure being maintained. Unless care is taken, these operations can greatly magnify the ordinary loading imposed on the structures.

An engineer should review maintenance operations that involve lowering wires at one or more structures. With level spans, the lowering of wires to the ground at one structure will cause an increase in tension in the wires that would almost double the original value unless there was longitudinal movement or insulator swing inward at the adjacent structures. This very simple maintenance operation can impose dangerous combined vertical and longitudinal loads on the adjacent structures in some conditions.

3.2 FALL PROTECTION LOADS

Fall protection loads are created when workers are attached to an anchorage and they fall from an elevated position. An anchorage is a secure point of attachment for a fall protection system. The fall protection system should meet all Occupational Safety & Health Administration (OSHA) and other government requirements as applicable. The "IEEE Standard for Fall Protection for Utility Work" [IEEE Standard 1307-04 (IEEE 2004)] provides guidance regarding loads and criteria for anchorages and step bolts.

The number and location of anchorages, number of workers attached at each anchorage, maximum expected arresting forces, equipment attached to anchorages, and type of climbing devices should be coordinated with operation and maintenance personnel.

3.3 LONGITUDINAL LOADS

Line structures may be required to resist longitudinal loads. Longitudinal loads resulting from inequalities of wind and/or ice on adjacent spans must be resisted to prevent a failure or line outage. Longitudinal loading resulting from wire breakage, insulator failure, or structural and component failure should be considered in the structure design to avoid a cascading failure of the transmission line. Additional information on the causes, effects, and mitigation of longitudinal loading is given in Appendix I.

3.3.1 Longitudinal Loads on Intact Systems

Transmission structures must be able to resist the longitudinal imbalances produced by different wind or ice loadings on adjacent spans or from temperature extremes on unequal spans. One such example is longitudinal imbalances resulting from unequal in-cloud ice deposits on adjacent spans. The imbalance is caused by the different wire exposures to the wind-driven clouds.

Unequal wire tensions must be resisted at each structure at which the attachment is not flexible. Attachment points on strain structures or ground-wire points on suspension structures are generally considered rigid. The flexibility of a typical conductor suspension assembly on a tangent structure will reduce the loading imbalances.

3.3.2 Longitudinal Loads and Failure Containment

Longitudinal loading events include all occurrences where breakage of conductors, insulators, hardware, and structural components can create severe load imbalances in the wire system capable of causing the partial or complete failure of the adjacent supports. Catastrophic transmission line failures occur whenever a multitude of support structures fail longitudinally or transversely along a line. These cascading failures of transmission lines cause significant damage and high economic losses because they may destroy complete sections of a line, requiring weeks or months of repair (EPRI 1997). The cascading failure risk of a transmission line can be reduced by several methods. The method selected is governed primarily by the characteristics of the line, the nature of the wire system, and the

design of the structures. These cascading failure mitigation methods are sometimes referred to as "security requirements."

Solutions to minimize cascading do not come easily but, at a minimum, designers of new lines should be aware of the mechanism by which a simple single structure failure can be transformed into an unexpected cascade. The awareness of the way in which the structures can fail can help when examining the damage after a high-intensity wind (HIW) strike; can permit a rapid evaluation of what happened and where; and also can indicate what might be done to reduce the possibility of another cascade.

One of the more important additions to a basic line design philosophy would be awareness of the significant contribution to the problem of cascading and longitudinal loading that can be made by the ground-wire system, especially when it is assessed against the overall conductor system. The overall characteristics of the conductor and ground-wire systems should be evaluated with considerations for cascading and failure containment. Line segments with limited amount of slack and slack transfer, or small longitudinal strength, may contribute to cascade failures.

3.3.2.1 Design All Structures for Longitudinal Loads. Figure 3-1 provides residual static load (RSL) factors as a function of the span/sag ratio and the span/insulator ratio (S/I). A wire tension multiplied by the RSL longitudinal load factors predicts the final residual static tension in the wire after all dynamic effects from the wire break have vanished. The calculation assumes rigid supports (i.e., the potential benefiting effects of the flexibility of the supports are neglected) and 10 equal length spans between the wire break and the next dead-end. The span/insulator ratio is the ratio of the average span length within a given tension section to the average effective insulator length (i.e., the insulator length free to swing longitudinally). The RSL longitudinal load factor for a ground wire equals 1.0.

It should be noted that the RSL longitudinal load factors suggested in Fig. 3-1 constitute the minimum required "static" loads to be resisted by the structures to avoid failure (i.e., the factors do not consider dynamic effects).

The calculated unbalanced longitudinal loads act on the support structure in the direction away from the initiating failure event, and should be considered to act concurrently with the effects of any permanently applied load imbalance. For a single-circuit line, unbalanced longitudinal loads should be applied to any single conductor phase or at any one ground-wire support. For a double-circuit line, unbalanced longitudinal loads should be applied to any two conductor phases, one or two ground-wire supports, or one conductor phase and ground-wire support.
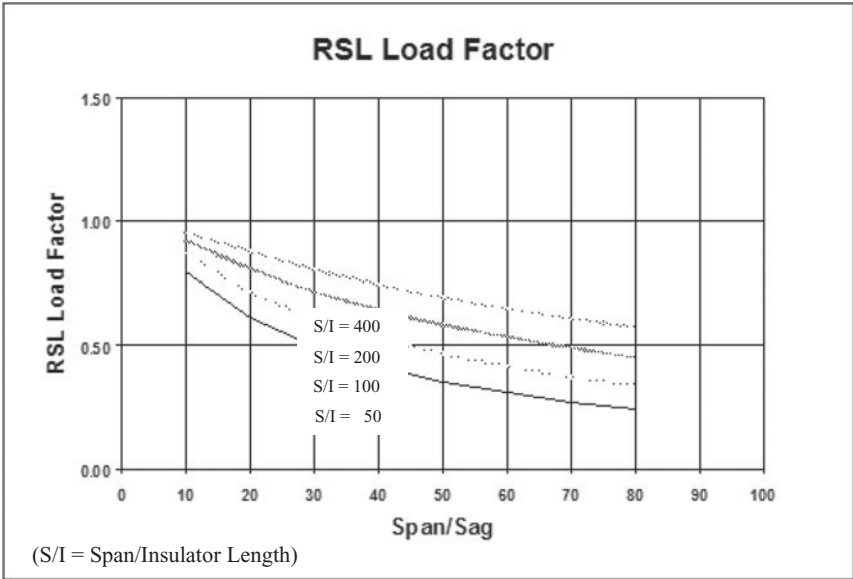
Figure 3-1. RSL load factor.

Rigid square-based latticed towers, longitudinally guyed V, Y, delta, or portal structures, and single pole supports are capable of resisting longitudinal loads and providing failure containment at a relatively low cost. Thus, it is common practice to specify longitudinal design loads that will provide a sufficient strength to resist cascading at every structure. Although all the structures are designed to resist cascading, the limited loss of structures adjacent to the origin of the failure can be anticipated.

Frequently, it is not economical for a utility to design or maintain a transmission line in a manner that provides sufficient strength to withstand the high dynamic loads at each structure. A successful and economic line design requires that the failure of a limited number of structures is acceptable if the overall system is protected from cascading. The acceptable number of structural failures should be determined based on the utility's design philosophy and targeted reliability levels. Lacking any more detailed analysis using one of the methods described in Appendix I, either Fig. 3-1 or 3-2 may be used to estimate the unbalanced longitudinal load.

Figure 3-2 provides longitudinal load factors as a function of the span/sag ratio and the stiffness of the support structures. This method was developed from the research works completed by the Electric Power Research Institute (EPRI 1997). Wire tensions multiplied by the
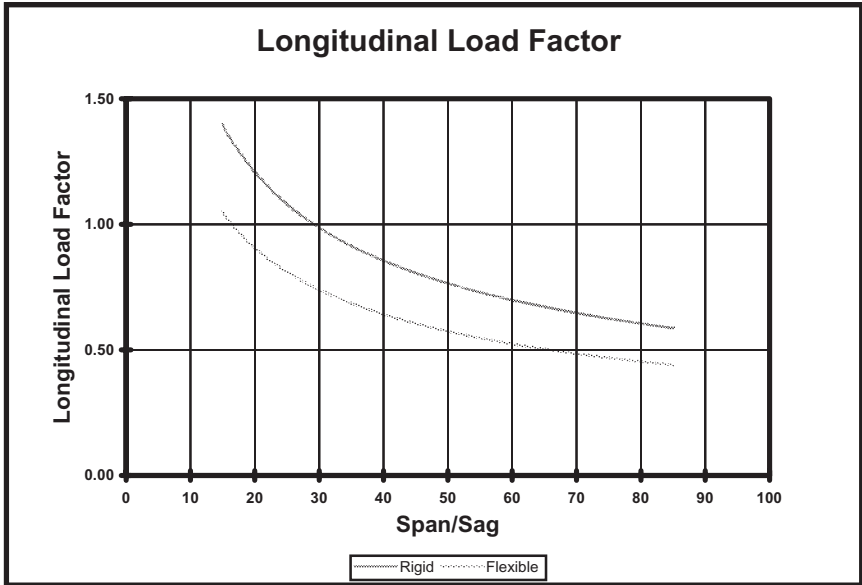
Figure 3-2. Longitudinal load factor.

longitudinal load factors provide approximate design loads that include dynamic effects, structural stiffness, and insulator lengths. The span/sag ratio is the ratio of the average span length within a given tension section to the sag of the average span for a given conductor or ground-wire tension. Longitudinal load factors are provided for "rigid" structures such as guyed or latticed structures of great stiffness, as well as for "flexible" structures such as single poles capable of enduring large elastic deformations.

It should be noted that the longitudinal load factors suggested in Fig. 3-2 are based on the assumption that the loss of one or two structures in each direction from the initiating event is acceptable to avoid a cascading failure. Therefore, the factors suggested are assumed to provide a balance between simplicity, economy, and reliability.

One other method developed by the Bonneville Power Administration (BPA) is described in Appendix I, Section I.3.3.

3.3.2.2 Install Failure Containment Structures at Specified Intervals.   H-frames and narrow-based, rectangular, latticed structures have little inherent ability to withstand the longitudinal loads of a cascading line. Additionally, the ground wires attached to these structures with near-rigid attachments may contribute to or initiate a cascade. It is

considered prudent design practice to employ methods to limit the length of a cascade, especially for existing lines with limited longitudinal strength. Generally, the cost of strengthening such structures to resist cascading at each support is likely to be prohibitive, and the addition of longitudinal guys might be undesirable or ineffective. Another option would be to insert failure containment structures (e.g., stop structures, anchor structures, anti-cascading structures) at prescribed intervals along the line to limit the extent of the damage caused by a component, structure, or foundation failure. Although there is no hard and fast rule for the interval between failure containment structures, intervals up to 10 miles are common. These intervals are based upon judgment considering length and importance of the line, longitudinal strength of the existing structures, terrain, land use, restoration time, emergency stocking levels, cost, and right-of-way access.

3.3.2.3 Install Release Mechanisms. Protection from cascading has been achieved with evident success by using slip- or release-type suspension clamps that limit the extreme event longitudinal loads that can be transferred to the structures. It is imperative that the design of the slip or release mechanism ensures consistent performance under any climatic and operational conditions throughout the expected service life of the transmission line. The performance of release mechanisms should be calibrated and verified in representative tests. Some release mechanisms may not be suitable to be used in areas where heavy ice buildups are frequent. A premature release of the device under unbalanced ice could result in a dangerous and undetected clearance to ground that may constitute a danger to the public.

3.4 STRUCTURE VIBRATION

Transmission line structures can be subjected to dynamic forces caused by the wind, conductor motions, and earthquakes. These forces have the potential to initiate complete structure or individual member vibration. Industry experience has demonstrated that structure and member vibrations generally do not occur or have not caused design problems, and only isolated occurrences have been reported.

The majority of reported problems have been with wind-induced vibration of individual members. These events have occurred on both tubular and structural shapes (such as single or double angles) and members with re-entrant cuts. The result of this type of vibration can cause (1) fatigue failure of the member or connection bolts, or (2) loosening of bolted connections. Design and detailing practices have been used to minimize individual member vibration. Tubular arms, before wires are

attached, may be susceptible to vibration. One solution to this potential problem is to temporarily suspend a weight at the end of the arm. Additional information on structure vibration is given in Appendix E.

3.5 CONDUCTOR GALLOPING

Galloping (the large-amplitude motion or dancing of wires) is a dynamic condition that occasionally occurs on transmission line ground wires and phase conductors with moderate winds blowing across ice-coated wires. Galloping is random in nature because only one or several of many phases and spans may be involved. The largely vertical amplitudes sometimes reach as much or more than the sags, although most common cases of galloping are less than a meter (Den Hartog 1932; Davison et al. 1961; EPRI 1979; Havard and Pohlman 1980; Rawlins 1981).

Galloping might cause electrical and structural/mechanical problems such as:

1. Flashovers or clashings of wires that lead to temporary or permanent outages due to the reduction of spacing between phases or a phase and a ground wire (Farr 1980; REA 1980).
2. Permanent additional conductor and ground wire sags caused by dynamic wire tensions in the inelastic range (Anjo et al. 1974; Richardson 1986).
3. Excessive wear, fatiguing, and failure of ground wires, conductors, and associated hardware and insulators of the suspension and dead-end assemblies (EPRI 1979).
4. The collapse of structural components and systems (Baenziger et al. 1993a, 1993b; White 1979).

Mitigation of galloping is the most desirable option. Some measures include detuning pendulums, interphase spacers, air flow spoilers, and modified conductor designs. These and other alternative measures and devices have been evaluated in field investigations (EPRI 1979; Havard and Pohlman 1980; Havard et al. 1982; Nigol and Havard 1978; Pohlman and Rawlins 1979; Whapam 1982). Experiences indicate varying degrees of success.

Although increasing the vertical and horizontal spacing between wires may eliminate flashovers or clashing, it will not eliminate the potential of the other problems associated with galloping. The galloping wires can produce large vertical and longitudinal loads at supports. Theoretical studies indicate that tensions at dead-ends can vary by ±60% and the vertical loads at support points by ±30%, the magnitudes depending on many factors (Brokenshire 1979; Gibbon 1984; Richardson 1986).

Measurements on actual galloping lines have found tension changes at dead-ends, cycling between 80% to 140% of the static tension (Anjo et al. 1974). When the wires are heavily coated with ice, these loads can cause tower failure. In the case of guyed masts, galloping movement can find a resonance and thus produce amplified motions that can destroy structural elements such as the ground wires masts or towers (White 1979). The cycling of vertical loads at support points, which were measured by Anjo et al. to be of the same magnitude as the tension changes, may not be visibly evident if the support point is rigid. The pounding over time can destroy hardware and insulators. At running angle suspension points, the vertical load fluctuations will be more evident and the vertical forces can result in violent beats and can create coupling effects on the adjacent spans. The load cycling has destroyed running angle suspension assemblies and the top parts of masts.

3.6 EARTHQUAKE LOAD

Transmission structures need not be designed for ground-induced vibrations caused by earthquake motion because, historically, transmission structures have performed well under earthquake events, and transmission structure loadings caused by wind/ice combinations and broken wire forces exceed earthquake loads. This may not be the case if the transmission structure is partially erected or if the foundations fail due to earth fracture or liquefaction.

Transmission structures are designed to resist large, horizontal loads of wind blowing on the wires and structures. These loads and the resulting strengths provide ample resistance to the largely transverse motions of the majority of earthquakes. Decades of experience with lines of all sizes has shown that very infrequent line damages have resulted from soil liquefaction or when earth failures affect the structural capacity of the foundation.

This page intentionally left blank

CHAPTER 4

WIRE SYSTEM

4.0 INTRODUCTION

This is a loading document; it is therefore necessary to understand the tension in the wire systems and the loads they impose on the support systems. The tensions change with temperature, time (creep), and under all the conditions of ice and/or wind, as well as the conditions imposed by construction and maintenance (C&M) operations.

The wire tensions must also be contained within limits to ensure the viability and survival of the wires themselves and the other components of the wire systems. The tensions also directly affect the loads applied to the strain and dead-end structures, and the transverse loads at all line angles; they also contribute to the vertical loads at all structures that sustain a vertical angle—those being above or below the level of adjacent structures. See Appendix A for the definitions of structure types.

Loads per unit length of conductor or ground wire have been discussed in Chapter 2. This chapter discusses the manner in which the wire systems respond to these unit wire loads, and some of the assumptions that may be used for determining the loads at the structure attachment points.

4.1 TENSION SECTION

If the supporting structure is a tangent structure (no line angle, $HA = 0$) and if the supporting points at the ends of the adjacent spans are at the same elevation (no vertical angle, $VA = 0$), then the loads at the attachment points in an intact line under everyday conditions do not depend on wire tensions. However, at any line angle (horizontal angle) or in any situation
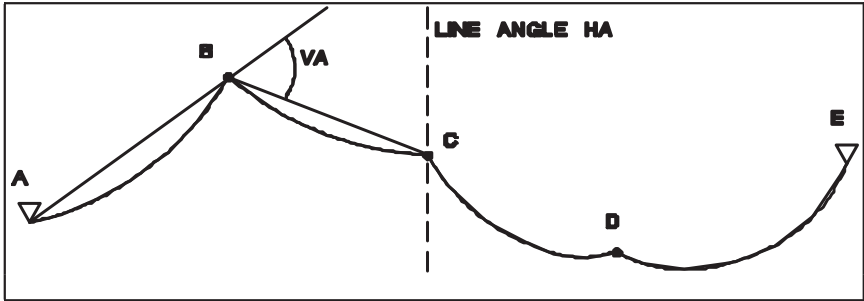
Figure 4-1. Profile of tension section.

where there is a vertical angle, the structure loads depend on wire tensions. Wire tensions depend on the factored unit loads, their initial sagging tensions, and also their loading history.

The wire system is normally broken down into tension sections. A tension section is a portion of conductor or ground wire strung between dead-end points, such as points A and E in Fig. 4-1. Intermediate wire attachment points between the dead-end points, such as points B, C, and D, are assumed to have some longitudinal flexibility as they attempt to equalize the horizontal components of tension in the various spans for various loading events. If points B, C, or D are at the lower ends of long suspension insulators, they have high longitudinal flexibilities. If they are located at the tips of post insulators, they may have less flexibility. If they represent ground-wire attachment clamps, they may have very little flexibility. In Fig. 4-1, points B and D are located at tangent structures and point C is located at a line angle. If the structures that support the wire at points B, C, and D are themselves very flexible, such as poles or H-frames, there is some coupling between the longitudinal displacements of B, C, and D with those of similar attachment points of other conductors or ground wires connected to the same structure.

The following sections discuss the different levels of approximation available to the designer to determine the loads imposed by the wire subsystem on the structures.

4.2 WIRE CONDITION

Wires, especially conductors, are subject to permanent elongations throughout their lifetime in service. They are in their "initial" condition if they are new wires and within a few hours of being sagged at construction time. The wires are in their "final after creep" condition if they have been in a line for several years and have permanently elongated under the relatively low, but ongoing, everyday tensions. The creep process

slows down exponentially with time, and estimates of future creep are usually based on a 10-year period. Therefore, the wire will spend most of its life at a condition very close to "final after creep" because the majority of the creep elongation occurs in the initial one or two years following the conductor installation. Although creep is almost certain to occur in conductors that contain aluminum, its magnitude is very much an estimate.

The wires are in their "final after load" condition if they have been permanently elongated by a high, but short-lived, tension due to a heavy load, generally an extreme load from ice, wind, or a combination of both. Examples of such extreme loads are the return period (RP_N) loads described in Chapters 1 and 2 of this document. Permanent elongation from heavy load can be determined more precisely than that from creep if the magnitude of the load is known. However, the heavy load magnitude is an arbitrary design assumption. Therefore, the resulting permanent elongation is also very much an estimate because that elongation may never occur.

In real cases, the total permanent elongation of the conductor (the impact of both creep and load elongations) will depend on the time loading history of the conductors. For example, if a severe weather load occurs very early in the life of the line, the permanent load elongation will cause the everyday conductor tension to drop and will subsequently reduce the creep rate. To overcome this difficulty, it has been an accepted practice in the industry to disassociate creep and load permanent elongation and assume them to be independent and not additive.

Compared to their initial values, everyday tensions are lower for "final after creep" and "final after load" conditions because the wires have developed some permanent elongations. Therefore, the calculation of wire tensions may be affected by the wire condition. A situation where a "final after creep" tension is lower than the corresponding "final after load" tension is sometimes referred to as a situation where "creep is a factor" or "creep controls."

Clearance calculations should be based on "final after creep" and "final after load" conditions, but the calculation of design structure loads is normally based on the "initial" condition. Structure loads computed with the "final after creep" condition may be used, even though there is a small probability they will be exceeded during the early life of the line. Structure loads should not be calculated with the "final after load" condition because such calculations are only valid if the heavy load causing the "final after load" condition has actually occurred.

4.3 WIRE TENSION LIMITS

Wires are normally sagged to perform within certain design limits. Limits on everyday tensions or everyday catenary constants (horizontal component of tension divided by unit weight) under initial and/or final

conditions are normally given to avoid or minimize the potential for wind vibration damage.

For example, in the United States, at 60°F (15°C) the National Electrical Safety Code (NESC) specifies a maximum initial unloaded tension of 35% of rated tension strength (RTS) and a maximum final unloaded tension of 25% of RTS. Many utilities specify stricter limits that may be based on experience or recommended by conductor manufacturers. It is important to understand that the everyday condition at which a limit is set should be "final after creep," not "final after load." Putting the limit on "final after creep" will result in the wire spending most of its life close to or below that limit, thus limiting vibration problems. If "creep does not control," putting the limit only on "final after load" may result in a wire enduring high tension all of its life or until the hypothetical heavy load occurs. This can cause unforeseen vibration problems.

Other limits are also specified under heavy loads to avoid significant permanent conductor stretching and to provide a safety margin against breakage. For its District Load Case, the NESC limits conductor tensions to 60% of RTS, but some conductor manufacturers recommend that the tension be limited to 50% of the rated RTS. However, it is unlikely that this NESC limit will be reached except on very small, distribution-size conductors if the usual limits for wind vibration control are used.

When the extreme RP_{50} (or RP_{100}, etc.) loads finally occur on the wire systems, all the components in series within these systems are highly stressed and need to have adequate remaining strength. Therefore, it is recommended that the maximum tensions caused by the fully factored loads from wind, ice, or combined wind and ice described in this manual never exceed 70% to 80% of the RTS. Conductors (especially the smaller ground wires) and the other components of the wire subsystem can deteriorate with time due to many causes. Lightning strikes can burn one or two strands of a three- or seven-strand ground wire, and fatigue caused by wire motions (aeolian vibration, subspan oscillations, or galloping) over many years, as well as corrosion of steel strands, will also reduce strength of the wire. It is critically important to protect the integrity of the wire system because a failure of the wire system under extreme loads can impose cascading-type loads on the structure system which otherwise would survive the extreme event.

4.4 CALCULATED WIRE TENSION

4.4.1 The Ruling Span Method

Assuming that the horizontal components of tension, H, in all the spans of a tension section are the same and the spans are in relatively flat terrain, then the entire tension section can be replaced by a single equivalent or

"ruling" span to calculate H (Thayer 1924). For high-temperature clearance calculations, H is determined by subjecting the ruling span to that high temperature. For load calculations, H is determined by subjecting the ruling span to the extreme RP_N loads or the fully factored unit loads (i.e., the load and ice thickness factors from Tables 1-1 and 1-2 in Chapter 1) must be applied to the unit loads prior to applying them to the ruling span.

The ruling span method implies that the same unit load is applied on all the spans of the tension section and that the intermediate support points have sufficient longitudinal flexibility. The ruling span is an approximation that has limits of validity (IEEE 1999) and can be computed as follows:

$$Ruling\ Span = \sqrt{\frac{S_1^3 + S_2^3 + S_3^3 + \ldots + S_n^3}{S_1 + S_2 + S_3 + \ldots + S_n}} \qquad (4\text{-}1)$$

where S_1, S_2, S_3, $\ldots S_n$, = the individual span lengths (horizontal projections) between dead-end or strain structures.

When correctly applied, the ruling span method (Eq. 4-1) enables the stringing and sagging-in of a line section (i.e., between dead-ends) of unequal spans in flat or hilly terrain so that the horizontal tensions in each span will be equal as designed. It is assumed that the wires are suspended by insulator assemblies that are free for limited swing along the line. The ruling span method is currently the only method of spotting, stringing, and sagging-in wire on a line section of unequal spans or uneven spans.

The ruling span method may not be accurate for conductor spans supported by rigid post insulators and for ground wires supported by rigid clamps. It may also not be accurate if suspension insulators are not sufficiently free to move in the longitudinal direction, for example, with short insulators (low voltage lines or short ground-wire suspension links) and at support points with substantial horizontal and vertical line angles. In such cases, the structural analysis options described in the next subsections are more appropriate. An alternative (but conservative) option to the structural analysis options is to assume all support points to be fixed, and to determine whether the post insulators or the clamp and the supporting structures can accommodate the resulting unbalanced longitudinal loads.

The ruling span method is not applicable to the calculation of unbalanced longitudinal loads caused by uneven ice on adjacent spans or other span-specific disturbances.

4.4.2 Structural Analysis of a Single Tension Section

If there is no significant interaction between parallel conductors or ground wires caused by the longitudinal displacement of their supporting

structures, then the tensions in the various spans of a tension section can be determined by modeling the entire section as a cable system with appropriate support conditions. Suspension supports can be modeled as cable elements or swinging rods. Post insulators can be modeled as small, cantilevered beams or longitudinal springs with appropriate longitudinal flexibilities. The model is then analyzed by accepted structural analysis methods that account for the longitudinal displacements of the wire attachment points.

This type of analysis is capable of handling unbalanced ice loads and will produce more accurate tension results than the ruling span method.

4.4.3 Structural Analysis of an Entire Line between Dead-Ends

If there is significant interaction between the conductors and ground wires in a line segment between two dead-end structures, then analyzing that segment as a single structural system, which includes all the wires in all the spans as well as detailed structural models of all supports, can be done. This rigorous approach produces a much more accurate analysis but, because of its complexity, is normally only justified in special situations.

4.5 LOADS AT WIRE ATTACHMENT POINTS

4.5.1 Using Wind and Weight Spans

At tangent locations, such as points B and D in Fig. 4-1, the transverse and vertical structure loads, L_T and L_V, can be determined as:

$$L_T = \text{Factored unit transverse wire load} \times \text{wind span} \qquad (4\text{-}2)$$

$$L_V = \text{Factored unit vertical wire load} \times \text{weight span} \qquad (4\text{-}3)$$

where the wind span represents the length of wire between mid-span points in the adjacent spans and the weight span is the length of wire between the low points in the adjacent spans. Wind span is normally calculated as one-half of the sum of the horizontal projections of the adjacent spans.

At line angle locations, such as point C in Fig. 4-1, the horizontal components of tensions in the adjacent spans cause an additional transverse pull. This additional transverse pull should be added to the transverse load in Eq. 4-2. This additional transverse pull is calculated as:

$$L_{T\text{-Angle}} = 2 \times T_H \, (\sin 0.5 HA) \qquad (4\text{-}4)$$

where
T_H = horizontal component of tension
HA = horizontal line angle

Calculating the weight span for a particular wire loading requires determining the equilibrium configuration of the wire for that loading. For example, the curves shown in Fig. 4-1 are elevation views of the wire in the spans for a particular loading.

The weight span is normally calculated as the horizontal distance between the low points in the adjacent spans. This is a good approximation for relatively flat terrain. However, in hilly terrain where the slope of the conductor may be significant, the weight spans to use in Eq. 4-3 should be substituted with the calculated actual length of wire between the low points.

A good approximation of the vertical load, L_V, can also be obtained by:

$$L_V = \text{Factored unit vertical wire load} \times \\ \text{wind span} + T_H \times 2 \times \tan[0.5VA] \tag{4-5}$$

where
VA = vertical line angle

4.5.1.1 Weight Span Change with Blow-Out on Inclined Spans. Extreme transverse winds on inclined spans can result in large blow-outs. This can produce changes to the weight spans at the supports. The location of the low point of the sag (or projected low point) can shift dramatically in the span. When slopes exceed 20%, the weight span at the upper support point can approach double that calculated by normal methods (which ignore the blow-out), and may even exceed the C&M loads, factored with the load factor of 2. Furthermore, the reduction of weight at the lower point may lead to excessive swing of the insulator strings and the possibility of flashover to the structure; also, the net vertical force may be an uplift that can collapse the crossarm. Some line design computer programs include calculation of the shift of weight spans with blow-out of inclined spans. As an alternative, the following manual method can be used to verify whether a problem exists. Two formulas are presented to locate the low point of a span: (1) the more precise Catenary Equation, and (2) a simpler but approximate Parabolic Equation. It must be noted that the Parabolic Equation should not be used if the difference in support elevation (B) is greater than approximately 20% of the span length (S).

Parabolic Formula. The position of the Low Point of Sag, X_1, on a parabolic curve is given by the following formula:

$$X_1 = \frac{S}{2 \times Midspan\ Sag} \times \left(Midspan\ Sag - \frac{B}{4} \right)$$

$$Midspan\ Sag = \frac{S \times D}{8 \times C} \qquad\qquad (4\text{-}6)$$

$$D = \sqrt{S^2 + B^2}$$

Catenary Formula. The position of the Low Point of Sag, X_1, on a cate-nary curve is given by the following formula:

$$X_1 = \frac{S}{2} - C \times \sinh^{-1} \left(\frac{\dfrac{B}{2}}{C \times \sinh\left(\dfrac{S}{2 \times C}\right)} \right) \qquad\qquad (4\text{-}7)$$

where
C = catenary constant or parameter of the catenary curve
S = span length
B = difference in elevation of supports
D = the straight-line distance between the supports
X_1 = distance from Low Point of Sag to lower support

Traditionally, the catenary constant, C, is calculated using the following:

$$C_{Traditional} = T_H / UR \qquad\qquad (4\text{-}8)$$

where
T_H = horizontal component of tension
UR = resultant unit wire load for this tension

Equations 4-6 and 4-7 give the correct answers when the conductor lies in the vertical plane, that is, when there is no transverse displacement (blow-out) of the wire due to wind. However, the resultant unit wire load (UR) is made up of vertical (UV) and transverse (UH, from wind) com-ponents. The orientation of this resultant is assumed to define the plane in which the wire lies in the blown-out state. Therefore, that plane is inclined by an angle of [$\tan^{-1}(UH\ /\ UV)$] from vertical. This potentially large angle causes the Low Point of Sag along the wire to move. In such a case, the horizontal distance, X_1, can still be determined by Eq. 4-6 or 4-7, as long as the traditional catenary constant of Eq. 4-8 is replaced by the following:

$$C_{Vertical} = T_H / UV \qquad\qquad (4\text{-}9)$$

If the span inclination exceeds about 25% and extreme winds are to be expected, more precise calculations may be considered, or else conservative vertical load values may be applied to the structures at the upper and lower support points. These calculations can be made analytically (Keselman and Motlis 1996, 1998) or with a finite element computer program (Peyrot 1985) by breaking the spans into short cable elements, each element responding automatically to a different local wind incidence. It is important to note that the analysis of this severe blow-out problem is very dependent on the horizontal angle at which the wind strikes the span, and on the vertical angle of approach of the wind. Both of these angles are likely to vary considerably and randomly in the rough or mountainous terrain where steeply inclined spans are to be found. Deviations from the orthogonal can greatly increase these distortions of the wire systems and increase or decrease the expected weight span changes. Thus, if a serious blow-out problem is anticipated, there is even greater justification for a conservative approach to the strengths of the upper and lower structures.

The weight span at structures that are higher than adjacent structures increases with lower temperatures because the low points will move downhill, away from the upper structures. The opposite is true at structures that are lower than adjacent structures. Therefore, in no-ice areas the largest vertical load, which can occur at a higher structure, is generally caused by the coldest temperature or sometimes by wind blow-out. Similarly, the coldest temperature or the wind blow-out can cause uplift and insulator swing problems at lower structures.

In icing areas, the weight span under ice should be used to calculate the vertical load with Eq. 4-3. For higher towers, it will almost certainly be found that the iced weight span is substantially less than the cold bare-wire weight span.

Equations 4-2 and 4-3 can be used to determine design loads on a new family of structures intended to have transverse and vertical capabilities based on assumed maximum (allowable) wind and weight spans. When these structures are spotted, their ability to carry their design loads at a particular location is simply checked by verifying that the actual (as spotted) wind and weight spans are less than the allowable values. In icing areas, the fact that iced weight spans are generally lower than cold bare-weight spans can be used to advantage by specifying shorter allowable weight spans under ice than under bare cold.

The concept of allowable wind and weight spans is extremely useful when spotting new lines, especially with families of standardized structures. However, for the design of custom structures at specific locations, for the checking of existing lines, or for parametric studies for possible upgrading or re-conducting, there is no need to be concerned with approximations in the wind and weight spans approach if the loads are

computed by a structural analysis method that accounts for the actual three-dimensional behavior of the wire system.

4.6 EXTREME WIND ON WIRE SYSTEM

It can be argued that the same lack of spatial correlation of wind gusts over a long span, which results in decreasing gust response factors with increasing span length as shown in Figs. 2-4 through 2-6 in Chapter 2, should be considered when calculating the wind response of an entire tension section. For example, when calculating the transverse load at point C, it is very unlikely that the same wind will blow simultaneously on spans AB and DE. Therefore, the tensions in spans BC and CD will very likely be less than what would be caused by a 90-mph wind uniformly blowing on all four spans. However, due to the complexity of calculating tensions in the wire systems for nonuniform span wind loads, and due to the uncertainty inherent in predicting those wind loads, it is recommended that the same unit wind load be conservatively applied to all the spans in the tension section.

Wire tensions calculated for the extreme wind loading case should be based on the temperature most likely to occur at the time of the extreme wind events. For example, it could be computed as the average of the minimum daily temperatures for the strong wind season.

4.7 COMBINED WIND AND ICE ON WIRE SYSTEM

In most loading districts in North America, the ice and wind combinations specified in this manual will typically produce factored unit wire loads greater than the loads currently specified by the NESC (2007). Consequently, the combinations suggested by this manual may generate calculated wire tensions that substantially exceed those produced by the NESC loading cases. Therefore, these ice and wind combinations, and not the NESC loading, may be the wire loading that should be used to determine the "after load" condition of the wire system.

In calculating wire tensions due to the combined ice and wind loads, it is recommended that a conductor temperature of 15°F (–10°C) for ice loading events be selected unless such a low temperature is unlikely to happen in the area. Though ice accretion typically occurs at temperatures around freezing, the 15°F temperature will account for a possible cold front passing after the icing event.

CHAPTER 5
EXAMPLES

5.0 LATTICED SUSPENSION TOWER LOADS

This example shows calculations for wire and structure loads. The loads are based on the tower shown in Fig. 5-1, Tables 5-1 through 5-3, and the design and wire data listed below.

Design Data

The transmission line is located in Utah.

Relative reliability factor = 1
Ruling span = 1,250 ft
Wind span = 1,500 ft
Weight span = 1,800 ft
Line angle = 5 degrees
Length of insulator assembly = 6 ft
Weight of insulator assembly = 200 lbs
Weight of ground-wire assembly = 50 lbs
No topographic effects, $K_{zt} = 1.0$

Wind pressures for the *Wind* and *Wind @ 30* loading cases are a function of the span length. They are generated using the wind span instead of the ruling span. However, for calculations of sags and tensions, the use of the ruling span is more appropriate.
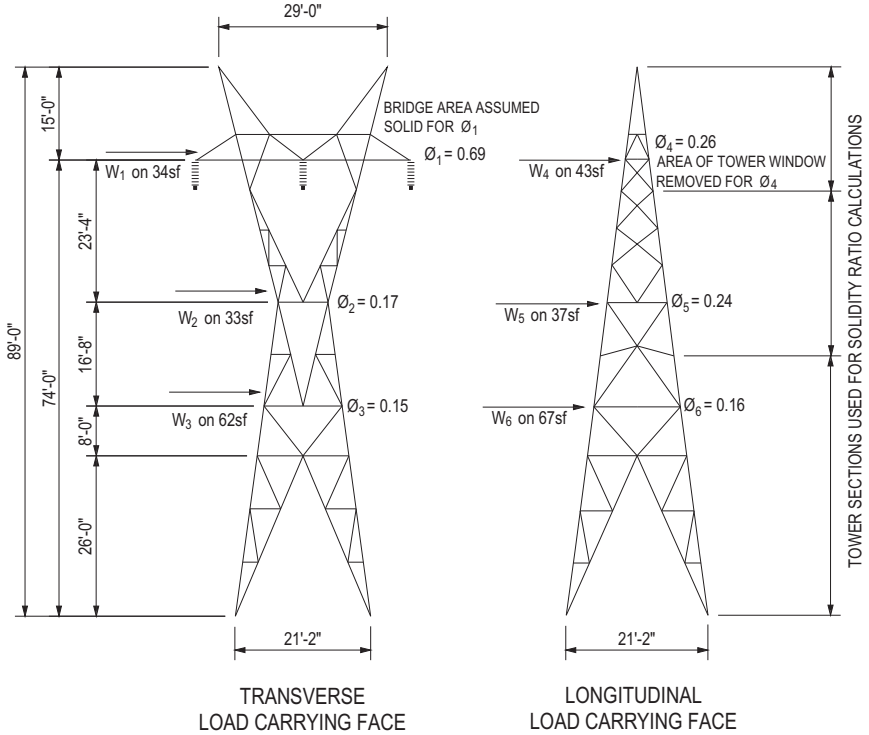
Figure 5-1. Suspension tower.

Extreme Wind (Chapter 2, Section 2.1)

Wind is normal to the ahead span, back span, and to the structure.
The structure is located on the perpendicular bisector of the line angle.
From the wind map (Fig. 1-1 in Chapter 1), V_{50} equals 90 mph. The exposure category is C.

Wind on Wires
Average wire height $(z_h) = [3(74) + 2(89)]/5$
$\qquad\qquad\qquad\qquad = 80$ ft $\qquad\qquad\qquad$ (Chapter 2, Section 2.1.4.3)
$K_z = 2.01(z_h/z_g)^{2/\alpha} = 2.01(80/900)^{2/9.5} = 1.21$ $\qquad$ (Eq. 2-3)
$E = 4.9(\kappa)^{1/2}(33/z_h)^{1/\alpha FM} = 4.9 (0.005)^{1/2}(33/80)^{1/7} = 0.305$ $\qquad$ (Eq. 2-6)
$B_w = 1/(1 + 0.8L/L_s) = 1/(1 + 0.8(1,500)/220) = 0.155$ $\qquad$ (Eq. 2-7)
$G_w = [1 + 2.7E(B_w)^{1/2}]/K_v^2$
$\qquad = [1 + 2.7(0.305)(0.155)^{1/2}]/1.43^2 = 0.648$ $\qquad\qquad$ (Eq. 2-4)
Wind pressure $= \gamma_w \, Q \, K_z \, K_{zt} \, (V_{50})^2 \, G_w C_f$
$\qquad\qquad\qquad = 1.0(0.00256)(1.21)(1.0)(90)^2(0.648)1.0$
$\qquad\qquad\qquad = 16.3$ psf $\qquad\qquad\qquad\qquad\qquad\qquad$ (Eq. 2-1a)

Table 5-1. Wire Data

Loading Case	Temp (°F)	Ice (in.)	Wind (psf)	954 kcmil 45/7 ACSR RAIL Conductor (d = 1.165 in., w = 1.075 lbs/ft)		7#8 Aluminum Clad Steel Ground Wire (d = 0.385 in., w = 0.262 lbs/ft)	
				Initial Sag (ft)	Initial Tension (lbs)	Initial Sag (ft)	Initial Tension (lbs)
Wind	60	0	16.3	43.7	8,598	39.0	2,939
Wind @ 30°	60	0	12.2	42.3	7,428	37.2	2,481
Wind and Ice	15	0.273	1.81	39.2	7,921	35.8	2,767
NESC	15	0.25	4	40.4	8,800	39.5	3,700
C&M	15	0	3	36.6	5,961	31.2	1,751
FC	30	0	0	37.5	5,615	31.6	1,623
No Wind	60	0	0	39.8	5,302	33.2	1,546

NESC, National Electrical Safety Code; C&M, construction & maintenance; FC, failure containment load.

Table 5-2. Load Summary[a]

Loading Case	Ground Wire			Conductor			Transverse Wind on Structure			Longitudinal Wind on Structure		
	V	T	L	V	T	L	W_1	W_2	W_3	W_4	W_5	W_6
Wind	0.5	1.0		2.1	3.1		1.3	2.2	4.3			
Wind @ 30°	0.5	0.8		2.1	2.4		1.1	1.9	3.7	1.2	1.1	2.3
Wind and Ice	0.9	0.5		3.0	1.1		0.1	0.2	0.5			
HIW @ 0 deg							3.9	6.7	13.0			
HIW @ 90 deg										7.5	6.7	13.8
HIW @ 45 deg							2.7	4.7	9.2	5.3	4.7	9.8
NESC	1.3	1.6		4.4	3.3		1.1	1.1	2.0			
C&M	1.3	0.5		4.7	1.4		0.3	0.5	0.9			
FC (Broken Wire)	0.3	0.1	1.6	1.2	0.2	3.9						
FC (Intact Wire)	0.5	0.1		2.2	0.5							

[a] All loads are in kips.
HIW, high-intensity wind; NESC, National Electrical Safety Code; C&M, construction & maintenance; FC, failure containment load.
See in-text definitions of V, T, and L.

Table 5-3. Weight Span Summary

		Upper Tower		Lower Tower	
Wire	C	Weight Span (ft)	Difference	Weight Span (ft)	Difference
Ground Wire	Traditional Chapter 5, Section 5.1	1,650 2,146	+23%	425 177	−140%
Conductor	Traditional Chapter 5, Section 5.1	1,608 1,888	+15%	446 306	−45%

C, catenary constant or parameter of the catenary curve.

Ground-Wire Loads
$V_l = 0.262(1,800) + 50 = 522$ lbs $= 0.5$ kips
$T = 16.3(0.385/12)(1,500) + 2,939 \sin(5/2)(2) = 1,041$ lbs $= 1.0$ kips

Conductor Loads
$V_l = 1.075(1,800) + 200 = 2,135$ lbs $= 2.1$ kips
$T = 16.3(1.165/12)(1,500) + 8,598 \sin(5/2)(2) = 3,124$ lbs $= 3.1$ kips

Wind on Structure
Two-thirds of the structure height $(z_h) = 2(89)/3$ (Chapter 2,
                                            $= 59.3$ ft   Section 2.1.4.3)
$K_z = 2.01(z_h/z_g)^{2/\alpha} = 2.01(59.3/900)^{2/9.5} = 1.13$ (Eq. 2-3)
$E = 4.9(\kappa)^{1/2}(33/z_h)^{1/\alpha FM} = 4.9 \, (0.005)^{1/2}(33/59.3)^{1/7} = 0.319$ (Eq. 2-6)
$B_t = 1/(1 + 0.56z_h/L_s) = 1/(1 + 0.56(59.3)/220) = 0.869$ (Eq. 2-7)
$G_t = [1 + 2.7E(B_t)^{1/2}]/K_v^2$
  $= [1 + 2.7(0.319)(0.869)^{1/2}]/1.43^2 = 0.882$ (Eq. 2-5)
Wind pressure $= \gamma_w \, Q \, K_z \, K_{zt} \, (V_{50})^2 \, G_t$
          $= 1.0(0.00256)(1.13)(1.0)(90)^2 \, 0.882 = 20.7$ psf   (Eq. 2-1a)

Figure 5-1 shows tower areas and solidity ratios.

Transverse Wind Loads
For $\Phi_1 = 0.69$, $C_{f1} = 1.8$, and $A_1 = 34$ ft^2
For $\Phi_2 = 0.17$, $C_{f2} = 4.1 - 5.2\Phi = 4.1 - 5.2(0.17) = 3.22$, and $A_2 = 33$ ft^2
For $\Phi_3 = 0.15$, $C_{f3} = 4.1 - 5.2\Phi = 4.1 - 5.2(0.15) = 3.32$, and $A_3 = 62$ ft^2

where force coefficient equations are from Table 2-4.
$W_1 = 20.7(1.8)(34) = 1,267$ lbs $= 1.3$ kips
$W_2 = 20.7(3.22)(33) = 2,200$ lbs $= 2.2$ kips
$W_3 = 20.7(3.32)(62) = 4,261$ lbs $= 4.3$ kips

Wind @30 (Extreme Wind @ 30-Degree Yaw Angle, Chapter 2, Section 2.1)

Wind is at a 30-degree yaw angle.

Wind on Wires
From the *Wind* load case, the wind pressure normal to the wires equals 16.3 psf.
Wind pressure = $16.3 \cos^2 \Psi = 16.3 \cos^2 (30) = 12.2$ psf   (Eq. 2-12)

Ground Wire Loads
$V_l = 0.262(1,800) + 50 = 522$ lbs $= 0.5$ kips
$T = 12.2(0.385/12)(1,500) + 2,481 \sin(5/2)(2) = 804$ lbs $= 0.8$ kips

Conductor Loads
$V_l = 1.075(1,800) + 200 = 2,135$ lbs $= 2.1$ kips
$T = 12.2(1.165/12)(1,500) + 7,428 \sin(5/2)(2) = 2,425$ lbs $= 2.4$ kips

Wind on Structure
From the *Wind* load case, the structure wind pressure equals 20.7 psf. Use the first alternative in Chapter 2, Section 2.1.6.2.3.

Transverse Wind Loads
Wind pressure = $20.7 \cos \Psi = 20.7 \cos(30) = 17.9$ psf   (Eq. 2-13a)
Force coefficients and areas are provided in the *Wind* loading case.
$W_1 = 17.9(1.8)(34) = 1,096$ lbs $= 1.1$ kips
$W_2 = 17.9(3.22)(33) = 1,902$ lbs $= 1.9$ kips
$W_3 = 17.9(3.32)(62) = 3,684$ lbs $= 3.7$ kips

Longitudinal Wind Loads
Wind pressure = $20.7 \sin \Psi = 20.7 \sin(30) = 10.4$ psf   (Eq. 2-13b)
For $\Phi_4 = 0.26$, $C_{f4} = 4.1 - 5.2\Phi = 4.1 - 5.2(0.26) = 2.75$, and $A_4 = 43$ ft^2
For $\Phi_5 = 0.24$, $C_{f5} = 4.1 - 5.2\Phi = 4.1 - 5.2(0.24) = 2.85$, and $A_5 = 37$ ft^2
For $\Phi_6 = 0.16$, $C_{f6} = 4.1 - 5.2\Phi = 4.1 - 5.2(0.16) = 3.27$, and $A_6 = 67$ ft^2

where force coefficient equations are from Table 2-4.
$W_4 = 10.4(2.75)(43) = 1,230$ lbs $= 1.2$ kips
$W_5 = 10.4(2.85)(37) = 1,097$ lbs $= 1.1$ kips
$W_6 = 10.4(3.27)(67) = 2,279$ lbs $= 2.3$ kips

where force coefficient equations are from Table 2-4.

Extreme Radial Glaze Ice with Wind, Chapter 2, Section 2.3

Wind on Wires
From the *Wind* load case, K_z equals 1.21 and G_w equals 0.648.
From the wind and ice map (Fig. 2-13), I_{50} equals 0.25 in. and V_I equals 30 mph.
Wind pressure $= Q\,K_z\,K_{zt}\,(V_I)^2\,G_w C_f$
$\quad\quad = 0.00256(1.21)(1.0)(30)^2(0.648)1.0 = 1.81$ psf $\quad\quad$ (Eq. 2-1a)
$I_z = I(z_h/33)^{0.10} = 0.25(80/33)^{0.10} = 0.273$ in. $\quad\quad$ (Eq. 2-15)

Ground-Wire Loads
$W_i = 1.24(d + I_z)I_z$
$\quad\quad = 1.24(0.385 + 0.273)0.273 = 0.223$ lbs/ft $\quad$ (Eq. 2-16)
$d_i = 2(0.273) + 0.385 = 0.931$ in.
$V_l = 1,800(0.262 + 0.223) + 50 = 923$ lbs $= 0.9$ kips
$T = 1.81(0.931/12)(1,500) + 2,767 \sin(5/2)(2) = 452$ lbs $= 0.5$ kips

Conductor Loads
$W_i = 1.24(d + I_z)I_z$
$\quad\quad = 1.24(1.165 + 0.273)0.273 = 0.487$ lbs/ft $\quad\quad$ (Eq. 2-16)
$d_i = 2(0.273) + 1.165 = 1.711$ in.
$V_l = 1,800(1.075 + 0.487) + 200 = 3,012$ lbs $= 3.0$ kips
$T = 1.81(1.711/12)(1,500) + 7921 \sin(5/2)(2) = 1,078$ lbs $= 1.1$ kips

Wind on Structure
From the *Wind* loading case, K_z equals 1.13 and G_t equals 0.882.
Wind pressure $= Q\,K_z\,(V_I)^2\,G_t$
$\quad\quad\quad\quad = 0.00256(1.13)(30)^2\,0.882 = 2.30$ psf $\quad\quad$ (Eq. 2-1a)

Transverse Wind Loads
Force coefficients and areas are provided in the *Wind* loading case.
$W_1 = 2.3(1.8)(34) = 141$ lbs $= 0.1$ kips
$W_2 = 2.3(3.22)(33) = 244$ lbs $= 0.2$ kips
$W_3 = 2.3(3.32)(62) = 473$ lbs $= 0.5$ kips

High-Intensity Wind, Chapter 2, Section 2.2

86% of the tornados are F2 or smaller (Table 2-8). This rating corresponds to a wind speed of 157 mph. Wind is applied on the structure and wire loads are assumed to be zero. Three loading cases are calculated: 0-, 90-, and 45-degree yaw angles.

Wind on Structure
$K_{zt} = K_z = G_t = 1.0$
Wind pressure $= Q\,K_z\,K_{zt}\,(V)^2\,G_t = 0.00256(1.0)(1.0)(157)^2\,(1.0) = 63.1$ psf

0-Degree Yaw Angle
Transverse Wind Loads
Force coefficients and areas are provided in the *Wind* loading case.
$W_1 = 63.1(1.8)(34) = 3,862$ lbs $= 3.9$ kips
$W_2 = 63.1(3.22)(33) = 6,705$ lbs $= 6.7$ kips
$W_3 = 63.1(3.32)(62) = 12,989$ lbs $= 13.0$ kips

90-Degree Yaw Angle
Longitudinal Wind Loads
Force coefficients and areas are provided in the *Wind and Ice* loading case.
$W_4 = 63.1(2.75)(43) = 7,461$ lbs $= 7.5$ kips
$W_5 = 63.1(2.85)(37) = 6,654$ lbs $= 6.7$ kips
$W_6 = 63.1(3.27)(67) = 13,825$ lbs $= 13.8$ kips

45-Degree Yaw Angle
Transverse Wind Loads
Wind pressure $= 63.1 \cos \Psi = 63.1 \cos(45) = 44.6$ psf   (Eq. 2-13a)
Force coefficients and areas are provided in the *Wind* loading case.
$W_1 = 44.6(1.8)(34) = 2,730$ lbs $= 2.7$ kips
$W_2 = 44.6(3.22)(33) = 4,739$ lbs $= 4.7$ kips
$W_3 = 44.6(3.32)(62) = 9,180$ lbs $= 9.2$ kips

Longitudinal Wind Loads
Wind pressure $= 63.1 \sin \Psi = 63.1 \sin(45) = 44.6$ psf   (Eq. 2-13b)
Force coefficients and areas are provided in the *Wind and Ice* loading case.
$W_4 = 44.6(2.75)(43) = 5,274$ lbs $= 5.3$ kips
$W_5 = 44.6(2.85)(37) = 4,703$ lbs $= 4.7$ kips
$W_6 = 44.6(3.27)(67) = 9,771$ lbs $= 9.8$ kips

National Electric Safety Code

From NESC (2007), Fig. 250-1, Utah is in the medium loading district. Rule 250C (Extreme Wind) is not included in this example.

Wind on Wires
Wind pressure $= 4$ psf

Ground-Wire Loads
$W_i = 1.24(d + I_z)I_z = 1.24(0.385 + 0.25)0.25 = 0.197$ lbs/ft   (Eq. 2-16)
$d_i = 2(0.25) + 0.385 = 0.885$ in.
$V_l = 1,800(0.262 + 0.197)(1.5) + 50(1.5) = 1,314$ lbs $= 1.3$ kips
$T = 4(0.885/12)(1,500)(2.5) + 3,700 \sin(5/2)(2)(1.65)$
    $= 1,638$ lbs $= 1.6$ kips

Conductor Loads
$W_i = 1.24(d + I_z)I_z = 1.24(1.165 + 0.25)0.25 = 0.439$ lbs/ft   (Eq. 2-16)
$d_i = 2(0.25) + 1.165 = 1.665$ in.
$V_l = 1,800(1.075 + 0.439)(1.5) + 200(1.5) = 4,388$ lbs = 4.4 kips
$T = 4(1.665/12)(1,500)(2.5) + 8,800 \sin(5/2)(2)(1.65) = 3,348$ lbs
   = 3.3 kips

Wind on Structure
Transverse Wind Loads
Wind pressure = 4(2.5) = 10 psf
Areas are provided in the *Wind* loading case.
The NESC force coefficient is 3.2.
$W_1 = 10(3.2)(34) = 1,088$ lbs = 1.1 kips
$W_2 = 10(3.2)(33) = 1,056$ lbs = 1.1 kips
$W_3 = 10(3.2)(62) = 1,984$ lbs = 2.0 kips

Construction and Maintenance, Chapter 3, Section 3.1

Wind on Wires
Wind pressure = 3 psf

Ground-Wire Loads
The pulling slope is 3 horizontal to 1 vertical.
$V_l = 1.5(1,751)(1/3) + 0.262(1,800)(1.5)/2 + 50(1.5)$
   = 1,304 lbs = 1.3 kips   (Alt. A controls)
$V_l = 0.262(1,800)(2) + 50(2) = 1,043$ lbs = 1.1 kips   (Alt. B controls)
$T = 3(0.385/12)(1,500)1.5 + 1751 \sin(5/2)(2)1.5 = 446$ lbs = 0.5 kips

Conductor Loads
$V_l = 1.5(5,961)(1/3) + 1.075(1,800)(1.5)/2 + 200(1.5)$
   = 4,732 lbs = 4.7 kips   (Alt. A controls)
$V_l = 1.075(1,800)2 + 200(2) = 4,270$ lbs = 4.3 kips   (Alt. B controls)
$T = 3(1.165/12)(1,500)1.5 + 5,961 \sin(5/2)(2)1.5 = 1,435$ lbs = 1.4 kips

Wind on Structure
Transverse Wind Loads
Wind pressure = 3(1.5) = 4.5 psf
Force coefficients and areas are provided in the *Wind* loading case.
$W_1 = 4.5(1.8)(34) = 275$ lbs = 0.3 kips
$W_2 = 4.5(3.22)(33) = 478$ lbs = 0.5 kips
$W_3 = 4.5(3.32)(62) = 926$ lbs = 0.9 kips

Failure Containment, Chapter 3, Section 3.3.2

This loading case is based on the residual static load of a broken conductor or ground wire (0 psf wind and 0 in. of radial ice at 30°F).

Ground-Wire Loads
The RSL load factor for a broken ground wire is 1.0.

Broken Wire
$V_l = 0.262(1,800)/2 + 50 = 286$ lbs = 0.3 kips
$T = 1,623 \sin(5/2)(1.0) = 71$ lbs = 0.1 kips
$L = 1,623 \cos(5/2)(1.0) = 1,621$ lbs = 1.6 kips

Intact Wire
$V_l = 0.262(1,800) + 50 = 522$ lbs = 0.5 kips
$T = 1,623 \sin(5/2)(2) = 142$ lbs = 0.1 kips
$L = 0.0$ kips

Conductor Loads
Ratio of the span to insulator length = 1,250/6 = 208
Ratio of the span to sag = 1,250/31.6 = 40
From Fig. 3-2 in Chapter 3, the RSL load factor is 0.7. Refer to Table 5-2.

Broken Wire
$V_l = 1.075(1,800)/2 + 200 = 1,168$ lbs = 1.2 kips
$T = 5,615 \sin(5/2)(0.7) = 171$ lbs = 0.2 kips
$L = 5,615 \cos(5/2)(0.7) = 3,927$ lbs = 3.9 kips

Intact Wire
$V_l = 1.075(1,800) + 200 = 2,135$ lbs = 2.2 kips
$T = 5,615 \sin(5/2)(2) = 490$ lbs = 0.5 kips
$L = 0.0$ kips

5.1 WEIGHT SPAN CHANGE WITH BLOW-OUT ON INCLINED SPANS

This example compares weight spans with and without wind for the center tower shown in Fig. 5-2. The equations are shown in Section 4.5.1.1 of Chapter 4. Wire data is from Section 5.0 above.

Ground Wire
No Wind
$C_v = H/w_v = 1,546/0.262 = 5,901$ ft   (Eq. 4-7)
$X_1 = S/2 - C_v \sinh^{-1}[(B/2)/C_v \sinh(S/2C_v)]$
  $= 1,250/2 - 5,901 \sinh^{-1}[(50/2)/5,901 \sinh(1,250/2(5,901))]$
  $= 390$ ft   (Eq. 4-5)
Weight span = 2(1,250 − 390) = 1,720 ft
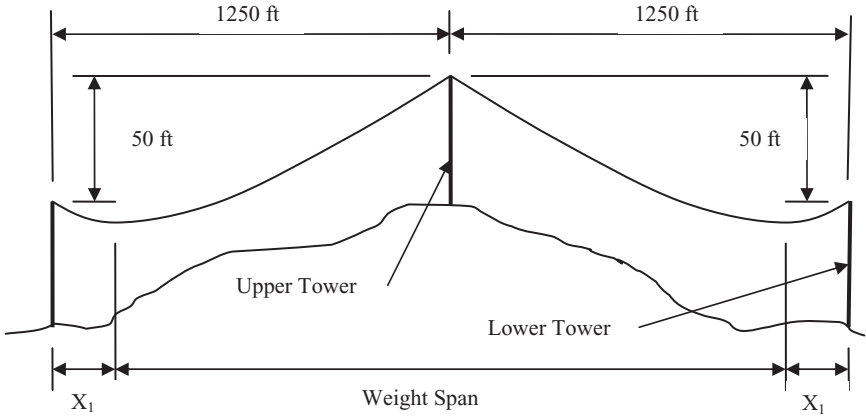
Figure 5-2. Weight span for center tower with inclined spans.

16.3-psf Wind
$C_v = 2,939/0.262 = 11,218$ ft   (Eq. 4-7)
$X_1 = 1,250/2 - 1,1218 \sinh^{-1}[(50/2)/11,218 \sinh(1,250/2(11,218))]$
  $= 177$ ft   (Eq. 4-5)
Weight span $= 2(1,250 - 177) = 2,146$ ft (*25% increase*)

Conductor
No Wind
$C_v = 5,302/1.075 = 4,932$ ft
$X_1 = 1,250/2 - 4,932 \sinh^{-1}[(50/2)/4,932 \sinh(1,250/2(4,932))] = 428$ ft
Weight span $= 2(1,250 - 428) = 1,644$ ft

16.3-psf Wind
$C_v = 8,598/1.075 = 7,998$ ft
$X_1 = 1,250/2 - 7,998 \sinh^{-1}[(50/2)/7,998 \sinh(1,250/2(7,998))] = 306$ ft
Weight span $= 2(1,250 - 306) = 1,888$ ft (*15% increase*)

5.2 TRADITIONAL CATENARY CONSTANT

This example compares weight spans to those in Section 5.1 using the traditional catenary constant. The traditional catenary constant is based on the resultant unit weight (w_r). The catenary constant in Section 5.1 is based on the vertical unit weight (w_v). Figure 5-2 shows the upper and lower towers and spans.

Ground Wire
16.3-psf Wind
$w_v = 0.262$ lbs/ft
$w_t = 16.3(0.385/12) = 0.523$ lbs/ft
$w_r = (0.262^2 + 0.523^2)^{1/2} = 0.585$ lbs/ft
$C_r = H/w_r = 2,939/0.585 = 5,025$ ft   (Eq. 4-6)
$X_1 = S/2 - C_r \sinh^{-1}[(B/2)/C_r \sinh(S/2C_r)]$
$\quad = 1,250/2 - 5,025 \sinh^{-1}[(50/2)/5,025 \sinh(1,250/2(5,025))]$
$\quad = 425$ ft   (Eq. 4-5)
Weight span $= 2(1,250 - 425) = 1,650$ ft

Conductor
Refer to Table 5-3.
16.3-psf Wind
$w_v = 1.075$ lbs/ft
$w_t = 16.3(1.165/12) = 1.582$ lbs/ft
$w_r = (1.075^2 + 1.582^2)^{1/2} = 1.913$ lbs/ft
$C_r = 8,598/1.913 = 4,494$ ft   (Eq. 4-6)
$X_1 = 1,250/2 - 4,494 \sinh^{-1}[(50/2)/4,494 \sinh(1,250/2(4,494))]$
$\quad = 446$ ft   (Eq. 4-5)
Weight span $= 2(1,250 - 446) = 1,608$ ft

The traditional catenary constant underestimates the vertical load on the upper tower and overestimates the vertical load on the lower tower.

APPENDIX A

DEFINITIONS, NOTATIONS, AND SI CONVERSION FACTORS

A.1 DEFINITION OF STRUCTURE TYPES

Tangent Structure: Minimum line deflection angle. Usually suspension or some type of post insulators (line post, braced line post, horizontal V) used to support the conductors and transfer wind and weight loads to the structure. In practice, structures with very small line angles, such as 2 degrees or less, are often referred to as tangent structures.

Angle Structure (change in direction in plan view):

a. May be similar to tangent structure, using suspension or post insulators to support the conductors and transfer wind, weight, and line angle loads to the structure.
b. May be similar to strain or dead-end structures, using insulators in series with the conductors to bring wind, weight, and line angle loads directly into the structure.

Strain Structure (usually has line angle, also): Similar to dead-end structure, using insulators in series with the conductors to bring wind, weight, and line angle loads directly into the structure. Also capable of resisting some unbalanced tensions in one direction of one or all wires on one face of the structure, but not capable of resisting the full unbalanced tensions of all wires removed on one face of the structure (i.e., with all ahead span or back span wires removed).

Dead-End Structure (usually has line angle, also): Uses insulators in series with the conductors to bring wind, weight, and line angle loads directly into the structure. Also (generally) capable of resisting the full

unbalanced tensions of all wires removed on one face of the structure (i.e., with ahead span or back span wires removed).

A.2 DEFINITIONS OF SPAN

Span. The distance, generally measured horizontally, between two points. Unless otherwise stated, span usually refers to the distance between two adjacent structures. See Fig. A-1.

Span Length. The horizontal distance between two adjacent structures.

Back Span. The span length in the span behind (generally in the direction of decreasing stationing) the structure in question. In Fig. B-1, span 1 is the back span of structure B.

Ahead Span. The span length in the span ahead (generally in the direction of increasing stationing) of the structure in question. In Fig. B-1, span 2 is the fore span (ahead span) of structure B.

Sag. The relative vertical distance of the straight line made by two adjacent supports to a point along a conductor.

Slack. The amount of conductor length difference between a straight line made by two adjacent supports and a sagging conductor.
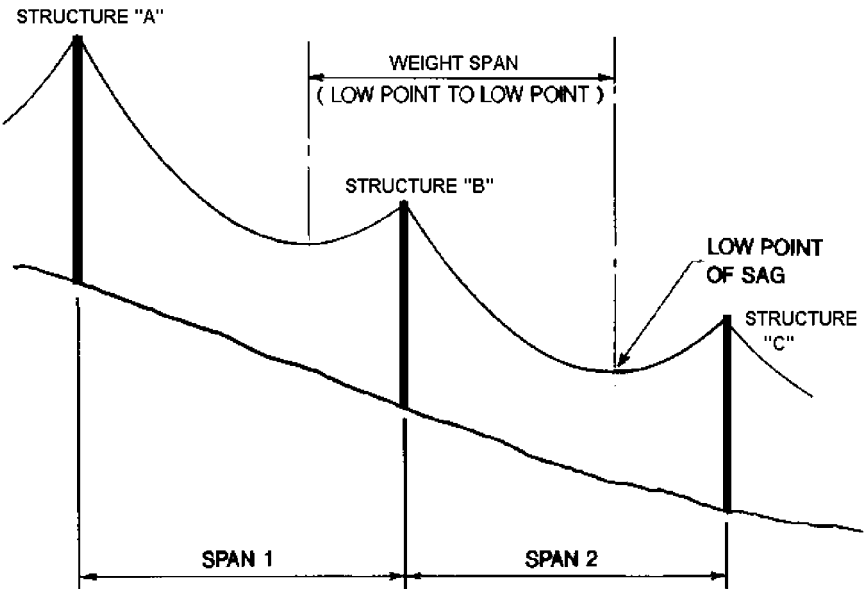
Figure A-1. Span usually refers to the distance between two adjacent structures.

Weight Span. The horizontal distance between the low point of sag in back span and the low point of sag in the ahead span. It is used in calculating the vertical load that the conductor imposes on the supporting structure.

Wind Span. The mathematical average of the back span and the fore span. It is used in calculating the wind load that the conductor imposes on the supporting structure. This may also be referred to as the horizontal span.

Vertical Span. The vertical span is the same as the weight span.

A.3 NOTATION

The following notation is used in this manual:

A	solid tributary area of surfaces projected normal to the wind, in square feet
A_i	cross-sectional area of ice accretion on a wire, in inches
A_m	the area of all members in the windward face of a structure, in square feet
A_{ml}	the area of all members in the face of the structure that, in a tangent structure, is parallel to the line, in square feet
A_{mt}	the area of all members in the face of the structure that, in a tangent structure, is perpendicular to the line, in square feet
A_o	the area of the outline of the windward face of a structure, in square feet
B	difference in elevation of supports, in feet
B_t	dimensionless response term corresponding to the quasi-static background wind loading on the structure
B_w	dimensionless response term corresponding to the quasi-static background wind loading on the wire (conductor or ground wire)
BWL	broken wire load
c	correction factor for aspect ratio
C	catenary constant or parameter of the catenary curve
C_f	force coefficient
C_{fl}	the force coefficient associated with faces of the structure that, in a tangent structure, are parallel to the line
C_{ft}	the force coefficient associated with faces of the structure that, in a tangent structure, are perpendicular to the line
C&M	construction and maintenance loads
COV_R	coefficient of variation of component strength
d	diameter of wire (conductor or ground wire), in inches
D	straight-line distance between the supports, in feet

DL dead loads from weights of components

e exclusion limit of component strength, in percentage

E exposure factor evaluated at the effective height of the wire or structure

f structure/member natural frequency, in cycles/second

f_t fundamental frequency of the free-standing structure in the transverse direction, in Hertz

f_w fundamental frequency for horizontal sway of the conductor or ground wire, in Hertz

F wind force, in pounds or kips (1,000 pounds)

F_1 wind force in the longitudinal direction, in pounds or kips

F_t wind force in the transverse direction, in pounds or kips

FC failure containment loads

FPP Fujita-Pearson tornado scale

G gust response factor

g_s statistical peak factor for gust response of a component

G_t gust response factor for the structure

G_w gust response factor for the wire (conductor or ground wire)

H height of hill or escarpment relative to the upwind terrain, in feet

HA horizontal line angle, in degrees

I_{RP} ice thickness having an RP-year return period, in inches

I_{50} ice thickness having a 50-year return period, in inches

I_Z design ice thickness, in inches

K_1 factor to account for shape of topographic feature and maximum speed-up effect

K_2 factor to account for reduction in speed-up with distance upwind of downwind effect

K_3 factor to account for reduction in speed-up with height above local terrain

K_v ratio of the 3-sec wind speed to the 10-min average wind speed in open country (Exposure C) at 33-ft (10-m) reference height

K_Z velocity pressure exposure coefficient

K_{zt} topographic factor

LEL lower exclusion limit

LL legislated loads

L_h distance upwind of crest to where the difference in ground elevation is half the height of hill or escarpment, in feet

L_m length of member, in feet

L_s transverse integral scale of turbulence, in feet

L_T transverse structure load, in pounds or kips

L_V vertical structure load, in pounds or kips

m_i mass of typical ice sample

PDF probability density function of a random variable

P_f	component annual probability of failure
Q	the numerical constant determined by air density
Q_D	design load effect in each component of a structure
Q_{RP}	weather-related load with an RP-year return period
Q_{50}	weather-related load with a 50-year return period
R	Reynolds number
R_n	nominal value of component strength
R_t	dimensionless resonant response term of the structure
R_w	dimensionless resonant response term of the wire
RP	return period of weather-related event, load, or load effect
RRF	relative reliability factor
RSL	residual static load for the broken wire loading condition
RTS	rated tension strength
s	member diameter or width normal to the wind, in feet
S	span length of the wires (conductor and ground wire), in feet
Str	Strouhal number
t	time
T_H	horizontal component of tension, in pounds or kips
UH	horizontal component of unit wire load for a certain tension, in pounds or kips
UR	resultant unit wire load for a certain tension, in pounds or kips
UV	vertical component of unit wire load for a certain tension, in pounds or kips
V	design wind speed (3-sec) at standard height of 33 ft (10 m) in open country (Exposure C), in miles per hour (mph)
V_{50}	wind speed at a 50-year return period (basic wind speed), 3-sec gust, in mph
V_{cr}	critical vortex-induced wind speed, in feet per second
V_l	vertical structure load, in pounds or kips
V_o	10-min average wind speed at the effective height of the wires and structure, in ft/sec
V_{RP}	wind velocity having an RP-year return period, 3-sec gust, in mph
VA	vertical line angle, in degrees
w	wire weight per unit length, in pounds per foot
Wi	weight of glaze ice, in pounds per foot
X_1	distance from the low point of sag to lower support, in feet
z	height above ground, in feet
z_g	gradient height, in feet
z_h	effective height above ground of the wire (conductor or ground wire) or structure, in feet
α	power-law coefficient for terrain factor equation
α_{FM}	power-law coefficient for sustained wind
γ	load factor applied to weather-related loads Q_{50}

γ_{CM}	load factor applied to construction and maintenance loads
γ_i	load factor applied to ice load
γ_w	load factor applied to wind load
ε	approximate coefficient for separation of the wire and structure response terms in the general gust response factor equations
κ	surface drag coefficient
ρ	mass density of air
ρ_i	ice density
Φ	the solidity ratio (A_m/A_o)
ϕ_{LL}	strength factor specified with legislated loads
ζ_t	structure damping to critical damping ratio
ζ_w	wire aerodynamic damping to critical damping ratio
Ψ	angle of yaw, in degrees

A.4 SI CONVERSION FACTORS

1 ft = 0.305 meter (m)
1 in. = 25.4 millimeters (mm)
1 pound (lb) force = 4.45 newtons (N)
1 lb/ft = 14.6 N/m
1 lb/ft^2 (psf) = 47.8 pascals (Pa) (N/m^2)
1 lb mass/ft^3 (pcf) = 0.016 gram/cubic centimeter (g/c^3)
1 mile per hour (mph) = 0.45 meter/second (m/s)
To convert temperature, θ, from °F to °C, θ (°C) = 5/9 [θ (°F) − 32°F]

APPENDIX B

LIMITATIONS OF
RELIABILITY-BASED DESIGN

B.1 GENERAL

Several valuable uses can be made of long-term and available data regarding weather events as well as of some knowledge of the dispersion of strength of at least two line components, but it is neither rational nor practical to claim that one can predict the annual probability or risk of failure of a transmission line by manipulating or combining such data.

The early claims with reliability-based design (RBD) were that with adequate weather data and knowledge of component strengths, one can make calculations and produce a design to reach a predictable failure rate of a given line design. The situation can be represented as shown in Fig. B-1, where the probability density function (PDF) of the load on the left and that PDF of the strength on the right can be used to determine the risk of failure. That risk is related to the overlapping of the upper tail of the load distribution and the lower tail of the strength distribution. Although this is a theoretically attractive proposal, when going from the theory to the realities of a transmission line, problems arise that make the proposal unworkable.

Looking first at the left side of the relationship, which is the PDF of the loads, the sources of error are the lack of enough years of weather data and also the transfer functions needed to convert the wind data into loads so that an RP_N load truly represents an RP_N wind event.

The theoretically precise probabilistic computations (which were expected to be far better than deterministic methods) run into the fact that deterministic transfer functions must be used to convert weather data into loads, and most of these functions cannot be defined with sufficient precision to validate the risk calculations.
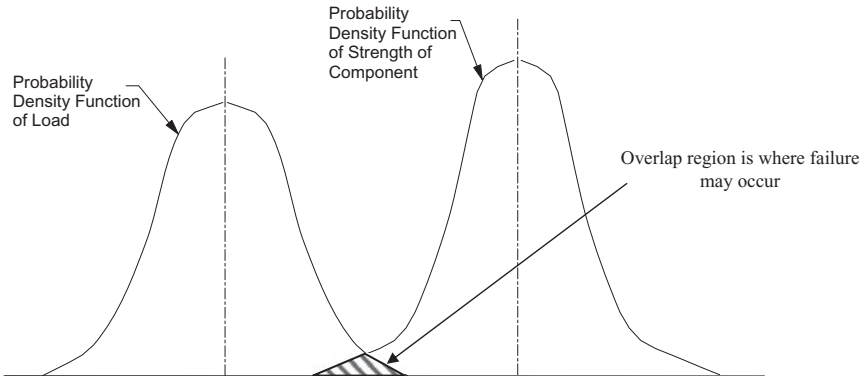
Figure B-1. Probability density function showing the region of failure, where the load is greater than the strength of the component.

B.2 UNCERTAINTIES IN LOADS

The conversion of wind speed data into, for example, wire and structure loads requires largely deterministic transfer functions such as:

1. The force coefficient, which can vary through a range of almost 100% depending on the Reynolds number. As can be seen from the spread of data in Figs. G-1 and G-2 of Appendix G, the Reynolds number itself is a function of diameter of wire and the wind speed.
2. A correction to adjust the time base of the wind speed data to the time base of pressure formula.
3. A wide range of mathematical assumptions regarding gust response factors as a function of span length and height.
4. More assumptions regarding corrections based on terrain and tree cover, which can vary widely along a line.
5. Corrections for the direction of each major line section with regard to the direction of the critical winds (not necessarily the prevailing wind direction).

The risk of failure also depends on the exposure, that is, the length of line as well as the number of structures and other components exposed to the wind or ice between switching stations.

The method used by line designers, with few exceptions, is to assume the worst of most parameters: Category C exposure (open, flat exposure typical of airports); the design wind speed blowing at the critical direction relative to the line orientation (which may or may not be perpendicular); and the line normal to the wind direction during severe ice storms. This

results in conservative designs arrived at by many deterministically controlled steps. However, the goal of the probabilistic process was not to produce conservative designs but, rather, to produce accurate values so the designer can then apply his or her own measure of conservatism.

B.3 UNCERTAINTIES IN STRENGTHS

Most common materials used in transmission structures—concrete, steel, and wood—have variable strength properties. The same is true of the wire system that consists of conductor, shield wires, insulators, hardware, and accessories that include dampers, spacers, jumpers, etc. Some of these properties degrade with time. In addition, the state of knowledge about structural behavior of individual structure components is imperfect. For example, it is impossible to predict precisely when a compression member in a latticed tower will fail. Therefore, it may not be possible to obtain an accurate PDF for the compression strength of a steel angle member in a particular location within a tower.

B.4 UNCERTAINTIES IN SPAN USE

Due to standardization and the limited number of structure types, many structures in a line are not used at their maximum design spans. Therefore, actual loads experienced by supporting structures may be smaller than those predicted on the basis of their limiting design span. This effect is similar to that caused by wind direction, discussed in Section B.7, where the design is based on wind acting from the critical direction to the line, whereas the actual extreme wind, or wind accompanying freezing rain, may blow at an angle and produce less severe loads. The fact that many structures are not loaded as expected contributes to an increase in overall reliability (Ghannoum and Orawaski 1987; White 1985). It is usual to ignore "span use."

The dispersion in "span use" can be much greater than the dispersions of the basic load and strength properties, and there can be many different critical "use factors" for any given structure. Each component may even have a different level of "usage" under a different load case. This "use" subject is a very complex one, made even more complex by the fact that a series of towers will be used by a utility for many lines, of different lengths, running in different directions, through varying terrain and ground covers, and so forth. It does not seem practical to change the limits of use of a standard set of structures because the next-to-be-built line is a short one or a long one or is routed in a different direction over different terrain.

B.5 PROBABILITY OF FAILURE

Referring once more to the set of curves of Fig. B-1, which show the theoretical basis for finding P_f, the probability of failure, can be determined mathematically. To calculate P_f demands that the two curves representing the load function and the strength function be precisely known and can be "drawn with a fine pen." In reality, as has been noted above, the load function curve is drawn with something like a very wide paintbrush and, as is seen, the strength function curve is also drawn with a very wide brush so that the probability of failure becomes difficult to predict.

Because of these problems with the application of the full RBD design concept, some very useful design concepts can be extracted from the overall probabilistic approach. These concepts help us make rational decisions regarding the selection of design climatic events and also regarding design strengths.

B.6 SPATIAL EFFECTS OF TRANSMISSION LINE STRUCTURES UNDER WIND AND ICE LOADS

The wind and ice maps (Fig. 1-1 in Chapter 1 and Figs. 2-13 through 2-18 in Chapter 2) provide extreme wind speeds and equivalent uniform radial glaze ice thicknesses at a point. Depending on the distribution type, an RP_N wind has a finite probability of being exceeded at least once in 50 years at a point structure, such as a small building, a microwave tower, or a switchyard, in most of the country. For example, for a given distribution, RP_{50}, RP_{100}, RP_{200}, and RP_{400} winds may have probabilities of 0.64, 0.39, 0.22, and 0.12, respectively, of being exceeded during 50 years. However, transmission lines are linear structures and thus are more exposed to extreme wind and ice loads. A long transmission line is hit by storms with 90-mph (40 m/s) gusts or ice storms with 1 in. of ice thickness more frequently than is a single microwave tower, and the frequency of that exposure increases with the length of the line. To obtain equal risks of exceeding the design load for a transmission line and a microwave tower in the same wind or ice climate, the transmission line must be designed for a higher wind speed or ice loads than is the microwave tower. Many studies of this spatial effect from windstorms, hurricanes, tornados, and ice storms have been published.

It has been suggested that one approximate way to take care of the spatial effect problem is to gather extreme wind data over the space of a line (i.e., to collect each year the largest wind observed over the entire length of a line) rather than the customary values at individual stations. This approach was followed by Behncke et al. (1998). They obtained an RP_{50} wind speed for a proposed 50-mile-long transmission line in Thai-

land that was about 9% higher than the maximum RP_{50} wind speed at a point along the line. They used the maximum annual speeds from six weather stations along the route in a Gumbel extreme value analysis to determine this extreme linear wind speed.

Vickery and Twisdale (1995) used an updated hurricane simulation methodology to compare fastest-mile wind speeds at a point in Miami and at any place along the Dade County, Florida coastline. They found that the fastest-mile wind along the coast was 147 mph (66 m/s), 16% higher than the fastest-mile wind speed in Miami.

There have been a number of studies on the risk of tornados to transmission lines. Twisdale and Dunn (1983) found that the tornado wind speed exceedance probability for a line can be estimated by increasing the point tornado wind speed exceedance probability by a factor of 10 times the length of the line in miles. An analysis in Twisdale (1982) shows that transmission lines designed using the NESC wind loading criterion will experience extreme winds more frequently than would be expected based on the RP_{50} wind speed, because the risk of tornado strikes is ignored in design. In a 1993 paper, the Australian Bureau of Meteorology quoted return periods for 100-mile (161-km)-long transmission lines in Oklahoma of 40 years for F2 tornados [wind speed greater than 112 mph (50 m/s)] and 120 years for F3 tornados [wind speed greater than 156 mph (70 m/s)]. Milford and Goliger (1997) developed a tornado risk model for tornado paths perpendicular to transmission lines that takes into account the damage length of the tornado and the length of the transmission line.

Golikova et al. (1983) present a simple method for determining the risk of ice storms to transmission lines compared to point structures. Their results indicate that the return period of an extreme ice load for a transmission line decreases as the ratio of the line length to the ice storm width increases. For a line length-to-storm width ratio of 2, for example, an RP_{50} point ice load has a return period of 17 years for the line. Laflamme (1993) used the maximum annual ice thickness from triads of passive ice meters, spaced about 50 km apart, to determine extreme ice thicknesses. The RP_{50} ice thickness obtained by Gumbel extreme value analysis of these maxima averaged 10% higher than that for the single stations.

B.7 EFFECTS OF WIND DIRECTION

The wind load effect on a structure is largest when the wind blows in the critical direction, which may or may not be perpendicular to the line. The designer usually assumes that the wind velocity, V_{RP}, acts in the critical direction. However, the data used to establish V_{RP} (such as those used to establish the wind map in this manual) usually do not include wind

direction. As a result, the loads determined are conservative. It has been determined (Dagher 1985; Peyrot and Dagher 1984) that using wind data from all directions as if they came from the critical direction increases a component reliability by a factor of approximately 4, provided the most critical winds are not correlated with directional tendencies.

The ice thicknesses in Figs. 2-13 through 2-18 were determined assuming the wind speed during freezing rain was perpendicular to the line to obtain the maximum effect of wind-blown raindrops on the accretion of ice. In regions where the wind direction during freezing rainstorms is consistently parallel to some wires, the ice thickness on these wires will be about 70% of the thicknesses in Figs. 2-13 through 2-18. Furthermore, the ice thickness on these lines does not increase with height above ground. The wind direction during freezing rain may vary from section to section along a line and may be significantly affected by the local topography.

B.8 EXTREME VALUE ANALYSIS—A BRIEF DISCUSSION

The gust wind speeds and radial ice thicknesses in the maps in Fig. 1-1 and Figs. 2-13 through 2-18 and the factors to adjust wind loads and radial ice thicknesses for return period (Tables 1-1 and 1-2 in Chapter 1) were determined by extreme value analyses of weather data. For both maps the stations were grouped into superstations (Peterka 1992) to increase the period of record and reduce sampling error in estimating the parameters of the extreme value distribution. Extreme wind speeds in non-hurricane regions were estimated by determining the parameters of a Gumbel distribution using maximum annual gust speeds. Along the Gulf and Atlantic coasts, the contours are based on hurricane models and Monte Carlo simulations of hurricanes striking the coast. Extreme radial ice thicknesses were estimated using the peaks-over-threshold method, estimating the parameters of the generalized Pareto distribution from radial ice thicknesses simulated from weather data. Both gust wind speeds and radial ice thicknesses are at 33 ft (10 m) above ground for exposure Category C. For further information, refer to ASCE 7-05 (ASCE 2005).

APPENDIX C

NUMERICAL CONSTANT, *Q*

The numerical constant (*Q*) converts kinetic energy of moving air into potential energy of pressure. The value of *Q* can be determined from Eq. C-1.

$$Q = \frac{1}{2}\rho \tag{C-1}$$

where ρ = mass density of air.

The value of the numerical constant, 0.00256 customary units (0.613 metric units), is based on the specific weight of air at 59°F (15°C) at sea level pressure of 29.92 in. (101.325 kPa) of mercury, and dimensions associated with wind speed in miles per hour and pressure in psf. The use of any other value should be based on good engineering judgment with sufficient weather data available to justify a different value for a specific design application.

The specific weight of air varies with temperature and atmospheric pressure. Table C-1 shows values of the air density factor as a function of air temperatures and pressures (elevations above sea level). The effect of moisture or variation in relative humidity is assumed negligible.

Table C-1. Numerical Constant, Q

Air Temp (°F)	Elevation above Sea Level (ft)					
	0	2,000	4,000	6,000	8,000	10,000
100	0.00238	0.00221	0.00205	0.00191	0.00177	0.00165
80	0.00246	0.00229	0.00213	0.00198	0.00184	0.00171
60	0.00256[a]	0.00237	0.00221	0.00205	0.00191	0.00178
40	0.00266	0.00247	0.00230	0.00214	0.00199	0.00185
20	0.00277	0.00257	0.00239	0.00223	0.00207	0.00192
0	0.00289	0.00268	0.00249	0.00232	0.00216	0.00201
−20	0.00293	0.00281	0.00261	0.00243	0.00226	0.00210
−40	0.00317	0.00294	0.00273	0.00254	0.00237	0.00220

[a] Recommended value.
Source: Brekke, G. N. (1959).

APPENDIX D

CONVERSION OF WIND SPEED AVERAGING TIME

It is recognized that wind speed values for a given wind speed record depend on the averaging time. Shorter averaging time corresponds to a higher wind speed, whereas longer averaging time would give a lower wind speed. It is often necessary to obtain equivalent wind speeds from different averaging periods. Conversion to another averaging time can be accomplished using the graph shown in Fig. D-1. This graph, prepared from results by Durst (1960), gives the ratio, (V_t/V_h), of probable maximum wind speed averaged over t seconds to hourly mean wind speed for Exposure C.

The following procedure is an example of converting a fastest-mile wind speed to a 3-sec gust speed.

Step 1.   Convert the fastest-mile wind speed to mean hourly wind speed. For example, a fastest-mile wind speed of 72 mph (averaging time of 50 sec) is 1.26 times the mean hourly wind speed (Fig. D-1). Thus, the equivalent mean hourly wind speed is 57 mph.

Step 2.   Convert the mean hourly wind speed to 3-sec gust speed. From Fig. D-1, it is seen that a 3-sec gust speed is 1.52 times the mean hourly wind speed. Hence, for the example problem, the 2-sec gust speed is 87 mph.

The Davenport equations for gust response factors, given in Appendix F, were originally developed based on 10-min average wind speed. To convert these equations to 3-sec wind, a constant, K_v, was introduced to account for the ratio of 3-sec gust wind speed to 10-min average wind
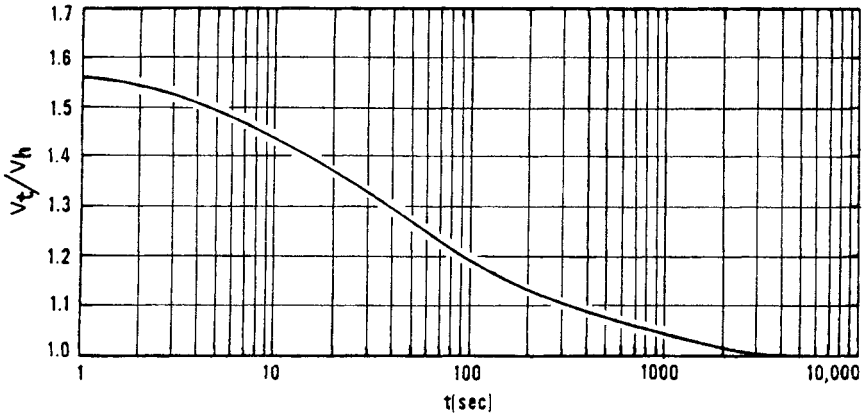
Figure D-1. Wind speed conversion, Exposure C.

speed in open country (Exposure C) at the 33-ft (10-m) reference height. This ratio (K_v) is equal to 1.43 (1.526/1.067).

Many other theories have been developed (IEC 2003) to address wind speed conversion. They often yield different results. This is particularly true for Exposure B and Exposure D, where only limited historical data are available under extreme wind events. With all the uncertainties related to wind and wind measurements, this committee recommends the use of a single numerical constant for the value of K_v under all exposure categories. Figures 2-4 through 2-7 in Chapter 2 are generated based on K_v equal to 1.43. It should be noted that IEC Standard 826 (IEC 2003) has recommended different conversion factors based on terrain exposure categories. Alternate values of K_v for Exposures B and D may be used as determined by the engineer from other sources or use of local wind data.

Some references related to the wind speed conversion can be found in the References at the end of this manual. This information, together with other related sources, may be used for this application.

APPENDIX E

SUPPLEMENTAL INFORMATION ON STRUCTURE VIBRATION

E.1 INTRODUCTION

A transmission structure is designed to support a system of electrically continuous conductors and overhead ground wires. A transmission line has a large number of structures located at sites with varying environmental and geographical exposures. The potential of a transmission structure being placed in an environment prone to vibration is much greater than that for a typical civil engineering structure.

Vibration of a transmission structure can consist of complete structure vibration modes, structure component modes, or individual member vibration modes. The initiation of these modes can be caused by induced vibration forces from the wind acting directly on the structure, from conductor and overhead ground wire vibrations (aeolian, subconductor oscillation, and galloping), or by induced ground motion such as that caused by an earthquake.

E.2 STRUCTURE VIBRATIONS

Structure or member vibrations can occur from conductor motions (aeolian, subconductor oscillation, and galloping) when the frequency of the vibrating conductor corresponds to one of the natural frequencies of the structure or its individual member(s). Approximate natural frequencies of conductor vibration for aeolian motions are 3 to 150 Hertz; for

subconductor oscillation 0.15 to 10 Hertz; and for galloping 0.08 to 3 Hertz (EPRI 1979). In most instances conductor systems can be designed, using dampers and spacer dampers, to prevent and/or reduce the effect of wind-induced vibration behavior. Although aeolian vibrations of wires have caused some instances of fatigue failures of structure or hardware elements, galloping wires have the potential to cause the most damage to the supporting structure (Brokenshire 1979; Gibbon 1984; White 1979). Latticed steel running angle suspension towers, guyed-mast dead-end structures, heavy-angle towers, and flexible "narrow-base" pole structures have been reported to be more susceptible to damage caused by conductor galloping motions. Field investigations have been conducted to study methods of suppressing conductor galloping (Pohlman and Havard 1979; Richardson 1983).

Wind-induced oscillation can cause vibration problems for a complete structure or the individual members. This type of vibration can be initiated by vortex shedding and/or aeroelastic instability. Tubular structures can respond in a complete tower vibration mode or as individual member vibrations. A latticed tower, in general, presents a complex aerodynamic shape to the wind such that consistent vortex shedding to cause complete oscillation of the structure over a prolonged period is almost impossible. Therefore, only individual member behavior of latticed steel towers to vortex shedding and aeroelastic instability has been studied (Modi and Slater 1983; Wardlaw 1967).

Alternate shedding of vortices from either side of the member causes vortex-induced vibration. This phenomenon is commonly known as Von Karman's vortices. Vibration can be initiated when the frequency of vortex shedding corresponds to a natural frequency of the structure or individual member. Vortex-induced vibration is more likely to occur when tubular structures (or components such as tubular arms) are installed without insulators and conductors. When stringing operations do not occur soon after installation of tubular arms, normal practice is to install a weight at the end of the arm or to tie the end the arm to the pole to reduce the possible vibrations due to vortex shedding. Equation E-1 can be used to calculate critical wind speed at which vortex-induced vibration may be initiated.

$$V_{cr} = \frac{fs}{Str} \qquad \text{(E-1)}$$

where
V_{cr} = critical vortex-induced wind speed, in ft/sec
f = structure or member natural frequency, in Hertz
Str = Strouhal number
s = across-wind dimension, in ft

Standard structural shapes have an average Strouhal number of 0.14. Strouhal numbers for a variety of structural shapes can be found in Simiu and Scanlan (1996). The structure's natural frequency can be determined using structural dynamic theory (Clough and Penzien 1975; Mathur et al. 1986; Paz 1980; Trainor et al. 1984). Vortex-induced motion can cause flexural, torsional, or coupled flexural-torsional vibration modes.

Structural shapes (Thrasher 1984) and cable components, such as guy wires and cable tension members, can be excited by vortex-induced vibration. In latticed steel towers, members (which are long and flexible) are particularly susceptible to wind-induced vibration caused by vortex resonance. Although general precautions during the initial design of transmission structures can be considered to reduce the possibility of vortex-induced vibration problems (ASCE 1961), the occurrence of vibration problems is highly dependent upon steady-state wind, terrain, and local conditions.

Large latticed structures for heavy-angle sites and river crossings frequently make use of stitched double-angle members for secondary and bracing members, and these have been found to be very susceptible to torsional flutter in moderate winds. For these double angles, slenderness ratios should not exceed 200. Vibration can be reduced using wind spoilers. One example of a wind spoiler for this application is the insertion of small, flat plates that project beyond the horizontal legs of the angle.

Utilities have experienced failures of the end connection plates or coped connecting members from this wind action. This phenomenon has been well defined by wind tunnel tests.

Solutions to vortex-induced problems developing during the service life of the tower can consist of changing the stiffness of the member, increasing the damping, or by adding a wind-spoiler system. Changing the member cross section or member boundary conditions (connections) can modify the member stiffness.

Although very infrequent in transmission structures, aeroelastic instability of certain structural shapes can be a potential problem. Wind forces acting on a structural shape that is inherently unstable at certain wind angles cause this wind-induced vibration. Additional information can be found in Houghton and Carruthers (1976), MacDonald (1975), Modi and Slater (1983), Sachs (1972), Simiu and Scanlan (1996), and Slater and Modi (1971).

This page intentionally left blank

APPENDIX F

EQUATIONS FOR
GUST RESPONSE FACTORS

F.1 INTRODUCTION

The gust response factor accounts for the load effects due to wind turbulence and dynamic amplification of flexible structures and cables. It represents the cumulative effect or the integration of the gusts and lulls of the wind over the range of span lengths typical of transmission lines, as well as the effect of the wind on the supporting structures. The equations for the gust response factor given in Chapter 2, Section 2.1.5 of this manual are based on equations derived by Davenport (1979) for estimating the response of transmission line systems to gusty winds.

The original Davenport equations were developed from statistical methods that involve the spatial correlation and energy spectrum of gusty winds as well as the dynamic characteristics of the line components. These equations included amplification factors that account for the possible resonant response of wires and the structural system. The decision to omit the resonant response features was noted in the previous (1991) edition of this manual. This decision is based on theoretical appraisal of transmission line behavior as well as the assessment of field-test data. Assumptions can be found in Section F.4.

These equations are based on idealized conditions that may or may not reflect the true weather events that are imposed onto the transmission line structure. Thus, the results obtained by the application of these equations within this context should be considered approximate.

The purpose of this appendix is to present the modified Davenport equations and define the various wind, exposure, and dynamic parameters used in these equations. Most of these parameters are taken directly

from Davenport's paper. However, some have been slightly modified to incorporate the relationships used in the development of ASCE Standard 7-05 (ASCE 2005) wind load criteria that form the basis for much of this manual.

The equations are given in this appendix without derivation. However, interested readers may refer to several papers that have been presented on this subject (Davenport 1961, 1967, 1977, 1979; Vellozzi and Cohen 1968).

F.2 NOTATION

The following notation is used in this appendix:

B_t dimensionless response term corresponding to the quasi-static background wind loading on the structure (see Eq. F-6)

B_w dimensionless response term corresponding to the quasi-static background wind loading on the wires (see Eq. F-4)

C_f force coefficient for the wires (see Chapter 2, Section 2.1.6)

d diameter of wire (conductor or ground wire), in inches

E exposure factor evaluated at the effective height of the wires or structure (see Eq. F-3)

f_t fundamental frequency of the free-standing structure in the transverse direction (see Table F-1), in Hertz

f_w fundamental frequency for horizontal sway of the conductor or ground wire (see Eq. F-9), in Hertz

g_s statistical peak factor dependent on the frequency characteristics of the response and sampling interval (for transmission line response and a 10-min sampling interval of the wind)

G_t gust response factor for structure wind loading (see Eq. F-2)

G_w gust response factor for conductor or ground-wire wind loading (see Eq. F-1)

K_v ratio of the 3-sec gust wind speed to the 10-min average wind speed at the 33-ft (10-m) reference height (see Appendix D)

L_s transverse integral scale of turbulence (see Table F-2), in feet

R_t dimensionless resonant response term of the structure (see Eq. F-7)

R_w dimensionless resonant response term of the wire (see Eq. F-5)

S design wind span, in feet

sag wire sag at mid-span, in feet

V design wind speed, in mph

V_o 10-min average wind speed at the effective height of the wires and structure, in ft/sec

z_g gradient height, in feet

Table F-1. Approximate Dynamic Properties for Transmission
Structures

Type of Structure	Fundamental Frequency (Hz), f_t	Damping Ratio, ζ_t
Latticed Tower	2.0–4.0	0.04
H-Frame	1.0–2.0	0.02
Pole	0.5–1.0	0.02

Table F-2. Exposure Category Constants

Exposure Category	Power Law Exponent Sustained Wind, α_{FM}	Gradient Height, z_g (ft)	Surface Drag Coefficient, κ	Turbulence Scale, L_s (ft)
B	4.5	1,200	0.010	170
C	7.0	900	0.005	220
D	10.0	700	0.003	250

z_h effective height above ground of the wires and/or structure (see
Chapter 2, Section 2.1.4.2)

α_{FM} power law exponent for sustained wind (see Table F-2)

ε approximate coefficient for separation of the conductor and
structure response terms in the general gust response factor
equations (for typical transmission line systems, ε is
approximately equal to 0.75)

κ surface drag coefficient (see Table F-2)

ζ_t structure damping to critical damping ratio (see Table F-1)

ζ_w wire aerodynamic damping to critical damping ratio (see Eq. F-10)

F.3 EQUATIONS

The wire and structure gust response factors, G_w and G_t, respectively,
are given by the following equations:

$$G_w = \left(1 + g_s \varepsilon E (B_w + R_w)^{0.5}\right)/k_v^2 \qquad \text{(F-1)}$$

$$G_t = \left(1 + g_s \varepsilon E (B_t + R_t)^{0.5}\right)/k_v^2 \qquad \text{(F-2)}$$

where g_s = 3.5 to 4.0 (3.6 is a typical value); $\varepsilon \approx 0.75$.

$$E = 4.9 \times (\kappa)^{0.5} \times (33/z_h)^{(1/\alpha_{FM})} \qquad \text{(F-3)}$$

$$B_w = 1/(1 + 0.8 \times S/L_s) \qquad \text{(F-4)}$$

$$R_w = (0.0113/\zeta_w) \times (z_h/S) \times (f_w \times z_h/V_o)^{-5/3} \qquad \text{(F-5)}$$

$$B_t = 1/(1 + 0.56 \times z_h/L_s) \tag{F-6}$$

$$R_t = (0.0123/\zeta_t) \times (f_t \times z_h/V_o)^{-5/3} \tag{F-7}$$

in which

$$V_o = 1.605 \, (z_h/z_g)^{(1/\alpha_{FM})} \times (88/60) \times (V/k_v) \tag{F-8}$$

$$f_w \approx (1/sag)^{0.5} \tag{F-9}$$

$$\zeta_w = 0.000048 \, (V_o/(f_w \times (d/12)) \times C_f \tag{F-10}$$

where C_f, d, f_t, f_w, S, sag, V, V_o, z_h, ζ_t, and ζ_w are given wire, structure, and wind parameters (see Section F.2); α_{FM}, z_g, κ, and L_s are constants listed in Table F-2 that depend on the given exposure category as defined in Chapter 2, Section 2.1.4.1.

The numerator terms in Eqs. F-1 and F-2 are taken directly from the Davenport (1979) gust response factor equations. The term in the denominators of these equations, k_v, is a wind speed conversion factor; see Appendix D. It represents the ratio of the 3-sec gust wind speed to the 10-min average wind speed at 33 ft (10 m) aboveground.

Approximate ranges in the fundamental natural frequency and damping ratio for free-standing suspension structures are given in Table F-1. The natural frequencies in this table are based on a limited review of typical suspension structure dynamic properties and are not intended to be applicable for every of transmission structure type. Since little data is available on damping ratio for transmission line structures, the values given in Table F-1 are conservative estimates for most structure types. Users are encouraged to perform dynamic tests in order to determine the appropriate dynamic properties.

F.4 ASSUMPTIONS

To derive the equations in Chapter 2, Section 2.1.5, some simplifying assumptions were made to the original Davenport equations. These assumptions are listed below.

1. The separation constant, ε, is equal to 0.75 and the statistical peak factor, g_s, is equal to 3.6, which are reasonable approximations for these constants for transmission line systems (Davenport 1979).
2. The resonant response terms for both structure and wire systems, R_t and R_w, can be neglected. This assumption is based on the observation that dynamic response is not present in transmission lines, and

the hypothesis that the peak vibration responses of the conductors, ground wires, and structures are unlikely to coincide with one another. Furthermore, the aerodynamic damping of the conductors and ground wires will significantly reduce their resonant responses such that the quasi-static background response will be the predominant response. For certain structures, users may consider including the resonant responses.

With these assumptions, Eqs. F-1 and F-2 are simplified to Eqs. 2-4 and 2-5 in Chapter 2, respectively. These simplified equations were used to generate the figures of gust response factor givens in Chapter 2, Section 2.1.5. Because the resonant response terms have been neglected, the given values for the gust response factors in Section 2.1.5 will be less than those given by equations in this appendix.

F.5 EXAMPLES

Resonant responses are neglected in these examples.

Structure Gust Response Factor

Assumed structure effective height 59.3 ft (18.1 m) in Exposure C

From Eq. F-2 $G_t = \left(1 + g_s \varepsilon E (B_t + R_t)^{0.5}\right)/k_v{}^2$

where $g_s = 3.6$, $\varepsilon \approx 0.75$, and $k_v = 1.43$.

From Eq. F-3 $E = 4.9 \times (\kappa)^{0.5} \times (33/z_h)^{(1/\alpha_{FM})}$

The value of κ and α_{FM} can be found in Table F-2.

$$E = 4.9 \times (0.005)^{0.5} \times (33/59.3)^{(1/7)} = 0.319$$

From Eq. F-5 $B_t = 1/(1 + 0.56 \times z_h/L_s)$

The value of L_s can be found in Table F-2.

$$B_t = 1/(1 + 0.56 \times 59.3/220) = 0.869$$

Assumed R_t can be neglected (see Section F.4); thus

$$G_t = \left(1 + g_s \varepsilon E (B_t + R_t)^{0.5}\right)/k_v{}^2$$
$$= \left(1 + 3.6 \times 0.75 \times 0.319 \times (0.869 + 0)^{0.5}\right)/(1.43^2) = 0.882$$

Wire Response Factor

Assumed wire effective height 80.0 ft (24.4 m) in Exposure C. Span length = 1,250 ft

From Eq. F-1 $G_w = \left(1 + g_s \varepsilon E (B_w + R_w)^{0.5}\right) / k_v^{2}$

where $g_s = 3.6$, $\varepsilon \approx 0.75$, and $k_v = 1.43$.

From Eq. F-3 $E = 4.9 \times (\kappa)^{0.5} \times (33/z_h)^{(1/\alpha_{FM})}$

The values of κ and α_{FM} can be found in Table F-2.

$$E = 4.9 \times (0.005)^{0.5} \times (33/80.0)^{(1/7)} = 0.305$$

From Eq. F-4 $B_w = 1 / (1 + 0.8 \times S / L_s)$

The value of L_s can be found in Table F-2.

$$B_w = 1 / (1 + 0.8 \times 1,250/220) = 0.180$$

Assumed R_w can be neglected (see Section F.4); thus

$$G_w = \left(1 + g_s \varepsilon E (B_w + R_w)^{0.5}\right) / k_v^{2}$$
$$= \left(1 + 3.6 \times 0.75 \times 0.305 \times (0.180 + 0)^{0.5}\right) / (1.43^2) = 0.660$$

APPENDIX G

SUPPLEMENTAL INFORMATION ON FORCE COEFFICIENTS

G.1 CONDUCTOR AND GROUND WIRE FORCE COEFFICIENTS

Wind tunnel test data, such as those shown in Fig. G-1, indicate that measured force coefficients for stranded wires can vary over a wide range depending on Reynolds number and the type of stranding. For this reason, there is also a wide variation in values recommended by the various design codes and guides as illustrated in Fig. G-2.

A force coefficient of 1.0 is recommended in Chapter 2, Section 2.1.6.2.1 for all conductors and ground wires. This is the same value recommended in NESC (2007). The data in Fig. G-1 indicate that the force coefficient can be significantly greater than 1.0, particularly for Reynolds numbers less than 3×10^4 (small wires under nominal wind speed). For Reynolds numbers above this value, the force coefficients are reduced to a value of 1.0 or less. For a 0.5-in.-diameter wire or larger, the Reynolds number will exceed 3×10^4 for the range of design wind speeds given in Chapter 1, Fig. 1-1. For this reason, a value of 1.0 has been chosen for all conductors and ground wires. However, force coefficients larger than 1.0 are often appropriate, especially on small-diameter (< ~0.5-in.) wire and wires with an ice coating.

G.2 MEMBER FORCE COEFFICIENTS

Table 2-6 in Chapter 2 lists force coefficients recommended for some common structural shapes used in pole and H-frame type transmission structures. Table G-1 lists force coefficients from various sources for these
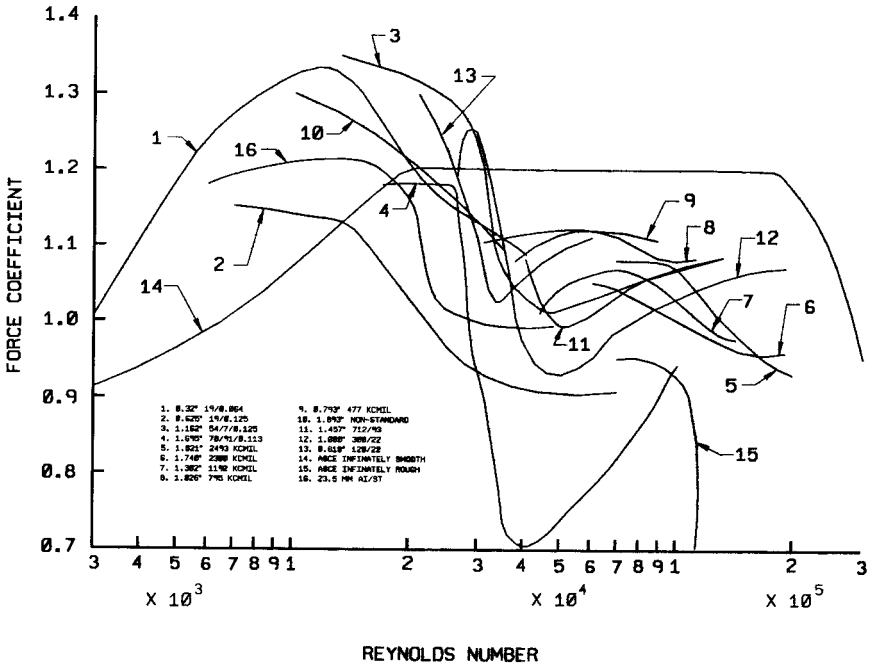
Figure G-1. Force coefficients for conductors based on wind tunnel tests. Sources: ASCE (1961); Birjulin et al. (1960); Castanheta (1970); Engleman and Marihugh (1970); Richards (1965); Watson (1955).

members and for additional shapes not shown in Table 2-6. For some shapes, values are given corresponding to variations in surface roughness, Reynolds number, corner radius ratio, yaw angle, or test conditions.

The force coefficients of unsymmetrical shapes are dependent on the wind direction with respect to the member's cross sections. No general equation exists for this condition; however, values have been determined by testing. These are shown in Table G-2.

G.3 ASPECT RATIO

The force coefficients given in Chapter 2, Section 2.1.6.2 and in Section G.2 above are for infinitely long members and are applicable to members with aspect ratios greater than 40. Adjustment factors for members with aspect ratios less than 40 may be applied as follows (MacDonald 1975):

$$C_f = (c)(C_f') \qquad \text{(G-1)}$$
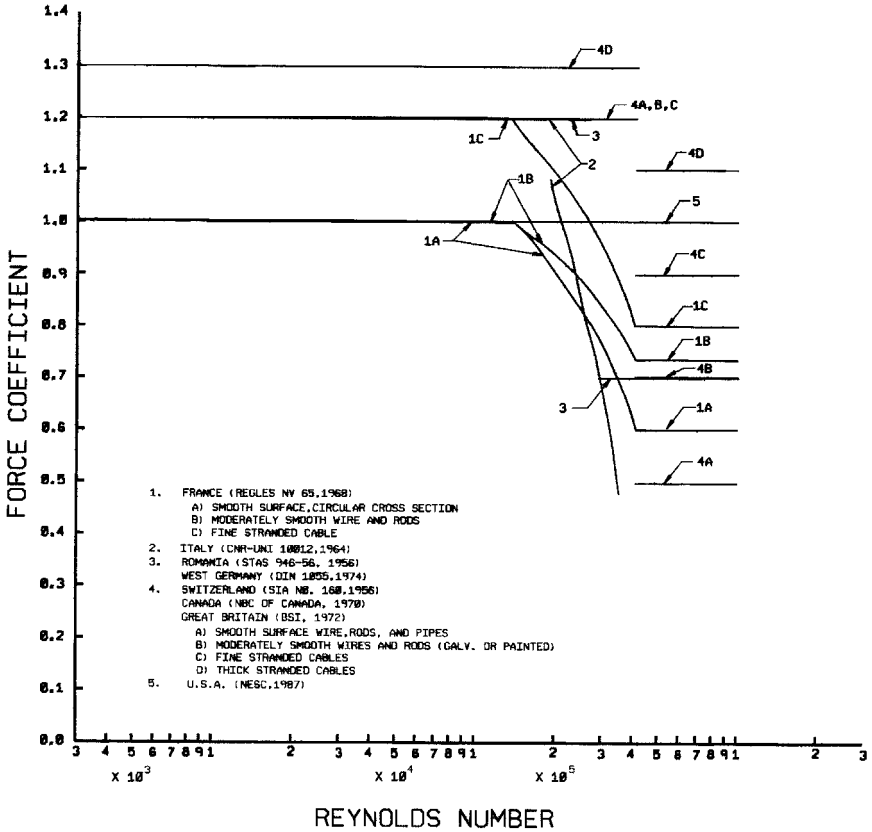
Figure G-2. Force coefficients for conductors based on code values.

where
c = correction factor from Table G-2
C'_f = force coefficient from Section 2.1.6.2 or Section G.2.

G.4 LATTICED TRUSS STRUCTURE FORCE COEFFICIENTS

The force coefficients given in Tables 2-4 and 2-5 in Chapter 2 of this guide represent the recommended values for square-section and triangular-section latticed structures having flat- and round-shaped members, respectively. The force coefficients in these tables, which were taken directly from ASCE Standard 7–88 (ASCE 1990b), account for the wind forces acting on the windward and leeward faces of the latticed tower. Therefore, they are influenced by the solidity ratio as defined by Eq. 2-10

Table G-1. Member Force Coefficients

PROJ. AREA = s x LENGTH

WIND

s
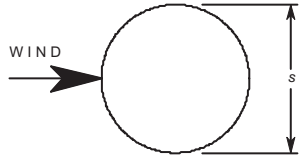
Circle Surface	Reynolds Number	Force Coefficient	Reference
Any	$<3.5 \times 10^5$	1.2	Scruton and Newberry, 1963
Any	$<4.1 \times 10^5$	1.2	MacDonald, 1975
Smooth	—	0.7	ASCE, 1990a
Smooth	$<10^5$	1.0	Sachs, 1978
Smooth	$<3.0 \times 10^5$	1.1	AASHTO, 1975
Smooth	$>3.5 \times 10^5$	0.7	Scruton and Newberry, 1963
Smooth	$>4.1 \times 10^5$	0.6	MacDonald, 1975
Smooth	$3 \times 10^5 < R < 6 \times 10^5$	$14.5 \times 10^6/R^{1.3}$	AASHTO, 1975
Smooth	$>6.0 \times 10^5$	0.45	AASHTO, 1975
Rough	$>4.1 \times 10^5$	1.2	MacDonald, 1975
Rough	—	0.9	ASCE, 1990a
Very rough	$>3.5 \times 10^5$	1.0	Scruton and Newberry, 1963
Very rough	—	1.2	ASCE, 1990a

PROJ. AREA = s x LENGTH
r = RADIUS OF CORNERS
R_c = RADIUS OF INSCRIBED CIRCLE

WIND

s
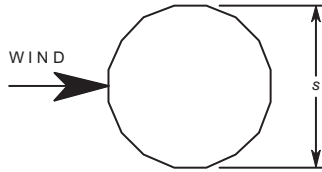
16-Sided Polygon

Corner Radius (r/R_c)	Reynolds Number	Force Coefficient	Reference
<0.26	$>6.0 \times 10^5$	$0.83–1.08(r/R_c)$	James, 1976
>0.26	$>6.0 \times 10^5$	0.55	James, 1976

PROJ. AREA = s x LENGTH
r = RADIUS OF CORNERS
R_c = RADIUS OF INSCRIBED CIRCLE

WIND

s
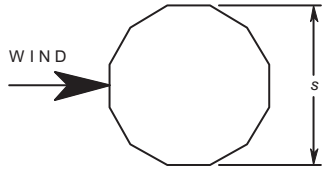
12-Sided Polygon

Corner Radius (r/R_c)	Reynolds Number	Force Coefficient	Reference
0	$<3.5 \times 10^5$	1.3	Scruton and Newberry, 1963
0	$<8.2 \times 10^5$	1.3	MacDonald, 1975
0	$>3.5 \times 10^5$	1.0	Scruton and Newberry, 1963
0	$>8.2 \times 10^5$	1.1	MacDonald, 1975
$0.09 < r/R_c < 0.34$	$>10^6$	$0.936–1.087(r/R_c)$	James, 1976
>0.125	$<3.0 \times 10^5$	1.2	AASHTO, 1975
>0.125	$3.0 \times 10^5 < R < 6.0 \times 10^5$	$2,322/R^{0.6}$	AASHTO, 1975
>0.125	$>6.0 \times 10^5$	0.79	AASHTO, 1975
>0.34	$>10^6$	0.57	James, 1976

PROJ. AREA = s x LENGTH
r = RADIUS OF CORNERS
R_c = RADIUS OF INSCRIBED CIRCLE

WIND
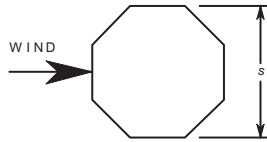
8-Sided Polygon

Corner Radius (r/R_c)	Reynolds Number	Force Coefficient	Reference
0	—	1.2	AASHTO, 1975
0	—	1.4	ASCE, 1990; MacDonald, 1975
$0.09 < r/R_c < 0.59$	$>10^6$	$1.422–1.368(r/R_c)$	James, 1976
>0.59	$>10^6$	$0.744–0.194(r/R_c)$	James, 1976

PROJ. AREA = s x LENGTH

WIND

2s
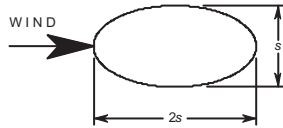
Ellipse, Wind on Narrow Side

Sides	Reynolds Number	Force Coefficient	Reference
Smooth	$<6.9 \times 10^5$	0.7	MacDonald, 1975
Smooth	$>6.9 \times 10^5$	0.2	MacDonald, 1975
Multi-sided	—	$(C/3)(4 - D/d)$	AASHTO, 1975
Where:	D = major diameter		
	d = minor diameter		
	$D/d = 2.0$		
	C = force coefficient of cylindrical shape with		
	diameter equal to D		
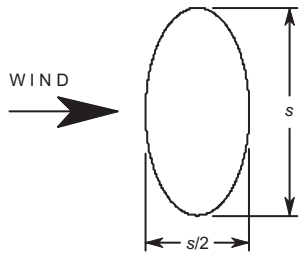
PROJ. AREA = s x LENGTH

Ellipse, Wind on Broad Side

Sides	Reynolds Number	Force Coefficient	Reference
Smooth	$<5.5 \times 10^5$	1.7	MacDonald, 1975
Smooth	$>5.5 \times 10^5$	1.5	MacDonald, 1975
Multi-Sided	—	$1.7(D/d - 1) + C(2 - D/d)$	AASHTO, 1975
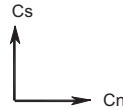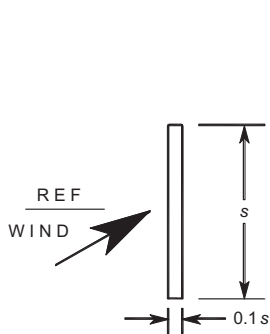
PROJ. AREA = s x LENGTH
C_n = COEFFICIENT NORMAL TO THE SURFACE
C_s = COEFFICIENT 90° to C_n

Flat Plate

Angle	Cn	Cs	Reference
0	2.0	0.0	Scruton and Newberry, 1963 Sachs, 1978
45	1.8	0.1	Sachs, 1978
90	0.0	0.1	Sachs, 1978

PROJ. AREA = s x LENGTH
Cn = COEFFICIENT NORMAL TO THE SURFACE
Cs = COEFFICIENT 90° to Cn
r = RADIUS OF CORNERS
R_c = RADIUS OF INSCRIBED CIRCLE
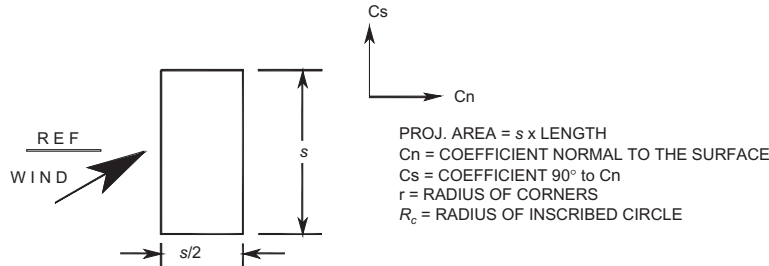
Rectangle

Corner Radius (r/R_c)	Angle	Cn	Cs	Reference
0	0	2.2	0.0	Scruton and Newberry, 1963
0	0	2.1	0.0	Sachs, 1978
0	45	1.4	0.7	Sachs, 1978
0	90	0.0	0.75	Sachs, 1978
0.08	0	1.9	0.0	MacDonald, 1975
0.25	0	1.6	0.0	Scruton and Newberry, 1963

PROJ. AREA = s x LENGTH
r = RADIUS OF CORNERS
R_c = RADIUS OF INSCRIBED CIRCLE
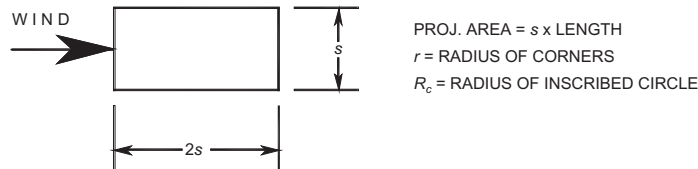
Rectangle

Corner Radius (r/R_c)	Reynolds Number	Force Coefficient	Reference
0.0	—	1.4	Scruton and Newberry, 1963
0.167	—	0.7	MacDonald, 1975
0.5	—	0.4	Sachs, 1978
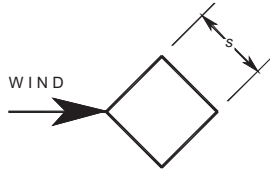
PROJ. AREA = 1.414 x s x LENGTH
r = RADIUS OF CORNERS
R_c = RADIUS OF INSCRIBED CIRCLE

Square, Wind at Apex

Corner Radius (r/R_c)	Reynolds Number	Force Coefficient	Reference
0.0	—	1.5	ASCE, 1990b
			Scruton and Newberry, 1963
0.33	$<6.86 \times 10^5$	1.5	MacDonald, 1975
0.33	$>6.86 \times 10^5$	0.6	MacDonald, 1975
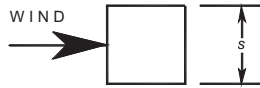
PROJ. AREA = s x LENGTH
r = RADIUS OF CORNERS
R_c = RADIUS OF INSCRIBED CIRCLE

Square, Wind at Side

Corner Radius (r/R_c)	Reynolds Number	Force Coefficient	Reference
0.0	—	2.0	ASCE, 1990b
			Scruton and Newberry, 1963
0.167	$<6.86 \times 10^5$	1.3	MacDonald, 1975
0.167	$>6.86 \times 10^5$	0.6	MacDonald, 1975
0.33	$<2.7 \times 10^5$	1.0	MacDonald, 1975
0.33	$>2.7 \times 10^5$	0.5	MacDonald, 1975

Table G-1. *Continued*

PROJ. AREA = s x LENGTH
Cn = COEFFICIENT NORMAL TO THE SURFACE
Cs = COEFFICIENT 90° to Cn
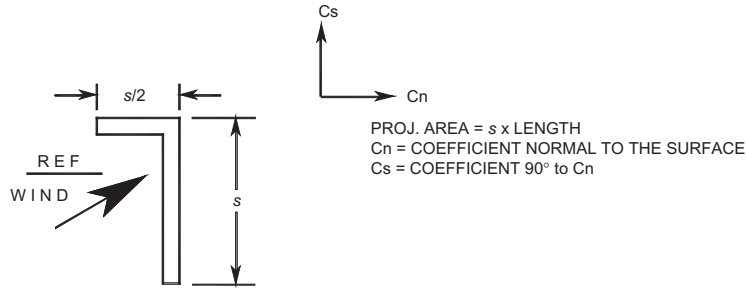
Unequal Leg Angle

Angle	Cn	Cs	Reference
0	1.9	0.95	Sachs, 1978
45	1.8	0.8	Sachs, 1978
90	2.0	1.7	Sachs, 1978
135	−1.8	−0.1	Sachs, 1978
180	−2.0	0.1	Sachs, 1978
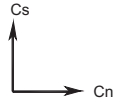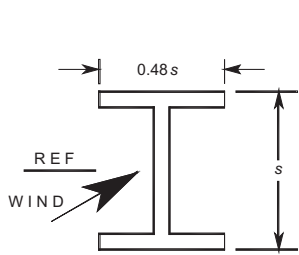
PROJ. AREA = s x LENGTH
Cn = COEFFICIENT NORMAL TO THE SURFACE
Cs = COEFFICIENT 90° to Cn

I-Beam

Angle	Cn	Cs	Reference
0	2.05	0.0	Sachs, 1978
45	1.95	0.6	Sachs, 1978
90	0.5	0.9	Sachs, 1978
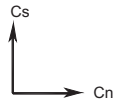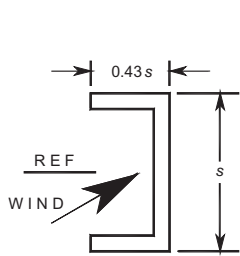
PROJ. AREA = s x LENGTH
Cn = COEFFICIENT NORMAL TO THE SURFACE
Cs = COEFFICIENT 90° to Cn

Channel

Angle	Cn	Cs	Reference
0	2.05	0.0	Sachs, 1978
45	1.85	0.6	Sachs, 1978
90	0.0	0.6	Sachs, 1978
135	−1.6	0.4	Sachs, 1978
180	−1.8	0.0	Sachs, 1978

PROJ. AREA = s x LENGTH
Cn = COEFFICIENT NORMAL TO THE SURFACE
Cs = COEFFICIENT 90° to Cn

Wide Flange

Angle	Cn	Cs	Reference
0	1.6	0.0	Sachs, 1978
45	1.5	1.5	Sachs, 1978
90	0.0	1.9	Sachs, 1978

PROJ. AREA = s x LENGTH
Cn = COEFFICIENT NORMAL TO THE SURFACE
Cs = COEFFICIENT 90° to Cn
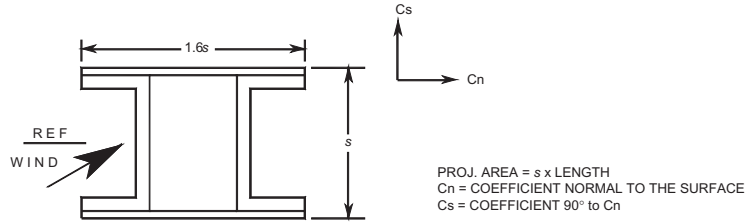
Built-Up Section

Angle	Cn	Cs	Reference
0	1.4	0.0	Sachs, 1978
45	1.2	1.6	Sachs, 1978
90	0.0	2.2	Sachs, 1978
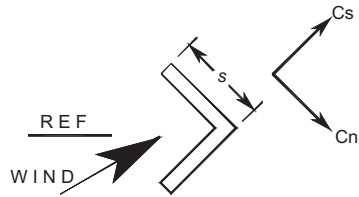
PROJ. AREA = s x LENGTH
Cn = COEFFICIENT NORMAL TO THE SURFACE
Cs = COEFFICIENT 90° to Cn

Equal Leg Angle

Angle	Cn	Cs	Reference
0	1.8	1.8	Sachs, 1978
45	2.1	1.8	Sachs, 1978
90	−1.9	−1.0	Sachs, 1978
135	−2.0	0.3	Sachs, 1978
180	−1.4	−1.4	Sachs, 1978
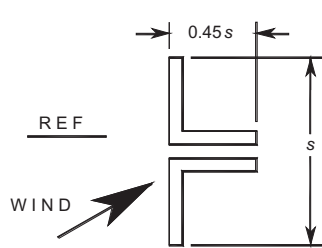
PROJ. AREA = s x LENGTH
Cn = COEFFICIENT NORMAL TO THE SURFACE
Cs = COEFFICIENT 90° to Cn

Double Angle

Angle	Cn	Cs	Reference
0	1.6	0.0	Sachs, 1978
45	1.5	−0.1	Sachs, 1978
90	−0.95	0.7	Sachs, 1978
135	−0.5	1.05	Sachs, 1978
180	−1.5	0.0	Sachs, 1978

Table G-1. *Continued*

PROJ. AREA = s x LENGTH
Cn = COEFFICIENT NORMAL TO THE SURFACE
Cs = COEFFICIENT 90° to Cn
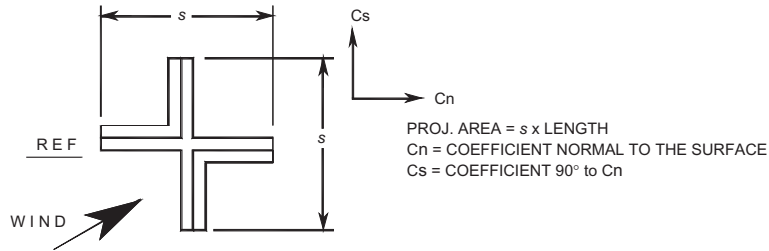
Built-Up Angles

Angle	Cn	Cs	Reference
0	1.75	0.1	Sachs, 1978
45	0.85	0.85	Sachs, 1978
90	−0.1	1.75	Sachs, 1978
135	−0.75	0.75	Sachs, 1978
180	−1.75	−0.1	Sachs, 1978

REF

WIND

PROJ. AREA = s x LENGTH
Cn = COEFFICIENT NORMAL TO THE SURFACE
Cs = COEFFICIENT 90° to Cn
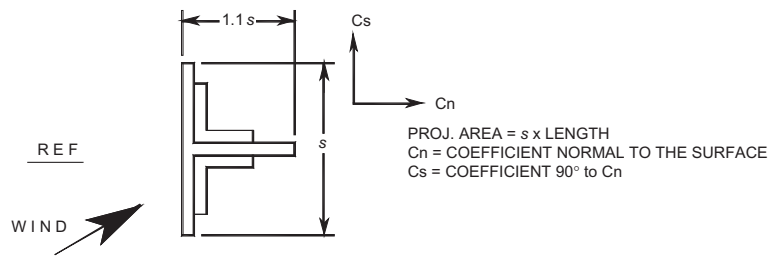
Tee Section

Angle	Cn	Cs	Reference
0	2.0	0.0	Sachs, 1978
45	1.2	0.9	Sachs, 1978
90	−1.6	2.15	Sachs, 1978
135	−1.1	2.4	Sachs, 1978
180	−1.7	2.1	Sachs, 1978

Table G-2. Aspect Ratio Correction Factors

Aspect Ratio	Correction Factor (c)
0–4	0.6
4–8	0.7
8–40	0.8
>40	1.0

Aspect ratio = L_m/s except for members attached to the ground where aspect ratio = $2L_m/s$, in which L_m = member length and s = member diameter or width.
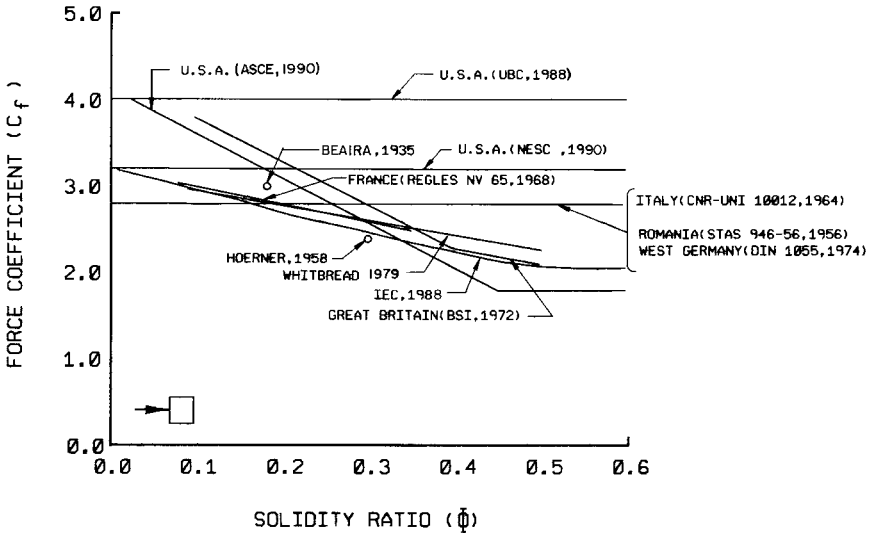
Figure G-3. Force coefficients for square-section towers having flat-sided members with face-on wind.

in Section 2.1.6-1 of this guide. As the solidity ratio increases, the force coefficient is reduced due to the shielding effect of the members in the windward face(s) of the tower.

Figures G-3 through G-6 provide information from various other codes, standards, and tests for force coefficients for latticed towers with face-on wind. These figures are for towers having either square or triangular cross sections and comprised of flat-sided or round-section members.

Figures G-7 through G-10 provide information from various codes and standards for force coefficients with yawed winds. These figures are for latticed tower structures having either square or triangular cross sections, and comprised of flat-sided or round-section members. Whitbread (1979) has published other data relating to wind forces on latticed towers having a wide variety of shapes, solidity ratios, and wind directions.
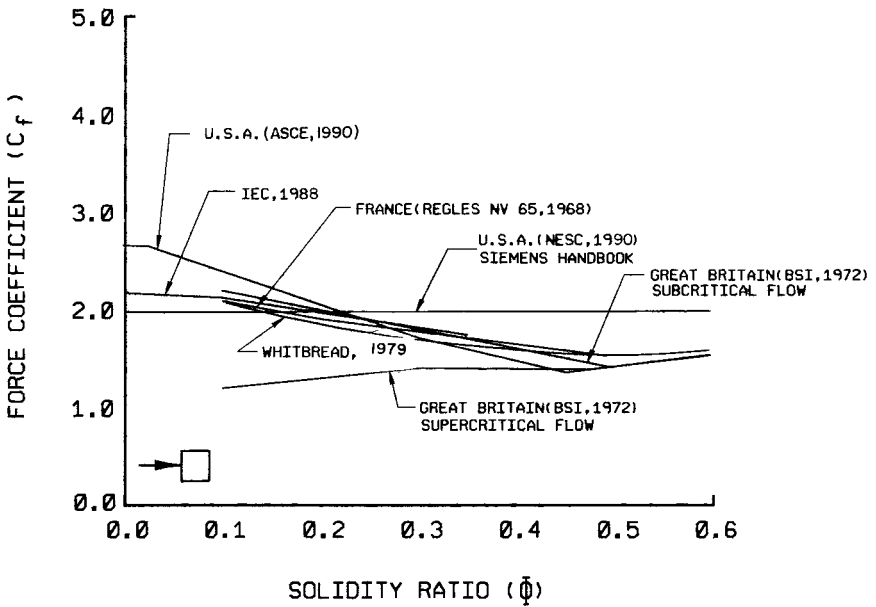
Figure G-4. Force coefficients for square-section towers having round-section members with face-on wind.
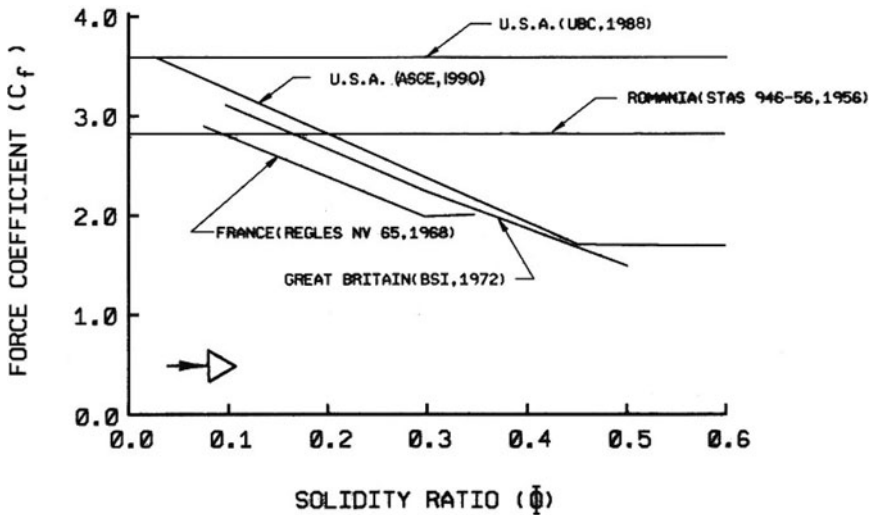
Figure G-5. Force coefficients for equilateral triangular-section towers having flat-sided members with wind normal to a face.
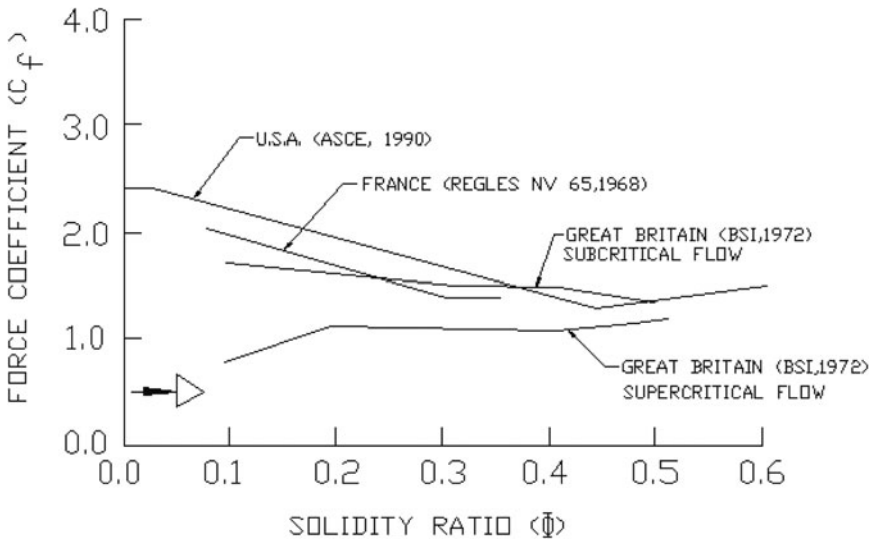
Figure G-6. Force coefficients for equilateral triangular-section towers having round-section members with wind normal to a face.
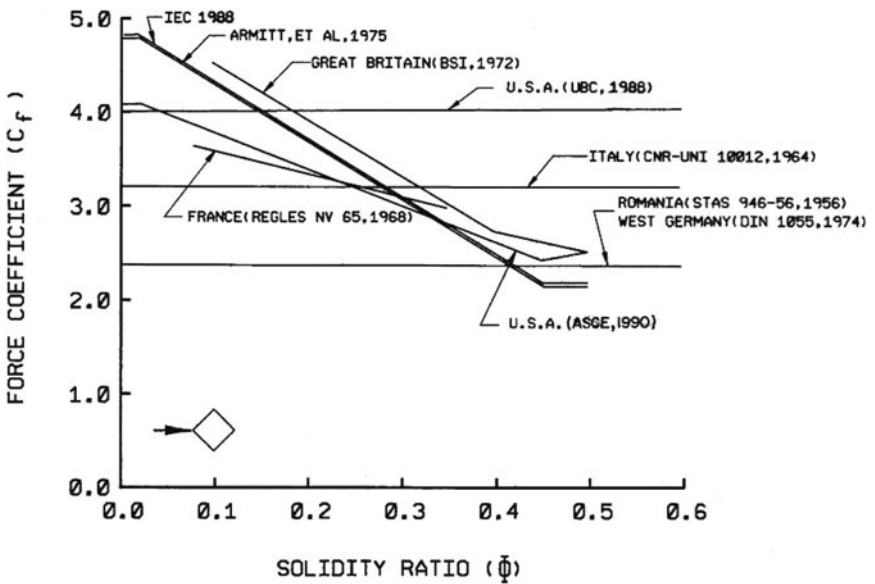
Figure G-7. Force coefficients for square-section towers having flat-sided members with diagonal wind.
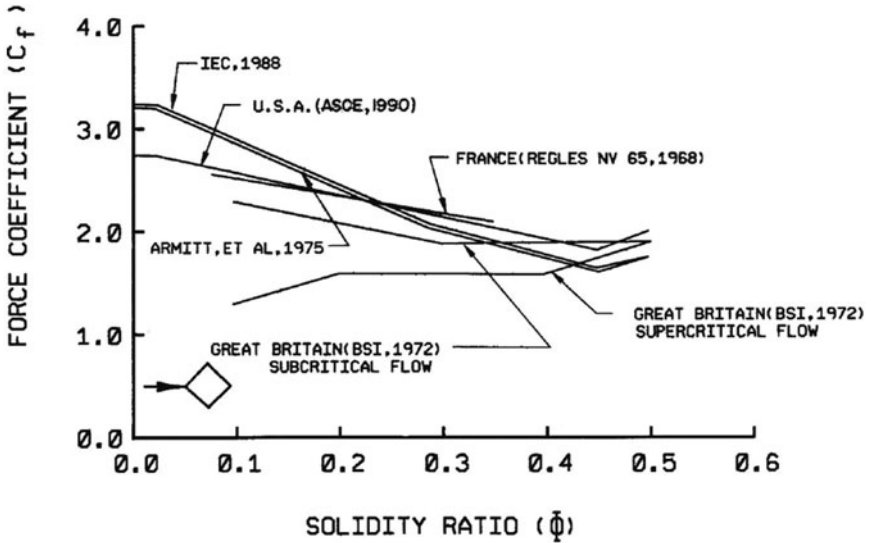
Figure G-8. Force coefficients for square-section towers having round-section members with diagonal wind.
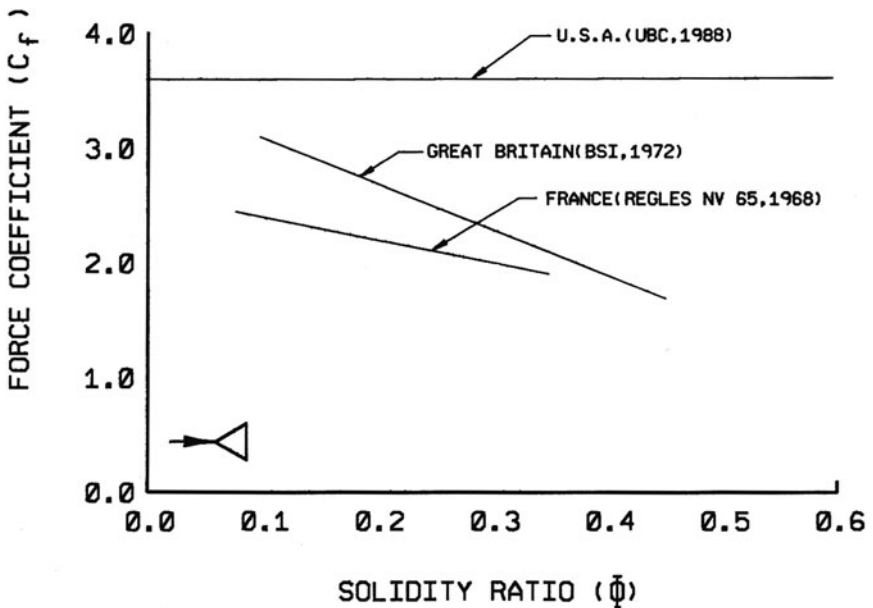
Figure G-9. Force coefficients for equilateral triangular-section towers having flat-sided members with wind onto a corner.
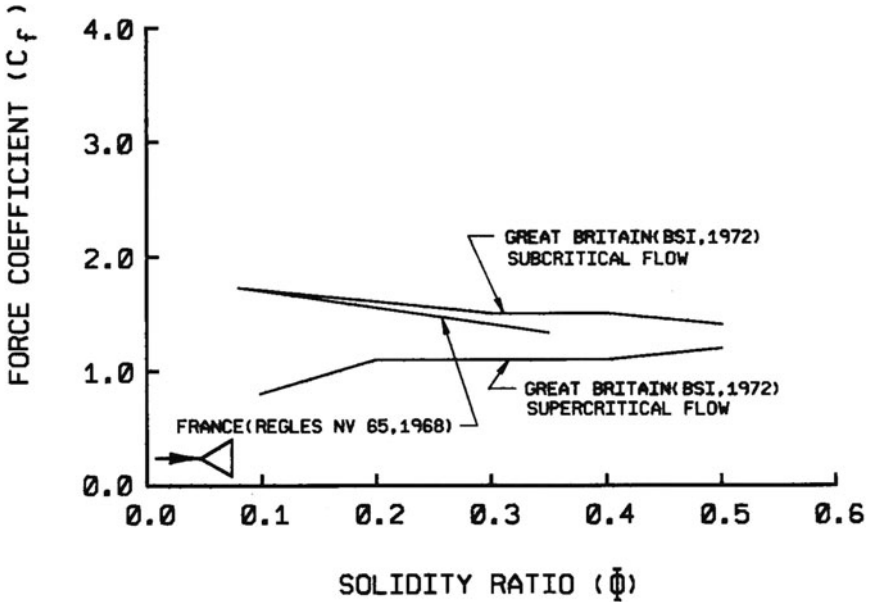
Figure G-10. Force coefficients for equilateral triangular-section towers having round-section members with wind onto a corner.

G.5 FORCE COEFFICIENTS OF ICED COMPONENTS

Both the International Standards Organization (ISO) and the International Electrotechnical Commission (IEC) suggest force coefficients of from 1.0 to 1.4 for wires covered with glaze or precipitation icing.

APPENDIX H

SUPPLEMENTAL INFORMATION ON ICE LOADING

H.1 THEORY AND CONDITIONS OF ICE FORMATION

In a general sense, the meteorological parameters that influence the type and amount of ice that forms under different conditions are well known. Liquid water content of supercooled clouds and precipitation intensity for freezing precipitation icing and sticky snow determine the amount of water available for ice formation. The ice properties are determined by the air temperature, wind speed, drop size, and supercooled liquid water content of clouds or fog or precipitation intensity and type. The icing phenomenon is best classified by the meteorological conditions that produce it. In the following paragraphs the various icing mechanisms are described because it is important for the engineer to understand the conditions that may cause severe loads on transmission lines.

H.1.1 Precipitation Icing

Freezing rain (or drizzle) is a common icing mechanism. Freezing rain occurs when warm, moist air is forced over a layer of subfreezing air at the Earth's surface. The precipitation usually begins as snow that melts as it falls through the layer of warm air aloft. The drops cool as they fall through the cold surface air layer and freeze on contact with structures or the ground to form glaze ice. Upper air data indicate that the cold surface air layer is typically between 1,000 ft (300 m) and 3,900 ft (1,200 m) thick (Young 1978), averaging 1,600 ft (500 m) (Bocchieri 1980). The warm air layer aloft averages 5,000 ft (1,500 m) thick in freezing rain, but in freezing drizzle the entire temperature profile may be below

32°F (0°C) (Bocchieri 1980). Precipitation associated with slowly moving frontal systems can alternate between snow and freezing rain to form a composite snow-glaze accretion on structures. The density of glaze is usually assumed to be 56 or 57 pcf (900 kg/m^3).

In freezing rain, the water impingement rate is often greater than the freezing rate. The excess water starts to drip off and may freeze as icicles, resulting in a variety of accretion shapes that range from a smooth, cylindrical sheath, through a crescent on the windward side with icicles hanging on the bottom, to large, irregular protuberances. The shape of a glaze accretion depends on the varying meteorological factors and the cross-sectional shape of the structural member or component, its spatial orientation, and flexibility.

H.1.2 In-Cloud Icing

This icing condition occurs when supercooled cloud or fog water droplets, 100 μm or less in diameter, collide with a structure. It occurs in mountainous areas where adiabatic cooling causes saturation of the atmosphere to occur at temperatures below freezing, in free air in supercooled clouds, and in supercooled fogs that exist in a stable air mass caused by a strong temperature inversion. Significant accumulations of ice can result. Large concentrations of supercooled droplets are not common at air temperatures below about 0°F (−18°C).

In-cloud icing forms rime or glaze ice with a density between about 10 and 56 pcf (150 to 900 kg/m^3). If the heat of fusion that is released by the freezing droplets is removed by convective and evaporative cooling faster than it is released, the droplets freeze on impact. The degree to which the droplets spread as they collide and then freeze governs how much air is incorporated in the accretion and, thus, its density. If the cooling rate is relatively low, not all the colliding droplets freeze. The resulting accretion will be clear or opaque ice, possibly with attached icicles.

The collision efficiency of a structure is defined as the fraction of cloud droplets in the volume swept out by the structure that actually collide with it. The basic theory of the collision efficiency of smooth, circular cylinders perpendicular to the flow of droplets carried by a constant wind was developed by Langmuir and Blodgett (1946). Collision efficiency increases with wind speed and droplet diameter and decreases as the diameter of the cylinder increases. For a given wind speed and droplet size, the theory defines a critical cylinder diameter beyond which accretion will not occur. This concept of a critical diameter has been confirmed by observation. Formulae for calculating collision efficiencies, based on an updated numerical analysis, are provided in Finstad and Lozowski (1988).

The amount of ice accreted during in-cloud icing depends on the duration of the icing condition and the wind speed, as well as on the liquid

water content and the size of the droplets in the supercooled clouds or fog. If, as often occurs, wind speed increases and air temperature decreases with height above ground, larger amounts of ice will accrete on higher structures. The accretion shape depends on the flexibility of the structural member or component. If it is free to rotate, such as a long guy or a long span of a single conductor or wire, the ice accretes with a roughly circular cross section. On more rigid structural members and components, the ice forms in pennant shapes extending into the wind.

H.1.3 Snow

Sticky snow that falls on a round cross-sectional structural member or component (such as a wire, cable, conductor, or guy) may deform and/or slide around it, as a result of either its own weight or aerodynamic lift. Because of the shear and tensile strength of the snow resulting from capillary forces, interparticle freezing (Colbeck and Ackley 1982), and/or sintering (Kuroiwa 1962), the accreting snow may not fall off the structural member during this process. Ultimately, the snow forms a cylindrical sleeve, even around bundled conductors and wires. The formation of the snow sleeve is enhanced by torsional rotation of flexible structural members or components because of the eccentric weight of the snow. The density of accreted snow ranges from below 5 up to 50 pcf (80 to 800 kg/m^3) and may be much higher than the density of the same snowfall on the ground.

Damaging snow accretions have been observed at surface air temperatures ranging from the low 20s up to about 36°F (−5° to 2°C). Snow with a high moisture content appears to stick more readily than drier snow. Snow falling at a surface air temperature above 32°F (0°C) may accrete even at wind speeds above 25 mph (10 m/s), producing dense [37- to 50-pcf (600- to 800- kg/m^3)] accretions. Snow with a lower moisture content is not as sticky, blowing off the structure in high winds. These accreted snow densities are typically between 2.5 and 16 pcf (40 and 250 kg/m^3) (Kuroiwa 1965). Even apparently dry snow can accrete on structures (Gland and Admirat 1986). The cohesive strength of the dry snow is initially supplied by the interlocking of the flakes, and ultimately by sintering, as molecular diffusion increases the bond area between adjacent snowflakes. These dry snow accretions appear to form only in very low winds and have densities estimated at between 5 and 10 pcf (80 to 150 kg/m^3) (Sakamoto et al. 1990; Peabody 1993).

H.1.4 Hoarfrost

Hoarfrost is an accumulation of ice crystals formed by direct deposition of water vapor from the air onto a structure. Because it forms when air

with a dew point below freezing is brought to saturation by cooling, hoarfrost is often found early in the morning after a clear, cold night. It is feathery in appearance and typically accretes up to about an inch (25 mm) in thickness with very little weight. Hoarfrost does not constitute a significant loading problem.

H.2 LOADING IMBALANCES

Unbalanced loads from in-cloud icing may be significant (White 1999). Because the rime density and thickness increase with wind speed, significant differences in ice loading can occur from one span to the next where the transmission line crosses a ridge, hill, or escarpment. This can result in a severe loading imbalance in the line, particularly if adjacent span lengths are significantly different. When a transmission line is to be located in a region where in-cloud icing occurs, the engineer would benefit from consulting a meteorologist to determine the severity and extent of the ice loads. With this information, the engineer can either relocate the line to reduce the exposure, or identify line sections with the greatest risk for in-cloud icing and design these sections accordingly.

Snow accretions may shed from wires in the process of formation, before forming a cylindrical sleeve around the wire. Low-density snow accretions formed in light winds may shed when the wind speed increases. When snow sheds from some but not all spans, the still-loaded spans will pull slack from the unloaded spans and the wire may sag down to the ground. This is more likely to occur when there is a thick layer of accumulated snow on the ground. Although this causes a clearance problem, the associated unbalanced loads are usually small.

Variations in ice loading during precipitation icing are typically gradual along the length of a transmission line. Therefore, unequal icing of adjacent spans is not significant.

Unbalanced longitudinal loadings associated with ice dropping or unequal ice formation on adjacent spans depend on the relationships between available slack, insulator lengths, and other factors. They have been found to be small in some cases (Cluts and Angelos 1977). Suggestions for the determination of unbalanced ice loads can be found in IEC Standard 60286 (IEC 2003) and the various national options of CENELEC Standard EN 50341 (CENELEC 2001).

H.3 ICE ACCRETION DATA AND MODELING

There is very little data in North America on equivalent uniform ice thicknesses from natural ice accretions on overhead lines. Therefore, ice loading studies often rely on mathematical models based on the physics

of the various types of icing and on meteorological data (precipitation amount and type, temperature, and wind speed) that are required as input to these models. Results from an ice accretion analysis typically give calculated ice thicknesses for past storms in which freezing precipitation has occurred. An extreme value analysis can then be applied to determine I_{RP}. Wind speeds during and after periods of freezing precipitation can also be extracted from the meteorological data base and analyzed to determine the wind speed to apply concurrently with I_{RP}.

There are a number of ice accretion models available that use weather data to determine accreted ice loads, including the conservative Simple model (Jones 1996a, 1998), similar to the Goodwin model (Goodwin et al. 1983), the U.S. Army Cold Regions Research and Engineering Laboratory (CRREL) model (Jones 1996b), the Makkonen model (Makkonen 1996), the Meteorological Research Institute (MRI) model (MRI 1977), and the Chaîné model (Chaîné and Castonguay 1974).

1. The Simple model determines the ice thickness, I, from the amount of freezing rain and the wind speed. I does not depend on the air temperature because it is assumed that all the available precipitation freezes, and I also does not depend on the wire diameter.
2. The CRREL model is less conservative than the Simple model, using a heat-balance calculation to determine how much of the impinging precipitation freezes directly to the wire and how much of the runoff water freezes as icicles. It calculates smaller ice loads than the Simple model when the air temperature is near freezing and wind speeds are relatively low; however, water that does not freeze immediately may freeze as icicles as it drips off the wire. The CRREL model requires the user to specify the diameter of the wire on which the accretion of ice is to be modeled. However, this model, like the MRI and Makkonen models, shows very little dependence of ice thickness on wire diameter.
3. The MRI model tends to determine smaller ice loads than the CRREL model because water that does not freeze immediately is ignored, rather than being allowed to freeze to form icicles. However, in using that model or the Goodwin model, the user is required to specify the fall speed of the rain drops and the model results depend significantly on the speed that is chosen. The MRI model also determines accreted snow loads and in-cloud icing loads; however, many of the significant parameters, including droplet size and liquid water content of the supercooled clouds, rime accretion density, and the snow sticking fraction and snow accretion density must be chosen by the user.
4. The Makkonen model for ice accretion in freezing rain tends to be almost as conservative as the Simple model, primarily because it assumes that a significant portion of the water that does not freeze

immediately is incorporated in the accretion. Thus, there is relatively little water available to freeze as icicles.

5. The Chaîné model is based on wind tunnel tests that were done by Stallabrass and Hearty (1967) to investigate sea-spray icing. A number of assumptions and extrapolations are made to mold these data into a formulation for freezing rain, and the results indicate a significant variation of uniform radial ice thickness with wire diameter.

There have been some attempts at model validation. Felin (1988) compared measured maximum ice thicknesses on cylinders of Hydro Quebec's Passive Ice Meters (PIMs) with MRI model results, assuming a drop fall speed of 9 mph (4.1 m/s). Yip and Mitten (1991) compared 61 PIM measurements with Chaîné, Makkonen, MRI, and Goodwin model results using weather data at nearby weather stations. Yip (1993) used annual maximum ice thickness data from 235 PIM sites from 1974 to 1990 and compared the factored ice thicknesses to annual maxima from the Chaîné model. Jones (1996b) compared the measured ice load on a horizontal cylinder in a single freezing rain storm with Chaîné, MRI, Makkonen, Simple, and CRREL model ice loads using collocated weather data. Newfoundland and Labrador Hydro et al. (CEA 1998) reported on the results of a 4-year Canadian Electrical Association (CEA) study comparing ice loads on three test spans with ice loads determined from the Chaîné, Makkonen, and MRI models using weather data measured at the test spans in 22 storm events. In all these comparisons, the ice accretion models as well as the user interface between the weather data and the model, and the assumptions made in determining the equivalent uniform radial ice thickness from the ice measurements, were tested.

An alternative approach to using meteorological data and ice accretion models is to establish ice and wind measurement stations at several locations in the utility's service area. The uniform radial thickness can be determined from the typical cross-sectional area A_i of the ice accretion on a wire of diameter d

$$I = -\frac{d}{2} + \left(\frac{d^2}{4} + \frac{A_i}{\pi} \right)^{1/2}$$

or from the mass, m_i, of a typical ice sample of length L:

$$I = -\frac{d}{2} + \left(\frac{d^2}{4} + \frac{m_i}{\pi \rho_i L} \right)^{1/2}$$

where ρ_i is the ice density.

In determining ice thicknesses for transmission lines from such data, the height above ground and orientation of the ice samples to the wind must be taken into account. With a sufficiently long period of record and a representative geographic distribution of these stations, extreme ice loads and concurrent wind speeds can be determined.

H.4 EXTREME ICE THICKNESSES FROM FREEZING RAIN AND CONCURRENT WIND SPEEDS

The map of 50-year return period ice thicknesses from freezing precipitation with concurrent wind speeds (Figs. 2-13 through 2-18 in Chapter 2) are taken from ASCE Standard 7-05 (ASCE 2005).

H.4.1 Continental United States and Alaska

Historical weather data from 500 National Weather Service (NWS), military, Federal Aviation Administration (FAA), and Environment Canada weather stations were used with the CRREL and Simple models to estimate glaze ice loads in past freezing rain storms on wires 33 ft (10 m) above ground, oriented perpendicular to the wind direction. The station locations are shown in Fig. H-1 for the continental United States and in Fig. 2-18 for Alaska. The period of record of the meteorological data at any station is typically 20 to 50 years.

Accreted ice was assumed to remain on the cylinder until after freezing rain ceases and the air temperature increases to at least 33°F (0.6°C). The maximum ice thickness and the maximum wind-on-ice load were determined for each storm. Severe storms—those with significant ice or wind-on-ice loads at one or more weather stations—were researched in *Storm Data* (NOAA 1959–present; a monthly publication that describes damage from storms of all sorts throughout the United States), newspapers, and utility reports to obtain corroborating qualitative information on the extent of and damage from the storm. Very little corroborating information was obtained about damaging freezing rain storms in Alaska, perhaps because of the low population density and relatively sparse newspaper coverage in the state. Extreme ice thicknesses were determined using the peaks-over-threshold method and the generalized Pareto distribution (Abild et al. 1992; Hoskings and Wallis 1987; Wang 1991). To reduce sampling error, weather stations were grouped into superstations (Peterka 1992) based on the incidence of severe storms, the frequency of freezing rain storms, latitude, proximity to large bodies of water, elevation, and terrain. A few stations that were judged to have unique freezing rain climatologies were not incorporated in superstations. Concurrent wind-on-ice speeds were back-calculated from the extreme wind-on-ice load and the extreme
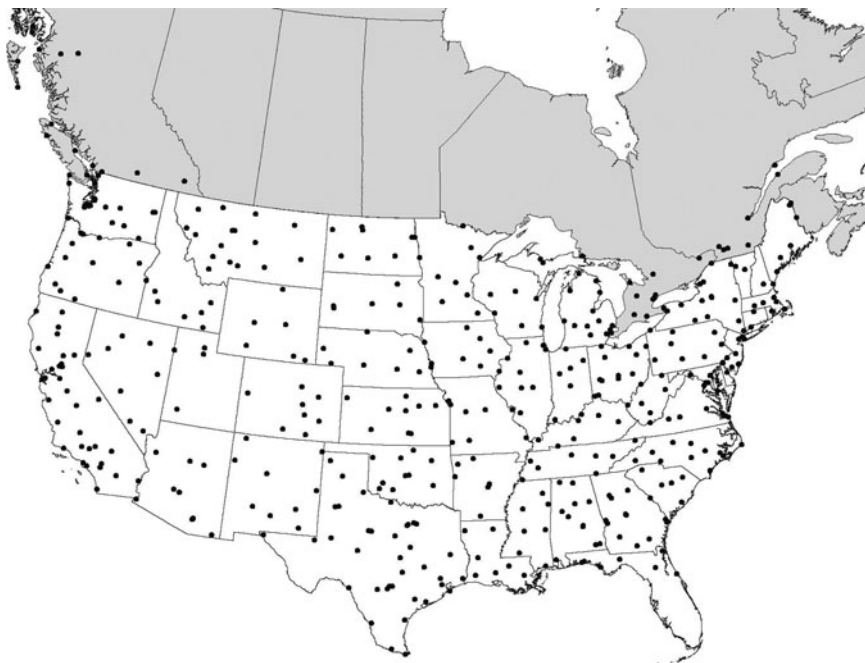
Figure H-1. Locations of weather stations used in preparation of Figs. 2-13 through 2-16. Source: ASCE (2005).

ice thickness. In calculating wind-on-ice loads, engineers should keep in mind that the actual projected area of a glaze ice accretion may be significantly larger than that obtained by assuming a uniform ice thickness. Thus, assuming a force coefficient of 1.0 will not be conservative.

Figures 2-13 through 2-18 represent the most consistent and best available nationwide maps for design ice loads. The icing model used to produce the map has not, however, been verified with a large set of co-located measurements of meteorological data and ice thicknesses. Furthermore, the weather stations used to develop this map are almost all at airports. Structures in more exposed locations at higher elevations or in valleys or gorges (for example, Signal and Lookout Mountains in Tennessee, the Ponatock Ridge and the edge of the Yazoo Basin in Mississippi, the Shenandoah Valley and Poor Mountain in Virginia, Mt. Washington in New Hampshire, and Buffalo Ridge in Minnesota and South Dakota) may be subject to larger ice thicknesses and higher concurrent wind speeds. On the other hand, structures in more sheltered locations (for example, along the north shore of Lake Superior within 300 vertical feet of the lake) may be subject to smaller ice thicknesses and lower concurrent wind speeds. Loads from accreted snow or in-cloud

icing may be more severe than those from freezing rain. In particular, in-cloud icing, possibly combined with freezing drizzle, appears to be the most significant icing process in eastern Colorado and New Mexico.

H.4.2 Special Icing Regions

Special icing regions are identified in Figs. 2-13 through 2-18. As described above, freezing rain occurs only under special conditions with a cold, relatively thin surface air layer, and a layer of warm, moist air aloft. Thus, severe freezing rain storms at high elevations in mountainous terrain will typically not occur in the same weather systems that cause severe freezing rain storms at the nearest airport weather station. Furthermore, in these regions ice thicknesses and wind-on-ice loads may vary significantly over short distances because of variations in elevation, topography, and exposure. In these mountainous regions, the values given in Fig. 2-13 should be adjusted, based on local historical records and experience, to account for possibly higher ice loads from both freezing rain and in-cloud icing.

H.5 EXTREME LOADS FROM IN-CLOUD ICING AND STICKY SNOW

Information to produce maps similar to Figs. 2-13 through 2-18 for in-cloud icing and snow accretions is not currently available.

H.5.1 In-Cloud Icing

In-cloud icing may cause significant loadings on transmission lines in both mountainous regions and level terrain. In the West, in-cloud icing occurs very frequently on exposed ridges and slopes in the mountains. Above the mean freezing level, heavy deposits can form during the numerous storms that strike the region in winter. Steep cliff faces and any exposed structures or obstacles to the wind can become covered with thick coats of ice. Although in-cloud icing does not commonly occur below elevations of about 3,000 ft (915 m), it does occasionally occur when freezing fog fills the basin regions of eastern Washington and Oregon during periods of strong wintertime temperature inversions. In the eastern plains of Colorado in February, 1978, severe rime ice loads were caused by an upslope fog with winds of 10 to 15 mph (4 to 7 m/s). In Arizona, New Mexico, and the panhandles of Texas and Oklahoma, the U.S. Forest Service specifies ice loads due to in-cloud icing for structures constructed at specific mountaintop sites (USFS 1994). In-cloud icing also occurs in the East, primarily on higher peaks in the Appalachian Mountains. On Mt. Washington in New Hampshire [6,280 ft (1,910 m)], the highest peak in

the Northeast, in-cloud icing occurs about 50% of the time from November through April, with icing episodes typically lasting less than a day and the temperature remaining below freezing between episodes. Typical liquid water contents are about 0.2 g/cm^3 and typical wind speeds during icing range from 45 to 70 mph (20 to 30 m/s), with winds greater than 90 mph (40 m/s) occurring 5% of the time. On the more numerous 4,000-ft (1,200-m) mountain summits, in-cloud icing is less severe because the peaks are not exposed to supercooled clouds as frequently and wind speeds are lower. In-cloud icing loads are very sensitive to exposure related to terrain and the direction of the flow of moisture-laden clouds. Large differences in ice thickness can occur over a few hundred feet and can cause severe load unbalances. Advice from a meteorologist familiar with the area is particularly valuable in these circumstances.

H.5.2 Snow

Snow accretions can occur anywhere that snow falls, even in regions that may experience only one or two snowstorms a year. In some regions, extreme accreted snow loads are greater than ice loads from freezing rain or drizzle. A heavy, wet snow storm on March 29, 1976 caused $15 million in damage to the electric transmission and distribution system of Nebraska Public Power District (NPPD 1976). Mozer and West (1983) report a transmission line failure on December 2, 1974 near Lonaconing, Maryland due to heavy, wet snow of 5-in. (127-mm) radial thickness on the wires with an estimated density of 19 pcf (304 kg/m^3). Goodwin et al. (1983) report measurements of snow accretions on wires in Pennsylvania with an approximate radial thickness of 4 in. (102 mm). The meteorological conditions along a transmission line that failed under vertical load in the Front Range of Colorado were analyzed after the failure. The study indicated that the failure was caused by a 1.7-radial-inch (43-mm), 30-pcf (480-kg/m^3) wet snow accretion with a 42-mph (19-m/s) wind. The return period for this snow load was estimated to be 25 years (McCormick and Pohlman 1993). In the winters of 1994–1995 and 1996–1997, Golden Valley Electric Association in Fairbanks, Alaska made 27 field measurements of the radial thickness and density of dry snow accretions. Densities ranged from 1.4 to 8 pcf (22 to 128 kg/m^3) and radial thicknesses up to 4.4 in. (112 mm). The heaviest were equivalent in weight to a 1-in. (25-mm) uniform radial thickness of glaze ice (GVEA 1997).

H.6 OTHER SOURCES OF INFORMATION

Bennett (1959) presents the geographical distribution of the occurrence of ice on utility wires from data compiled by various railroad, electric

power, and telephone associations covering the 9-year period from the winter of 1928–1929 through the winter of 1936–1937. The data include measurements of all forms of ice accretion on wires, including glaze ice, rime ice, and accreted snow, but does not differentiate between them. Ice thicknesses were measured on wires of various diameters, heights above ground, and exposures. No standardized technique was used in measuring the thickness. The maximum ice thickness observed during the 9-year period in each of 975 squares, 60 miles (97 km) on a side, in a grid covering the contiguous United States is reported. In every state except Florida, thickness measurements of accretions with unknown densities of approximately one radial inch were reported. The map shows measurements as high as 2 in.(51 mm) in the Northeast, Southeast, and South; 1.75 in. (44 mm) in the Midwest; 2.4 in. (61 mm) in the High Plains; and 3 in. (76 mm) in the West. Information on the geographical distribution of the number of storms in this 9-year period with ice accretions greater than specified thicknesses is also included in the Bennett report.

Tattelman and Gringorten (1973) reviewed ice load data, storm descriptions, and damage estimates in several meteorological publications to estimate maximum ice thicknesses with a 50-year return period in each of seven regions in the United States.

In *Storm Data*, storms are sorted by state within each month. The compilation of this qualitative information on storms causing damaging ice accretions in a particular region can be used to estimate the severity of ice and wind-on-ice loads. The Electric Power Research Institute (EPRI) has compiled a database of icing storms from the reports in *Storm Data*. Damage severity maps have also been prepared (Shan and Marr 1996).

Robbins and Cortinas (1996) and Bernstein and Brown (1997) provide information on freezing rain climatology for the 48 contiguous states based on meteorological data. For Alaska, what information is available indicates that moderate to severe ice loads of all types can be expected. The measurements made by Golden Valley Electric Association are consistent in magnitude with visual observations across a broad area of central Alaska (Peabody 1993). Several meteorological studies using ice accretion models to determine ice loads have been conducted for high voltage transmission lines in Alaska (Richmond 1985, 1991, 1992; Gouze and Richmond 1982a, 1982b; Peterka et al. 1996). Glaze ice accretions for a 50-year return period range from 0.25 to 1.5 radial in. (6 to 38 mm), snow from 1.0 to 5.5 radial in. (25 to 140 mm), and rime from 0.5 to 6.0 radial in. (12 to 150 mm)). The assumed accretion densities were glaze 57 pcf (910 kg/m^3), snow 5 to 31 pcf (80 to 500 kg/m^3), and rime 25 pcf (400 kg/m^3). These ice thicknesses are valid only for the particular regions studied and are highly dependent on the elevation and local terrain features. Large accretions of snow have been observed in most areas of Alaska that have overhead lines.

In areas where little information on ice loads is available, it is recommended that a meteorologist familiar with atmospheric icing be consulted. Factors to be kept in mind include the fact that taller structures may accrete more ice because of higher winds and colder temperatures aloft, and that the influences of elevation, complex relief, proximity to water, and potential for unbalanced loading are significant.

H.7 CURRENT PRACTICE

A 1979 survey of design practices for transmission line loadings (ASCE 1982) obtained responses from 130 utilities operating 290,000 miles (470,000 km) of high voltage transmission lines. Fifty-eight of these utilities specifically indicated "heavy icing areas" as one reason for special loadings in excess of NESC requirements. Design ice loads on conductors ranged from no ice (primarily in portions of the southern United States), up to a 2- or 2.25-in. (50- or 57-mm) radial thickness of glaze ice in some states. Radial glaze ice thicknesses between 1.25 and 1.75 in. (32 to 45 mm) are commonly used. Most of the responding utilities design for heavy ice on the wires with no wind and less ice with wind. Few utilities consider ice on the supporting structures in design.

Minimum ice and wind loads are specified in the current edition of the National Electrical Safety Code (NESC 2007) for three geographical loading districts. According to a discussion published with the third edition of the code (NESC 1920):

> The assumed ice loadings have been chosen after careful consideration of data obtained from the U.S. Weather Bureau, from electric companies, and from engineers. The values chosen do not represent the most severe cases recorded, but do represent conditions that occur more or less frequently. Ice loading of 1/2 inch is frequently exceeded, particularly near the northern and eastern borders of the U.S., and on occasions ice has been known to collect to a thickness of 1.5 inches and even more.

In addition to NESC loading districts (heavy, medium, and light), utilities have been using the 50-year glaze ice map in the previous edition of this manual (ASCE 1991) to establish ice loading criteria.

APPENDIX I

SUPPLEMENTAL INFORMATION ON SPECIAL LOADS

I.1 INTRODUCTION

The assessment of the required longitudinal strength for transmission line structures has been the subject of countless debates and studies. The objective of this appendix is to present a discussion of the causes and the effects of extreme event loads. An attempt is also made to provide guidance on how to mitigate the effects of such loads.

Generally, the calculation of vertical and transverse loads for a transmission structure is well established because the weight, wind, and ice loads applied to the wire systems are directly transferred to the support structures. However, load inequalities resulting from the disturbance or disruption of the wire system are likely to produce extreme event loads that are a function of the characteristics of the loaded wire system.

The elastic and inelastic behavior of the wire and the movement of the support system (suspension insulator swing and/or structure deflection) affect the magnitude of the unbalanced loads that are resisted by the structures. It should be noted that there is a difference between supports where suspension insulator strings permit flexibility in the direction of the line that may reduce the unbalanced loads through load sharing, and strain structures and ground-wire peaks that provide very little flexibility.

I.2 WEATHER-RELATED LONGITUDINAL LOADS

I.2.1 Suspension Supports

Unequal wind or ice loads on adjacent spans and conductor temperature variation on unequal adjacent spans can result in differential tensions. These differential tensions can produce significant load imbalances that are usually reduced by the swing of the suspension strings (Cluts and Angelos 1977). The longitudinal loads transmitted to the structures by the inclined suspension strings rarely exceed 10% to 20% of the conductor bare wire tension, except in hilly or mountainous terrain where in-cloud icing is a hazard. Suggestions for the determination of unbalanced ice loads can be found in IEC Standard 60286 (IEC 2003) and the various national options of CENELEC Standard EN 50341 (CENELEC 2001).

In the case of in-cloud icing, the longitudinal loads can be significant because ice deposits vary greatly from span to span (see Chapter 2, Section 2.3.6 and Appendix H). Unloaded adjacent spans with significant slack (defined as the difference between the actual wire length and the straight-line distance between the attachment points) permit the insulator to swing sufficiently to turn the suspension assembly into a strain support that is likely to transfer nearly all the differential tension to the structure. Problems have been observed in areas where the slack difference of adjacent spans exceeds twice the length of the insulator strings.

Assuming level spans and using the parabolic approximation of the catenary, the following relationships may be used:

$$\text{sag} \cong wS^2/8T_H \tag{I-1}$$

$$\text{slack} \cong 8\,\text{sag}^2/3S = \frac{S^3}{24(T_H/w)^2} \tag{I-2}$$

where
w = wire unit weight
S = straight-line span length
T_H = horizontal component of tension

It should be noted that for a given T_H/w ratio (catenary constant, C), slack is proportional to the cube of the span. For example, using a T_H/w ratio of 5,000 ft, the slack of an 800-ft span equals 0.85 ft, the slack of a 1,600-ft span equals 6.8 feet, and the slack of a 2,400-ft span equals 23 ft.

I.2.2 Strain Supports

Strain supports must resist the differential tensions from adjacent spans because the unbalanced loads are only reduced by the flexibility of the support structure, which is usually negligible for latticed towers.

Experience shows that the ground-wire support (with clamps or short suspension link) of suspension structures may pose the highest risk for failure because the differential ground-wire tensions could be significantly higher than the differential conductor tensions produced by the same conditions. Therefore, ground-wire supports of structures located in in-cloud icing areas are especially vulnerable.

Several methods have been used to reduce the risk of failures resulting from differential ground-wire tensions caused by in-cloud icing. Suspension links with lengths of 1 to 5 ft (0.3 to 1.5 m) have been installed in attempts to provide sufficient flexibility to permit wire tensions to equalize; slip or release clamps have been installed to limit the maximum load acting on a support point; and, in some cases, ground-wire supports have been designed to act as fuses to collapse at defined loads, thereby preventing more serious damage. As a final measure, some utilities have removed the ground wires from lines located in areas likely to experience in-cloud icing.

Due to unequal spans, ground-wire peaks can be subjected to large longitudinal loads even without icing. High differential tensions can exist in the ground wire during low ambient temperatures, which can generate substantial longitudinal loads.

I.3 FAILURE-RELATED LONGITUDINAL LOADS

Failure-related load requirements, such as the broken wire load (BWL), have been used successfully to ensure the satisfactory performance of structures and to mitigate the effects of severe differential wire tensions. Based on past experience (EPRI 1997), the breakage of conductors, ground wires, and components as well as line cascades (thousands of structures in the last 30 years) are serious problems. The potential for a cascade exists when sufficient slack is introduced into a span so that the unbalanced longitudinal load at the adjacent structure is significant enough that it could fail that structure. As the second structure fails to resist residual load, it allows the wire to move on to the next structure and repeat the sequence. It is this wire movement that leads to cascading. To stop the cascading, it is necessary to arrest the wire movement or, as will be seen, to accommodate the movement with some structure flexibility.

Unbalanced longitudinal loads for cascading failure containment can be calculated using any of the following methods.

I.3.1 Residual Static Load

The extreme event loading can be defined as the residual static load (RSL) that corresponds to a broken wire condition. The RSL is the residual static longitudinal load (no dynamic amplification) at a wire support

point after breakage of a phase (all wires of a bundle) or of a ground wire. The RSL is generally calculated for the bare wire (no ice or wind) loading condition at an average temperature. The reduction in the load magnitude resulting from the insulator swing and support deflection may be considered in the calculation of the RSL. Computer programs (EPRI 1983; Mozer et al. 1977; Peyrot 1985) and design charts (Comellini and Manuzio 1968; EPRI 1978) might be available to assist in the calculation of the RSL magnitudes. RSL values derived from the Comellini and Manuzio charts are based on insulator string length and span length and will approximate 60% to 70% of everyday tensions. The RSLs are applied to a nominal one-third of the conductor support points or to one (or both) ground-wire support point(s). RSLs are to be applied in one direction only, along with 50% or more of the intact wire vertical load. Other support points carry full wire vertical loads. Generally, the effects of wind are not considered when using the RSLs.

I.3.2 Electric Power Research Institute Method

EPRI developed another methodology for calculation of unbalanced longitudinal loads. This method calculates loads as a function of the horizontal wire tension, the span/sag ratio, the span/insulator ratio, and the support flexibility (EPRI 1997). Due to the complexity of this approach, this method is not presented herein.

I.3.3 Failure Containment (Bonneville Power Administration Method)

A system approach can be followed to mitigate the effects of failure-related unbalanced longitudinal loads on transmission lines. The system approach (Kempner 1997) uses a "failure containment" philosophy that accepts the failure of one tower on each side of the initiating event. The longitudinal loading case assumptions are (1) only one wire or phase is broken at one time, and (2) the break occurs during an everyday load situation, which is defined as no ice, no wind, a conductor temperature of 30°F (−1.1°C), and initial sag. The conductor tension obtained under these conditions is multiplied by an impact factor. Standard suspension towers (0- to 3-degree line angle) and "heavy" suspension towers (0- to 6-degree line angle) have an impact factor of 1.33. The impact factor for "light" suspension towers (no line angle) is 0.67.

Suspension Tower Conductor. The broken conductor load condition consists of:

1. A vertical load at the broken conductor attachment point [i.e., 50% of the conductor weight and hardware at 30°F (−1.1°C)] and the

vertical load at the intact conductors (i.e., the weight of the conductors and hardware).

2. A longitudinal load at the support (i.e., bare wire everyday tension multiplied by the appropriate impact factor (light suspension tower, 0.67; standard suspension tower, 1.33; and heavy suspension tower, 1.33).

3. A transverse load caused by line angle. Only one phase is assumed broken for both single- and double-circuit towers. Each conductor attachment point shall be considered individually. For a double-circuit tower, this load case shall be repeated with only one circuit strung.

Strain Dead-End Conductor. The load case consists of:

1. A vertical load (i.e., weight of the conductor and hardware) at 0°F (−17.8°C).

2. A transverse wind load on the tower and wires [i.e., at 40 mph (18 m/s)] with no ice.

3. A longitudinal load equal to 125% of sagging tension. The vertical, transverse, and longitudinal wire load is multiplied by a 1.5 load factor. For double-circuit towers, this load case shall be repeated with only one circuit strung.

Ground Wire. The load consists of:

1. A vertical load of the iced overhead ground wire (i.e., weight of glaze ice equivalent to 1.5 times the working load overhead ground-wire design ice thickness at maximum working tension). The equivalent glaze ice thicknesses are light suspension tower, 0.75; standard suspension tower, 1.125; and heavy suspension tower, 1.125. The vertical load is the sum of one-half the equivalent iced wire weight for 1.5 times the transverse span plus one-half the bare weight of 0.5 times the transverse span. Additionally, a vertical conductor load equal to the equivalent ice-coated wire weight is applied to 1.0 times the transverse span.

2. The longitudinal load of the overhead ground wire equals the horizontal tension and is applied to all ground-wire peaks.

I.3.4 Percent of Everyday Wire Tension

A design longitudinal load, historically known as broken wire load (BWL) (ASCE 1991), can also be used. It is equal to the everyday bare wire tension (EDT) of the ground wire and is equal to about 70% of the EDT of a conductor, applied as a single load at any one support point. This

load has been used successfully in the past to mitigate the effects of broken wires. Experience has shown that flat or horizontal configuration, single-circuit lines designed with the BWL concept produced transmission lines with a sufficient level of longitudinal strength to contain the effects of broken wires and other comparable failures that may have otherwise resulted in a cascade. It should be noted that frequently occurring heavy ice conditions or stiff, brittle supports may require a larger longitudinal load.

I.4 FAILURE CONTAINMENT REQUIREMENTS

Infrequent failures of a few structures or components must be accepted as a result of erecting transmission lines exposed to severe wind and ice loads and other causes of mishaps, such as the impact of aircraft or vehicles, footing washouts, and tornados. It is recommended that the design of the line anticipate such unusual events by providing a longitudinal strength level that will limit the damage to a few structures from the initiating event to prevent a cascading failure.

Successful failure containment may be achieved by providing sufficient longitudinal strength: (1) on all structures, or (2) on special resistance structures inserted at regular intervals. Angle structures may be used as special resistance structures if their longitudinal strength is sufficient to resist the unbalanced loads and to arrest a cascading failure.

I.4.1 General Rules

Experience demonstrates that it is almost impossible to anticipate the manner and form of the initial failure. A train derailment, a major tornado, a low-flying aircraft, or a freak ice storm may bring several structures to the ground, accompanied by component and wire failures creating dynamic forces at adjacent structures that cannot be assessed. The inability to quantify the dynamic energy or impact component at the adjacent structures has directed attention to the security (or survival) of the second, third, fourth, or fifth structure away from the initial failure (Thomas 1981; EPRI 1997; Kempner 1997).

Depending on the importance of the line, it is generally agreed that if the second, third, fourth, or fifth structure from the initiating event does not fail, there will be no cascade and most of the energy released by the failure will have dissipated. Therefore, the problem of failure containment may be reduced to the problem of determining the required longitudinal strength to resist the differential tensions at the second, third, fourth, or fifth structure, respectively, while allowing the failure of one or more structures to dissipate the released energy.

I.4.2 Basic Assumptions

Longitudinal cascades of high-voltage lines (Frandsen and Juul 1976) have resulted from initial failures other than broken ground wires or conductors. In one case, failure of a heavy angle structure introduced excessive conductor slack and longitudinal loads that triggered cascading failures on both sides of the fallen angle structure. It should be noted that any event that permits the creation of excessive slack is likely to produce longitudinal loads that may lead to a cascading failure.

I.4.3 Special Resistance Structures

Most rigid and guyed single-circuit structures are capable of resisting significant longitudinal loads, but some structures cannot be economically designed to provide a sufficient level of resistance. In such instances, it is recommended that special resistance structures be provided at selected intervals along the line to limit the length of a cascading failure to an acceptable number of structures. Special resistance structures are typically rigid lattice, frame, or pole suspension structures that provide a sufficient level of strength to resist the unbalanced longitudinal loads caused the failure of components, wires, or structures.

The decision to install or create anti-cascade or stop towers at intervals along an existing line requires an awareness of the means by which a longitudinal cascade is propagated. Failure to appreciate the mechanics involved may negate the entire effort.

As discussed, a strain-type structure could stop a cascade if it has sufficient strength to resist the unbalanced loads (bare wire or iced, as required) and prevent the movement of wire along the line. A suitably strong strain-type angle tower will serve this purpose. In new line construction, the frequent need for angle structures may be accepted as a design alternative to building the anti-cascade strength into each suspension structure.

The alternative of either inserting or converting a suspension-type structure to perform the anti-cascading duty is attractive but not always possible if the suspension strings are long, as with high voltage (HV) and extra high voltage (EHV) lines. It is possible that enough wire movement will be passed on through the stop tower so the failures continue. The swing of the insulator string will produce a longitudinal load equal to the vertical load being supported at the point, multiplied by the tangent of the angle of swing of the insulator string. This secondary effect must be checked.

For HV and EHV lines, the attempt to use a rigid and relatively inflexible suspension structure as a stop tower will not succeed even if the tower itself has great longitudinal strength. Allowing the wire movement

to pass on down the line will ensure continuance of the cascade even though the stop towers may remain standing.

On the other hand, at low-voltage H-frames or portal structures, the length of the insulator strings will approximately equal the available deflection, so the application of longitudinal storm guys, and possibly the installment of metal crossarms on structures at appropriate intervals, can be a rational means of removing the threat of long cascades.

I.4.4 Failure Containment for Icing Events

In areas where icing events are frequent, utilities may adopt failure containment loads with iced conductors as a design requirement for important lines. Specially reinforced structures (guyed or not) may be used at regular intervals to resist the extremely large differential tensions and to arrest a cascading failure.

I.5 TRANSVERSE CASCADES

I.5.1 Characteristics of a Transverse Cascade

Most cascades are longitudinal in nature, starting with a certain event that severed some or all of the wire system or introduced enough slack into the system such that it generated enough longitudinal loads to overwhelm structures in a line section. Transverse cascades are differentiated from longitudinal cascades in that the "pull" of the wire system after the collapse of the initiating structure failure is predominately in the transverse direction. Successive structural failures in a transverse cascade collapse in a generally transverse direction; as such, they may be incorrectly considered a failure caused by a broad front wind.

Most transverse cascades are instigated by the initial impact of a high-intensity wind (HIW) on the line, with one or two structures brought down by a tornado. These small, local failures frequently become transverse cascades of dozens of structures. These failure scenarios have often been misjudged as multiple failures caused by a "wall of wind" overcoming all the fallen structures, when the actual failure mechanism was a transverse cascade.

It is important to be able to recognize a transverse cascade and to distinguish between the near-simultaneous transverse failure of many structures caused by a broad wind versus a transverse cascade triggered by failure of one or (at most) a few structures. Failure of many towers from widespread transverse wind is not common except in areas subject to cyclones, hurricanes, or seaside gales. The differences between the two types of multiple transverse failures are easy to recognize.

These transverse cascades produce stresses throughout the wire system that will probe the tower system in ways not common to other load scenarios. A different and new type of behavior of the wire system promotes this transverse type of cascading, and such transverse cascades are restricted almost totally to failures triggered by HIWs.

It is useful to understand and appreciate the loads generated in the wire system after the transverse collapse of one or two structures from HIWs. Awareness of the line systems (wires and structures) that are vulnerable to these loads is important, as is the conception of design modifications that will reduce the vulnerability of new or existing lines.

I.5.2 Wire Behavior of a Transverse Cascade

A significant parameter in what follows is that of the slack, which is the difference in length between the straight line joining the points of support and the length of the suspended wire. This exercise uses a parabolic equation because the added precision of working with catenaries is not required.

$$sag = \frac{w \times span^2}{8 \times T_H} \quad slack = \frac{w^2 \times span^3}{24 \times T_H^2}$$

where
$T_H =$ the horizontal tension in the cable
$w =$ the cable's weight per unit length

Rearranging the above formulas:

$$slack = \frac{8 \times sag^2}{3 \times span}$$

Thus, *sag* is a function of *span²* and *slack* is a function of *span³*.

The ratio of T_H/w is generally referred to as the catenary or parabolic constant. For typical spans with the parabolic constant of tension/unit weight of 1,600 ft, we would find the values in Table I-1.

It may be noted at this point that the conductors are supported on suspension insulator strings permitting restricted longitudinal swing varying with the length of the string, whereas the ground wires are almost always firmly attached to the tops of the ground-wire peaks of the structures.

With the transverse failure of a single structure, the added length to the wire system can be calculated as well as the transverse and

Table I-1. Typical Span Characteristics

Spans	Sag	Slack
400 ft (121.9 m)	12.5 ft (3.81 m)	1.04 ft (0.317 m)
800 ft (243.8 m)	50.0 ft (15.24 m)	8.33 ft (2.54 m)
1,200 ft (365.8 m)	112.5 ft (34.29 m)	28.13 ft (8.57 m)
1,600 ft (487.7 m)	200.0 ft (60.96 m)	66.67 ft (20.32 m)

TOP VIEW   **Trigger or Initial Failure**
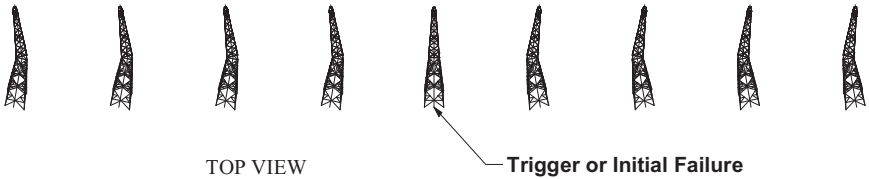
Figure I-1. Plan view of typical transverse cascade.

longitudinal loads applied to the adjacent structures. The insulator strings will swing toward the fallen structure, pulling slack from adjacent spans of conductors. However, it is evident that, with the resistance offered by the inclined insulator strings, there will be a great increase in all conductor tensions. These tensions exert longitudinal forces on these towers, as well as significant transverse loads.

Ground-wire tensions will increase more rapidly with no relief due to insulator string swing, and the pulls exerted on the tops of the ground-wire peaks will be limited only by the slip strength of the clamps or the fusing capacity of the ground-wire peak itself.

These loads can overwhelm the adjacent two structures, leading to a compression buckling of the mast or nearest corner leg of a latticed structure. However, as the structure starts to fall, the inward tensions start to relax while the tensions back to the next set of adjacent structures will increase. The falling structures will therefore describe an arc in falling, pulled first toward the failed structure but then away from it. Crossarms will strike the ground slightly away from the trigger structure, sometimes as much as 3 ft (1 m). A plan view (top view) of a typical transverse cascade is illustrated in Fig. I-1.

This pattern of structures falling slightly away from the trigger structure can be readily discerned on-site if the investigator is aware of the phenomenon. If the structures on the ground almost "point" back toward the trigger tower and there is further evidence of the failed and outwardly splayed corner legs of a latticed structure, the sequence of events can be confirmed. It is important to be able to recognize or identify a transverse cascade event.

I.5.3 Conditions Leading to Transverse Cascading

By examining the parameters that will create the greatest diagonal pulls on adjacent structures, it can be noted that:

1. Short spans contain little slack to relieve the high tensions produced by the falling structure. Short spans also create the greatest tension increases after the failure of one structure.
2. Tall structures (such as double-circuit vertical configurations), in falling transversely, lead to large increases in wire loads of upper conductor phases and of the ground wires.
3. The short insulator strings of low-voltage lines restrict movement of slack from adjacent spans.

On the other hand, EHV lines are inherently safer with regard to transverse cascading, for several reasons:

1. Longer insulator strings permit greater equalization or reduction of conductor tensions.
2. Strength requirements for carrying the bundled conductors of an EHV line minimize the influence of the ground-wire system that usually is similar to that used for lower voltages.
3. The longer spans usually associated with EHV also contain larger amounts of slack and do not tighten as quickly when one structure falls.

It should be noted that the reduced influence of the ground-wire system on EHV lines may be threatened by the increasing trend of replacing conventional small steel or aluminum-clad steel wire stranding with much larger, heavier, and stronger optical ground wire (OPGW). Replacement with OPGW may require a corresponding strengthening of the clamping and the ground-wire peaks themselves.

The ground-wire system can, and in most cases does, contribute a major part of the cascade-inducing forces because it is the highest part of the wire system, and the direct clamp system permits no equalization or reduction of tension. The stronger the ground-wire system comprising the wires, clamps, and ground-wire peaks, the greater the potential for a transverse cascade.

This page intentionally left blank

APPENDIX J

INVESTIGATION OF
TRANSMISSION LINE FAILURES

J.1 INTRODUCTION

Line failures provide a unique and highly valuable opportunity to increase our understanding of transmission line behavior. Not all damage or failures can be avoided, and it is anticipated that failures will occur under extreme conditions that exceed the code required and utility-established design criteria. A systematic investigation can provide information that may be used to reaffirm or improve design criteria and maintenance practices. The investigation may reveal that the conditions were in excess of design criteria and no modification of the criteria or maintenance practices is justified. The goal of the failure investigation is to establish the cause of the failure and try to reconstruct or understand the behavior of the line subsequent to the failure initiation.

There has been much public reporting of failures in recent years, but little has been published dealing with the technical aspects of transmission line failures. Information on structural failure investigations may be found in publications by Carper (1986) and Janney (1979), and in 1973 a series of papers on transmission line failures (Griffing and Leavengood 1973) was published.

The correct interpretation of the causes of transmission line failures has, at times, led to significant modifications of line design practices. The investigator should be certain that the assumed failure mechanism is consistent with the evidence.

J.2 THE NEED FOR AND BENEFIT OF THOROUGH INVESTIGATIONS

In any failure event, the utility's responsibility is to ensure public safety and to promptly restore service. Therefore, a predefined emergency response plan should be established so repair crews can be mobilized quickly and a qualified engineer has adequate time to perform a thorough investigation. Time is the vital factor and, unless plans have been made before the event and priority directives issued, significant evidence and data could be lost.

A utility/transmission line owner should have an established phone list that identifies key failure investigation personnel. These individuals should be familiar with the utility's investigation procedures and policy. The list should be distributed to the utility's line construction and maintenance office(s).

The reasons for attempting to get to the root causes of a failure event are many:

1. The cause may be an actual overload of ice, wind, or a combination of the two that exceeded the design specifics and will require an assessment of future risks and costs. The accurate assessment of the actual ice and wind loads is imperative to determine whether there was excessive loading or whether there was a problem or defect within the system.
2. Detection of a deficiency or defect may permit modifications to components to prevent further failures, or may lead to modifications of current design practices or specifications.
3. The cause may be attributed to the deterioration of specific line components that may justify increased inspection and replacement policies.
4. Unanticipated dynamic behavior may be detected.
5. The investigation may uncover a specific loading case that was not originally considered.
6. A systematic and thorough failure investigation should provide the line engineer a greater familiarity with the ways in which the various components of the wire and structural support systems interact when the system is severely stressed.

J.3 CAUSES OF FAILURE

The following lists represent some of the more general causes of transmission line failures.

J.3.1 Natural Phenomena (Exceeding Design Criteria)

- Extreme wind
- Extreme ice
- Combination of ice and wind
- Landslides
- Avalanches
- Ice movement on rivers or lakes (for structures located in the water)
- Flooding (causing damage to structure or to foundation)
- Soil liquefaction

J.3.2 Manmade Causes

- Sabotage, vandalism, or theft of members and bolts
- Accidental damage caused by equipment and vehicles

J.3.3 Structure Deficiencies (When Design Criteria Were Not Exceeded)

- Design inadequacies of structure
- Missing members or loose bolts caused by vibration or omitted during erection
- Erroneously fabricated members
- Improperly installed foundations
- Deterioration or corrosion of structures

J.3.4 Conductor, Ground-Wire, and Hardware Deficiencies

- Improper wire splices
- Faulty or inadequate hardware
- Fatigue failure of wire or hardware components
- Insulation failures

J.3.5 Construction-Related Causes

- Excessive vertical load during stringing
- Excessive longitudinal load during stringing
- Improper stringing sequence

J.4 FAILURE INVESTIGATIONS

A failure investigation can be a very simple and quick observation of the facts represented by the evidence. At other times, it will result in a study involving many engineers over a period of years. The least demanding of investigations are those that follow an accident caused by an obvious event, such as aircraft contact, foundation washout, and so forth. The emphasis in the investigation will be directed toward finding means of preventing recurrence and determining whether the postfailure behavior of adjacent structures was satisfactory.

A more difficult problem will be encountered when the cause can be identified as a wind or ice storm but the evidence indicates that the failure occurred at lower than the expected design values. These situations require an examination of the evidence to determine whether there was a structure design deficiency. For example, bolts or members may have been missing, foundations may have had inadequate cover, or guy anchors may have had inadequate uplift capacity. In other cases, consideration of yawed or longitudinal wind loads may have been omitted from the design criteria, or probable uplift loads were not considered.

In the case of line damage with multiple failures caused by ice or wind load equal to or exceeding design values, the investigation should attempt to determine the line section that has failed by the initial ice and/or wind event. This should be inspected separately from other sections that may have failed due to secondary events. This is an important finding to better understand the behavior of the line, but it is often difficult to distinguish between them.

J.5 POSTFAILURE BEHAVIOR OR FAILURE CONTAINMENT

The investigation should establish the cause of failure and whether the line performed as designed. If needed, make recommendations regarding:

1. Strengthening of the existing structures
2. Improvement of maintenance and inspection procedures
3. Possible change of load design criteria for future lines

Another function is to identify any evidence of a cascading failure. An initial failure with collapsed structures or broken wires may cause damage to one or two structures adjacent on either side. It is difficult to prevent such damage in all cases because the nature of the initial event and the impact and energy release may not be easily absorbed. If subsequent structures fail, a cascade is more likely. The investigator should also determine the effectiveness of any existing anti-cascade measures.

J.6 PREPARATION

J.6.1 Failure Investigation Equipment

1. Measuring tape and pocket scale
2. Micrometer (if material sizing is in question)
3. Notebook and sketch pad
4. Markers and identification tags
5. Cardboard pieces or 8 × 11-in. paper pad and marker to place in foreground of all photos for future identification.
6. A voice recorder
7. High-resolution digital camera with video capability and extra batteries
8. Binoculars
9. Cell phone or radio

J.6.2 Technical Preparation

If time and access permit, the investigators should familiarize themselves with the appropriate line data, conductor and structure loadings, design characteristics, and any special construction records. When possible, discuss the failure briefly with a group of key design personnel.

J.7 FAILURE INVESTIGATION CHECKLIST

The investigators should initiate complete photo documentation, make an overall survey of the damaged area, and listen to viewpoints and evidence of any witnesses or earlier arrivals.

The following information may be used as a summary checklist for failure investigation but does not cover all the tasks that could be performed during an investigation.

J.7.1 After Arriving at the Site

1. The line crews may have already arrived at the site and will be ready to start repair operations. If this happens, try to obtain a visual inspection of the damaged portion of the line. An overall picture taken at this time may provide information and detail that could be lost after the repair activity begins.
2. The first impression of the site can result in a multitude of ideas about the failure, and it is valuable for the investigator to record these thoughts.

3. Prepare a sketch of the line showing the positions of conductors, insulators, structures, and any indication of the conductors having been pulled across the ground. Also note the structure configuration, such as the position of the guy anchors, deflected shape of structures, and final position of footing stubs and/or structure legs.

4. If the event is an ice storm, attempt to gather representative ice samples from the fallen wires, record the length of each sample, and store them in plastic bags for later weighing. Sample ice weights are the best way to accurately measure the ice load that was on the wires.

5. An awareness of conductor and shield wire behavior is important because these tie the structures together. Observe how conductor tension was affected by the collapse of the structures.

6. If wind is the suspected cause of failure, look for surrounding damage to trees, buildings, etc. The Beaufort Scale (Baumeister et al. 1978), given in Table J-1, can provide valuable information as to the approximate wind speed.

7. Look for signs of the following:
   a. Rust on sheared surfaces indicating that the bolt or member may have partially failed previously
   b. Burn marks on the conductor or structure indicating initial point of fault to ground
   c. Evidence of loose or missing bolts
   d. Shiny steel and worn galvanizing at joints, indicating possible vibration

8. If hardware, insulators, conductors, or overhead ground wires are broken, they may have been triggered by the initial failure or may have been caused by a secondary event. Retrieve and mark some specimens as needed.

9. If there are broken wires, note whether the ends of the strands indicate a prior fracture due to fatigue, or a cup cone failure with necking indicative of a tensile failure.

10. It may be desirable to remove test sections of steel members for material tests to determine material properties. Record the location of the member samples. Avoid taking samples in the area of high stress because the cold working of the steel will significantly alter its physical properties. If a torch is used to remove the sample, be sure to obtain a sample large enough that a testing coupon can be prepared that has not been degraded due to the localized effects of heat.

11. Individuals in the nearby area of the failure may be a possible source of information. These individuals can frequently tell of vibration, galloping, and other unusual meteorological events that may have occurred.

Table J-1. Beaufort Scale of Wind Intensity

Beaufort Number	Wind Speed (mph)	Wind Effects Observed on Land	Terms Used in USWB Reports
0	<1	Calm, smoke rises vertically.	Light
1	1–3	Direction of wind shown by smoke drift but not by wind vanes.	
2	4–7	Wind felt on face, leaves rustle, ordinary vane moved by wind.	
3	8–12	Leaves and small twigs in constant motion, wind extends light flag.	Gentle
4	13–18	Raises dust, loose paper; small branches are moved.	Moderate
5	19–24	Small trees in leaf begin to sway, crested wavelets form on inland waters.	Fresh
6	25–31	Large branches in motion, whistling heard in telegraph wires, umbrellas used with difficulty, wind is heard in buildings.	Strong
7	32–38	Whole trees in motion, difficult walking against wind.	
8	39–46	Breaks branches off trees, generally impedes progress.	
9	47–54	Slight structural damage occurs; chimney pots, slates removed.	Gale
10	55–63	Seldom experienced inland; trees uprooted, considerable structural damage occurs, telephone poles break.	Whole Gale
11	64–72	Very rarely experienced, accompanied by widespread damage.	
12	>73	Very rarely experienced, disastrous damage.	Hurricane

Source: Baumeister et al. (1978).
USWB, U.S. Weather Bureau.

J.7.2 After Returning to the Office

1. Look for design inadequacies:
   a. Conductor weaker than structure
   b. Combined loading producing critical member stresses not previously considered
   c. Foundation or anchor failures
2. Obtain weather data from the nearest local weather station.
3. Study field data carefully; try to match field data with postulated cause of failure.
4. If the structure appears to have failed below the design load, a more detailed analysis may be warranted, taking into account secondary stresses due to bending and nonlinearities.
5. Examine conductor behavior after the failure event and its potential effect on the remaining transmission line system.
6. Ascertain why damage terminated where it did.

J.7.3 Preparation of Report

The report should summarize and document the following:

1. Field investigation, observations made, and data collected. The data collected in the field (primarily photographs, sketches, interviews, and notes) should be cataloged for future reference.
2. Overview of the physical characteristics and layout of the line, design practices, inspection methods, maintenance practices, and construction techniques prior to the failure.
3. Documentation of the failure summarizing the environmental conditions, cause of the failure, identification of initial failure location, sequence of failure, and contributing or mitigating factors.
4. Conclusions and recommendations, including adequacy of design criteria, inspection and maintenance practices, effectiveness of failure containment, and recommendations for improvement or modification of new or existing facilities.
5. Follow-up evaluation of failure investigation.

J.8 ADDITIONAL REFERENCES (Failure Investigation-Specific)

Chapter 5, "Forensic Analysis of Failures." In Overhead Transmission Inspection and Assessment Guidelines—2004. Electric Power Research Institute (EPRI), Palo Alto, Calif., 2004 (1002007).

The Fundamentals of Forensic Investigation Procedures Guidebook. EPRI, Palo Alto, Calif., 2003 (1001890).

Guidelines for Failure Investigation. American Society of Civil Engineers (ASCE), Task Committee on Guideline for Failure Investigation, Technical Council on Forensic Engineering, 1989.

"Forensic Engineering." In *Proc., First Congress, Forensic Engineering Division of American Society of Civil Engineers*. ASCE, 1997.

Guidelines for Forensic Engineering Practice. ASCE Forensic Engineering Practice Committee, Technical Council on Forensic Engineering, 2003.

This page intentionally left blank

REFERENCES

Abbey, R. E., Jr. (1976). "Risk probabilities associated with tornado wind-speeds." *Proc., Symposium on Tornadoes: Assessment of Knowledge and Implications for Man*, Texas Tech University, Lubbock, Tex., 177–236.

Abild, J., Andersen, E. Y., and Rosbjerg, L. (1992). "The climate of extreme winds at the Great Belt, Denmark." *J. Wind Eng. Ind. Aerod.*, 41–44, 521–532.

American Concrete Institute (ACI) (2002). "Building code requirements for structural concrete with commentary." ACI-318-05, Farmington Hills, Mich.

American Association of State Highway and Transportation Officials (AASHTO) (1975). *Standard specifications for structural supports for highway signs, Iuminaires, and traffic signals*. AASHTO, Washington, D.C.

American Institute of Steel Construction (AISC) (2001). "Load and resistance factor design." *Manual of steel construction*, 3rd ed., Chicago, Ill.

AISC. (2005). *Specification for structural steel buildings*. AISC 360-05, Chicago, Ill.

Anjo, K., Yamasaki, S., Matsubayashi, Y., Nakayama, Y., Otsuki, A., and Fujimura, T. (1974). "An experimental study of bundle conductor galloping on the Kasatori-Yama test line for bulk power transmission." *Proc., CIGRE 25th session*, Vol. 1 (22-04).

American National Standards Institute (ANSI) (2002). *Specifications and dimensions for wood poles*, ANSI Standard 05.1, American National Standards Institute, New York, N.Y.

Armitt, J., Cojan, M., Manuzio, C., and Nicolini, P. (1975). "Calculation of wind loads on components of overhead lines." *Proceedings IEE*, 122(11), 1247–1252.

Arya, S. P. S., Capuano, M. E., and Fagen, L. C. (1987). "Some fluid modeling studies of flow and dispersion over two dimensional hills." *Atmos. Environ.*, 21(4), 753–764.

American Society of Civil Engineers (ASCE). (1961). "Wind forces on structures." *Transactions*, 126(Part II), Paper No. 3269, New York, ASCE, 1124–1198.

ASCE. (1982). "Loadings for electrical transmission structures." *J. Struct. Div.*, ASCE, 108(ST5), 1088–1105.

ASCE. (1984). "Guidelines for electrical transmission line structural loading." *Proc., ASCE Annual Convention and Exposition*, San Francisco, Calif., Oct. 1–5.

ASCE. (1988). *Guide for design of steel transmission towers*. ASCE Manuals and Reports on Engineering Practice No. 52, New York.

ASCE. (1990a). *Design of steel transmission pole structures*. ASCE Manuals and Reports No. 72, New York.

ASCE. (1990b). *Minimum design loads for buildings and other structures*. ASCE 7-88 (revision of ANSI A58. 1-1982), New York.

ASCE. (1991). *Guidelines for electrical transmission line structural loading*. ASCE Manuals and Reports on Engineering Practice No. 74, New York.

ASCE. (1997a). *Design of guyed electrical transmission structures*. ASCE Manuals and Reports on Engineering Practice No. 91, New York.

ASCE. (2000a). *Design of latticed steel transmission structures*. ASCE 10-97, Reston, Va.

ASCE. (2000b). *Minimum design loads for buildings and other structures*. ASCE 7-98, Reston, Va.

ASCE. (2005). *Minimum design loads for buildings and other structures*. ASCE 7-05, Reston, Va.

ASCE. (2006). *Reliability-based design of utility pole structures*. ASCE Manuals and Reports on Engineering Practice No. 111, Reston, Va.

Baenziger, M. A., James, W. D., Wouters, B., Li, L., and White, H. B. (1993a). "Dynamic loads on transmission line structures due to galloping conductors, and discussion by B. White." WM 078-6 PWRD, IEEE, Piscataway, N.J.

Baenziger, M. A., Gupta, S., Wipf, T. J., Fanous, F., Hahm, Y. H., and White, H. B. (1993b). "Structural failure analysis of 345 kV transmission line, and discussion by B. White." SM 441-6 PWRD, IEEE, Piscataway, N.J.

Baumeister, T., and Avallone, E. A., eds (1978). *Standard handbook for mechanical engineers*. 8th ed. New York, McGraw-Hill, 9–167.

Behncke, R. H., Clark, A. M., Sparrow, L. J., Tong, Y. K., White, H. B., Opaschaitat, P. (1998). "500 kV compact line design for the greater Bangkok area." Paper 22–33, *CIGRE*, Session 22, Paris, France.

Behncke, R. H., Milford, R. V., and White, H. B. (1994). "High intensity wind and relative reliability-based loads for transmission line design." Paper 22–205, *CIGRE*, Session 22, Paris, France.

Bennett, I. (1959). "Glaze, its meteorology and climatology, geographical distribution and economic effects." *Technical Report EP-105*. Natick,

Mass., U.S. Army, Quartermaster Research and Engineering Center, Environmental Protection Research Division, 217.

Bernstein, B. C., and Brown, B. G. (1997). "A climatology of supercooled large drop conditions based upon surface observations and pilot reports of icing." *Proc., 7th Conf. on Aviation, Range and Aerospace Meteorology*, Long Beach, Calif., Feb. 2–7.

Birjulin, A. P., Burgsdorf, V. V., and Makhlin, B. J. (1960). "Wind Loads on Overhead Lines," Paper 225, *CIGRE*, International Conference on Large Electric Systems, Paris, France.

Bocchieri, J. R. (1980). "The objective use of upper air soundings to specify precipitation type." *Monthly Weather Review*, Boston, Mass., 108, 596–603.

Brekke, G. N. (1959). "Wind pressures in various areas of the United States." Catalog No. C13.29. Washington, D.C., U.S. Weather Bureau.

Britter, R. E., Hunt, J. C. R., and Richards, K. J. (1981). "Air flow over a two-dimensional hill: Studies of velocity speed-up, roughness effects and turbulence." *Q. J. Roy. Meteor. Soc.*, 107, 91–110.

Brokenshire, R. E. (1979). "Experimental study of the loads imposed on welded steel support structures by galloping 345-kV bundled conductors." Paper A 79 551-3. IEEE Power Engineering Society. Piscataway, N.J.

Carper, K. L., ed. (1986). *Forensic engineering: Learning from failures*. American Society of Civil Engineers, New York, N.Y.

Canadian Electrical Association (CEA). (1998). "Validation of ice accretion models for freezing precipitation using field data." 331 T 992 (A-D). Newfoundland and Labrador Hydro, Ontario Hydro Technologies, and École de Technologie Supérieure.

Castanheta, M. N. (1970). "Dynamic behavior of overhead power lines subject to the action of the wind," Paper No. 22-08 *CIGRE*, Session 22, Paris, France.

European Committee for Electrotechnical Standardization (CENELEC) (2001). Standard EN 50341, Brussels, Belgium.

Chaîné, P. M., and Castonguay, G. (1974). "New approach to radial ice thickness concept applied to bundle-like conductors." *Industrial Meteorology—Study IV*. Environment Canada, Atmospheric Environment, Toronto, Canada.

Clough, P. W., and Penzien, P. (1975). *Dynamics of structures*. New York, McGraw-Hill.

Cluts, S., and Angelos, A. (1977). "Unbalanced forces on tangent transmission structures." Paper No. A77-220-7. IEEE Winter Power Meeting, New York, N.Y.

Colbeck, S. C., and Ackley, S. F. (1982). "Mechanisms for ice bonding in wet snow accretions on power lines." *Proc., First Int. Workshop on*

Atmospheric Icing of Structures, Special Report 83-17. Hanover, N. H., U.S. Army CRREL, 25–30.

Comellini, E., and Manuzio, C. (1968). "Rational determination of design loadings for overhead line towers." Paper 23-08. *CIGRE*, Session 22, Paris, France.

Coppin, P. A., Bradley, E. F., and Finnigan, J. J. (1994). "Measurements of flow over an elongated ridge and its thermal stability dependence: The mean field." Boundary-Layer Meteorology, 69, 173–199.

Dagher, H. J. (1985). "Reliability-based analysis and design of transmission line structures." Ph.D. dissertation, University of Wisconsin, Department of Civil and Environmental Engineering, Madison, Wis.

Dagher, H. J., Kulendran S., Peyrot, A. H., Maamouri, M., and Lu, Q. (1993). "System reliability concepts in design of transmission structures." *J. Struct. Eng.*, 119(1), 323–340.

Davenport, A. G. (1961). "The response of slender line-like structures to a gusty wind." *Proc., Institution of Civil Engineers*, 23, 389–408.

Davenport, A. G. (1967). "Gust loading factors." *J. Struct. Div ..*, ASCE, 93(5T3), 11–34.

Davenport, A. G. (1977). "The prediction of the response of structures to gusty wind." *Proc., Int. Research Seminar on the Safety of Structures under Dynamic Loading*, Trondheim, Norway, Norwegian Institute of Technology, 1, 257–284.

Davenport, A. G. (1979). "Gust response factors for transmission line loading." *Proc., Fifth Int. Conf. on Wind Engineering*. U. E. Cermack, ed., New York, Pergamon Press, 2, 899–909.

Davison et al. (1961). "Alcoa overhead engineering data no. 4." Alcoa.

Den Hartog, J. P. (1932). "Transmission line vibration due to sleet." Trans. American Institute of Electrical Engineers, 51, 1074–1086.

Durst, C. S. (1960). "Wind speeds over short periods of time." *Meteorological Magazine*, 89, 181–186.

Electric Power Research Institute (EPRI). (1978). "Longitudinal unbalanced loads on transmission line structures." Project 561, Report EL-643. Palo Alto, Calif.

Engleman, W. C., and Marihugh, D. (1970). "Forces on Conductors at High Wind Velocities," *Transmission and Distribution*, Oct.

EPRI. (1979). *Transmission line reference book*. Palo Alto, Calif.

EPRI. (1983). "Longitudinal unbalanced loads on transmission structures." Report EL-2943-CC7, Palo Alto, Calif.

EPRI. (1997). "Longitudinal load and cascading failure risk assessment (CASE)." M. Ostendorp, principal investigator. TR-107087, Vol. I-IV, Palo Alto, Calif.

Farr, H. H. (1980). "Transmission Line Design Manual," United States Department of the Interior, Water and Power Resources Service, Denver, Co.

Felin, B. (1988). "Freezing rain in Quebec: Field observations compared to model estimations." *Proc., Fourth Int. Workshop on Atmospheric Icing of Structures*, GIVRAGE, Paris, 119–123.

Finnigan, J. J., Raupach, M. R., Bradley, E. F., and Aldis, G. K. (1990). "A wind tunnel study of turbulent flow over a two-dimensional ridge." *Boundary-Layer Meteorology*, 50, 277–317.

Finstad, K., and Lozowski, E. (1988). "Computational investigation of water droplet trajectories." *J. Atmos. and Ocean Sci.* Tech., 5, 160–170.

Frandsen, A. G., and Juul, P. H. (1976). "Cascade of tower collapses: Design criteria." Paper 22-10. *CIGRE* Session 22, Paris.

Fujita, T. T., and Pearson, A. D. (1973). "Results of FPP classification of 1971 and 1972 tornadoes," *Preprints, Eighth Conference on Severe Local Storms*, American Meteorological Society, Boston, Mass., 142–145.

Ghannoum, E. (1983). "Probabilistic design of transmission lines, part I: Probability calculations and structural reliability, and part II: Design criteria corresponding to a target reliability." *IEEE Trans. on Power Apparatus and Systems*, Vol. PAS-102, No. 9, 3057–3079.

Ghannoum, E., Bell, N., Binette, L., Ouellet, P., and Manoukian, B. (1994). "Use of reliability techniques in the design of Hydro-Quebec's 1100 km Radisson-Nicolet-des-Cantons 450 kV HVDC line." Paper 22-201, *CIGRE*, Session 22, Paris, France.

Ghannoum, E., and Orawaski, G. (1987). "Reliability based design of transmission lines according to recent advances by IEC and CIGRE." *Probabilistic methods applied to electric power systems*. Pergamon Press, New York, 125–142.

Gibbon, R. R. (1984). *Damage to overhead lines caused by conductor galloping*. Art. ELT_094_4, *CIGRE*.

Gland, H., and Admirat, P. (1986). "Meteorological conditions for wet snow occurrence in France—calculated and measured results in a recent case study on 5 March 1985." *Proc., Third Int. Workshop on Atmospheric Icing of Structures*. Canadian Climate Program in 1991, Vancouver, Canada, 91–96.

Golikova, T. N., Golikov, B. F., and Savvaitov, D. S. (1983). "Methods of calculating icing loads on overhead lines as spatial constructions." *Proc., First Int. Workshop on Atmospheric Icing of Structures*, CRREL Special Report, June, 83–17, 341–346.

Gong, W., and Ibbetson, A. (1989). "A wind tunnel study of turbulent flow over model hills." *Boundary-Layer Meteorology*, Springer, Netherlands, 49, October, 113–148.

Goodwin, E. J., Mozer, J. D., DiGioia, A. M., Jr., and Power, B. A. (1983). "Predicting ice and snow loads for transmission line design." *Proc., Third Int. Workshop on Atmospheric Icing of Structures*. Canadian Climate Program in 1991, Vancouver, Canada, 267–275.

Gouze, S. C., and Richmond, M. C. (1982a). *Meteorological evaluation of the proposed Alaska transmission line routes*. Meteorology Research, Inc., Altadena, Calif.

Gouze, S. C., and Richmond, M. C. (1982b). *Meteorological evaluation of the proposed Palmer to Glennallen transmission line route*. Meteorology Research, Inc., Altadena, Calif.

Griffing, K. L., and Leavengood, D. C. (1973). "Transmission line failures, part I: Meteorological phenomena—severe winds and icing." *Proc., IEEE Winter Power Meeting*. Paper No. 73 CH0816-9-PWR, 5–14.

Gringorten, I. I. (1963). "A plotting rule for extreme paper." *J. Geophys. Res.*, 68, 813–814.

Golden Valley Electric Association (GVEA) (1997). Unpublished data of Golden Valley Electric Association, Fairbanks, Alaska.

Havard, D. G., and Pohlman, J. C. (1980). "Control of galloping conductors by detuning." Paper 22-05. *CIGRE*, Paris, France.

Havard, D. G., Paulson, A. S., and Pohlman J. C. (1982). "The economic benefits of controls for conductor galloping." Paper 22-02, *CIGRE*, Session 22, Sept. 1–9, Paris, France.

Hoerner, S. F. (1958). *Fluid-dynamic drag*. Hoerner Fluid Dynamics, Bakersfield, Calif.

Hoskings, J. R. M., and Wallis, J. R. (1987). "Parameter and quantile estimation for the generalized Pareto distribution." *Technometrics*, 29(3), 339–349.

Houghton, E. L., and Carruthers, N. B. (1976). *Wind forces on building and structures*. John Wiley & Sons, Inc., New York.

International Electrotechnical Commission (IEC). (2003). "Loading and strength of overhead transmission lines." International Standard IEC 60826, 3rd ed. International Organization for Standardization (ISO), Technical Committee 11, Geneva, Switzerland.

Institute of Electrical and Electronic Engineers (IEEE). (1999). "Limitations of the ruling span method for overhead line conductors at high operating temperature." *IEEE Trans. on Power Delivery*, 14(2).

IEEE. (2003). "IEEE guide to the installation of overhead transmission line conductors." IEEE Standard 524–03.

IEEE. (2004). "IEEE standard for fall protection for utility work." IEEE Standard 1307–04.

Ishac, M. F., and White, H. B. (1995). "Effect of tornado loads on transmission lines." IEEE, *Transactions on Power Delivery*, 10(1), 445–451.

International Standards Organization (ISO). (1999). *Atmospheric icing of structures*. ISO 12494 Preliminary International Standard. Technical Committee ISO/TC 98, Subcommittee SC3, ISO, Geneva, Switzerland.

James, W. D. (1976). "Effects of Reynolds number and corner radius on two-dimensional flows around octagonal, dodecagonal, and hexde-

cagonal cylinders." Ph.D. dissertation. November, Iowa State University, Ames, Iowa.

Janney, J. R. (1979). *Guide to investigation of structural failures*. American Society of Civil Engineers, New York.

Jones, K. (1996a). "A simple model for freezing rain loads." *Proc., Seventh Int. Workshop on Atmospheric Icing of Structures*, Chicoutimi, Quebec, Canada June 3–7, 1996, 412–416.

Jones, K. F. (1996b). "Ice accretion in freezing rain." CRREL Report 96-2, Cold Regions Research and Engineering Laboratory (CRREL), Hanover, N.H.

Jones, K.F. (1998) "A simple model for freezing rain ice loads." *Atmospheric Research*, 46(1–2), 87–97.

Kempner, L. Jr. (1997). "Longitudinal impact loading on electrical transmission line towers—a scale model study." Ph.D. dissertation, Portland State University, Department of Civil and Environmental Engineering, Portland, Oregon.

Keselman L. M., and Motlis, Y. (1996). "Enhanced analytical design method for overhead line conductors in non-level spans." *Proc., IEEE/PES T and D Conference*. 359–366, Los Angeles, Calif.

Keselman L. M., and Motlis, Y. (1998). "Application of the ruling span concept for overhead lines in mountainous terrain." *IEEE Trans. on Power Delivery*, 13(4), 1385–1390.

Kuroiwa, D. (1962). "A study of ice sintering." Res. Rep. 86, U.S. Army CRREL, Hanover, N.H.

Kuroiwa, D. (1965). "Icing and snow accretion on electric wires." Res. Paper 123, U.S. Army CRREL, Hanover, N.H.

Laflamme, J. (1993). "Spatial variation of extreme values in the case of freezing rain icing." *Proc., Sixth Int. Workshop on Atmospheric Icing of Structures*. Hungarian Electricity Board, Budapest, Hungary, 19–23.

Langmuir, I., and Blodgett, K. (1946). "Mathematical investigation of water droplet trajectories." *The collected works of Irving Langmuir*. Pergamon Press, Elmsford, N.Y., 335–393.

Lilien, J. L., Erpicum, M., Wolfs, M. (1998). "Overhead line galloping. Field experience during one event in Belgium on last February 13, 1997." *Proc., Eighth Int. Workshop on Atmospheric Icing of Structures*, Reykjavik, Iceland, June 8–11, 293–298.

Lott, J. N., and Sittel, M. C. (1996). "The February 1994 ice storm in the southeastern U.S." *Proc., Seventh Int. Workshop on Atmospheric Icing of Structures*. Chicoutimi, Quebec, Canada, June 3–7, 259–264.

Lowry, M. D., and Nash, J. E. (1970). "A comparison of methods of fitting the double exponential distribution function." *J. Hydrol.*, 10, 259–275.

MacDonald, A. (1975). *Wind loading on buildings*. John Wiley & Sons, Inc., New York.

Makkonen, L. (1996). "Modeling power line icing in freezing precipitation." *Proc., Seventh Int. Workshop on Atmospheric Icing of Structures*. Chicoutimi, Quebec, Canada, June 3–7, 195–200.

Mathur, R. K., Shah, A. H., Trainor, P. G. S., Popplewell, N. (1986). "Dynamics of guyed transmission tower system." Paper 86 SM 414-7. IEEE Power Engineering Society, Piscataway, N.J.

Mehta, K. C., and Lou, T. (1983). "Force coefficients for transmission towers," *EPRI Report*, Technical Agreement TPS 82–623.

Mehta, K. C., Minor, J. E., and McDonald, J. R. (1976). "Windspeed analysis of April 3–4, 1974 tornadoes," *J. Struct. Div.* ASCE, 102(5T9), Proc. Paper 12429, 1709–1724, New York.

McComber, P., Martin, R., Morin, G., Van, L. V. (1982). "Estimation of combined ice and wind load on overhead transmission lines," *Proc., First Int. Workshop on Atmospheric Icing of Structures*, Hanover, N.H., 143–153.

McCormick, T., and Pohlman, J. C. (1993). "Study of compact 220 kV line system indicates need for micro-scale meteorological information." *Proc., Sixth Int. Workshop on Atmospheric Icing of Structures*. Budapest, Hungary.

McDonald, J. R. (1983). "A methodology for tornado hazard probability assessment." NUREG/CR-3058, Nuclear Regulatory Commission, Washington, D.C., Oct.

Milford, R. V., and Goliger, A. M. (1997). "Tornado risk model for transmission line design." *J. Wind Eng. Ind. Aerod*. 72(1–3), 469–478.

Minor, J. E., McDonald, J. R., and Mehia, K. C. (1977). "The tornado: An engineering-oriented perspective," *NOAA Technical Memorandum ERL* NSSL-82, National Severe Storms Laboratory, Norman, Okla.

Modi, V. J., and Slater, J. E. (1983). "Unsteady aerodynamics and vortex-induced aeroelastic instability of a structural angle section." *J. Wind Eng. and Indust. Aerod*. 11(1–3), 321–334.

Mozer, J. D., and West, R. J. (1983). "Analysis of 500 kV tower failures." *Proc., Pennsylvania Electric Association*. 1983.

Mozer, J. D., Pohlman, J. C., and Fleming, J. F. (1977). "Longitudinal load analysis of transmission line system." *IEEE Trans. on Power Apparatus and Systems*. PAS-96(5), 1657–1665.

Meteorological Research Institute (MRI). (1977). "Ontario Hydro wind and ice loading model." MRI 77 FR-1496. Ontario Hydro, Toronto.

National Electrical Safety Code (NESC). (1920). *National electrical safety code*. National Bureau of Standards, Washington, D.C.

NESC. (2007). *National electrical safety code*. ANSI C2. IEEE, Piscataway, N.J.

Nigol, O., and Havard, D. G. (1978). "Control of torsionally induced conductors by detuning." Paper A 78 125-7. IEEE, Piscataway, N.J.

National Oceanic and Atmospheric Administration (NOAA). (1959–Present). Storm data. NOAA, Washington, D.C.

Nojima, T. (1998). "Observations of ice load and galloping on a full scale 500 kV test line by Nojima, Shimizu, Nosaka and Shibata." *Proc., Int. Workshop on Atmospheric Icing on Structures*. IWAIS, Reykjavik, Iceland.

Nebraska Public Power District (NPPD). (1976). "The storm of March 29, 1976." NPPD, Public Relations Department, Columbus, Neb.

Precast/Prestressed Concrete Institute (PCI). (1983). "Guide for design of prestressed concrete poles." *J. Prestressed Concr. Inst.*, 28(3), 22–87.

PCI. (1997). "Guide for design of prestressed concrete poles," *J. Prestressed Concr. Inst.*, 42(6), 94–134.

Paz, M. (1980). *Structural dynamics—theory and computations*. Van Nostrand Reinhold, New York, N.Y.

Peabody, A. B. (1993). "Snow loads on transmission and distribution lines in Alaska." *Proc., Sixth Int. Workshop on Atmospheric Icing of Structures*, Budapest, Hungary.

Peterka, J. A. (1992). "Improved extreme wind prediction for the United States." *J. Wind Eng. Ind. Aerod.*, 41–44, 533–541.

Peterka, J. A., Finstad, K., and Pandy, A. K. (1996). *Snow and wind loads for Tyee transmission line*. Cermak Peterka Petersen, Inc., Fort Collins, Colo.

Peyrot, A. H. (1985). "Microcomputer-based nonlinear structural analysis of transmission line systems." *IEEE Trans. on Power Apparatus and Systems*, PAS-104(11).

Peyrot, A. H., and Dagher, H. J. (1984). "Reliability-based design of transmission lines." *J. Struct. Eng.*, New York, N.Y., 110(11), 2758–2777.

Pohlman, J. C., and Havard, D. (1979). *Field research on the galloping of iced conductors—a status report*. IEEE Power Engineering Society, Paper A 79 551–3.

Pohlman, J. C., and Rawlins, C. B. (1979). "Field testing an anti-galloping concept on overhead lines." *Proc., 7th IEEE/PES Transmission and Distribution Conference and Exposition*, April 1–6, Atlanta, Ga.

Rawlins, C. B. (1981). "Analysis of conductor galloping field observations—single conductors." *IEEE Trans. on Power Apparatus and Systems*, PAS-100(8), 3744–3751.

Rural Electrification Administration (REA). (1980). "Design manual for high voltage transmission lines." *Rural Electrification Administration Bulletin 62-I*, United States Department of Agriculture, Washington, D.C.

Richardson, A. S. (1983). *The windamper method of galloping control*. National Technical Service, U.S. Department of Commerce, DOE/CE/15102T1, Springfield, Va.

Richardson, A. S. (1986). "Longitudinal dynamic loading of steel pole transmission lines." Paper WM 189-5. IEEE Power Engineering Society, Piscataway, N.J.

Richards, D. J. W. (1965). "Aerodynamic properties of the severn crossing conductor." Paper 8, Symposium 16, National Physical Laboratory, Department of Scientific and Industrial Research, Teddington, Middlesex, England.

Richmond, M. C. (1985). "Meteorological evaluation of Bradley Lake hydroelectric project 115 kV transmission line route." M. C. Richmond Meteorological Consultant, Torrance, Calif.

Richmond, M. C. (1991). "Meteorological evaluation of Tyee Lake hydroelectric project transmission line route, Wrangell to Petersburg." M. C. Richmond Meteorological Consulting, Torrance, Calif.

Richmond, M. C. (1992). "Meteorological evaluation of Tyee Lake hydroelectric project transmission line route, Tyee power plant to Wrangell." M. C. Richmond Meteorological Consulting, Torrance, Calif.

Richmond, M. C., Gouze, S. C., and Anderson, R. S. (1977). *Pacific northwest icing study*. Meteorology Research, Inc., Altadena, Calif.

Robbins, C. C., and Cortinas, J. V. Jr. (1996). "A climatology of freezing rain in the contiguous United States: Preliminary results." *Preprints*, 15th AMS Conference on Weather Analysis and Forecasting, American Meteorological Society, Norfolk, Va, August 19–23.

Sachs, P. (1972). *Wind forces in engineering*. Pergamon Press, New York, N.Y.

Sachs, P. (1978). *Wind forces in engineering*. 2nd ed. Pergamon Press, New York, N.Y.

Sakamoto, Y., Mizushima, K., and Kawanishi, S. (1990). "Dry snow type accretion on overhead wires: growing mechanism, meteorological conditions under which it occurs and effect on power lines." *Proc., Fifth Int. Workshop on Atmospheric Icing of Structures*, Paper 5–9, Japanese Society of Snow and Ice, Tokyo, Japan,

Schwarzkopf, M. L. A., and Rosso, L. C. (1993). "Riesko de tornados y corrientes descedentes en la Argentian." *Proc., Workshop on High Intensity Winds on Transmission Lines*, CIRSOC, Buenos Aires, Argentina, April 19–23.

Schaefer, J. T., Kelly, D. L., and Abbey, R. F. (1985). "A minimum assumption tornado hazard probability model," *NOAA Technical Memorandum NWS NSSFE-8*, National Severe Storms Forecast Center, Kansas City, Mo., 30.

Scruton, C., and Newberry, C. W. (1963). "On the estimation of wind loads on buildings and structural design," *Proc., Inst. of Civil Engineers*, 25(6), 97–126.

Shan, L., and Marr, L. (1996). *Ice storm data base and ice severity maps*. Electric Power Research Institute, Palo Alto, Calif.

Simiu, E., and Scanlan, R. H. (1978). *Wind effects on structures: An introduction to wind engineering*. John Wiley & Sons Inc., New York, N.Y.

Simiu, E., and Scanlan, R. H. (1996). *Wind effects on structures: Fundamentals and applications to design*. 3rd ed. John Wiley & Sons Inc., New York, N.Y.

Slater, J. E., and Modi, V. J. (1971). "On the wind-induced vibration of structural angle sections." *Proc., IAWE, Third Int. Conf. on Wind Effects on Building and Structures*, Tokyo, Japan.

Snyder, W. H., and Britter, R. E. (1987). "A wind tunnel study of the flow structure and dispersion from sources upwind of three-dimensional hills, atmospheric environment." *Atmospheric Environment*, 21, 735–751.

Stallabrass, J. R., and Hearty, P. F. (1967). "The icing of cylinders in conditions of simulated sea spray." *Mechanical Engineering Report MD-50*. National Research Council of Canada, Ottawa, Canada.

Tattelman, P., and Gringorten, I. (1973). "Estimated glaze ice and wind loads at the earth's surface for the contiguous United States." *Report AFCRL-TR-73-0646*. Air Force Cambridge Research Laboratories, Bedford, Mass.

Taylor, T. A., Mason, P. J., and Bradley, E. F. (1987). "Boundary layer flow over low hills, a review." *Boundary Layer Meteorology*, 39(1–2), 107–132.

Tecson, J. J., Fujita, T. T., and Abbey, R. F. Jr. (1979). "Statistics of U.S. tornadoes based on the DAPPLE tornado tape," *Preprints, Proc., 11th Conference on Severe Local Storms*, American Meteorological Society, Boston, Mass.

Thayer, E. S. (1924). "Computing tensions in transmission lines." *Electrical World*, 2, 72–73.

Thomas, M. B. (1981). "Broken conductor loads on transmission line structures," Ph.D. dissertation, University of Wisconsin, Madison, Wis.

Thrasher, W. J. (1984). "Halt redundant member failure on 765-kV towers." *Transmission and Distribution*, May.

Trainor, P. G. S., Popplewell, N., Shah, A. H., Wong, C. K. (1984). "Estimation of fundamental dynamic characteristics of transmission towers." Paper 84 SM 525-2. IEEE Power Engineering Society, Piscataway, N.J.

Twisdale, L. A. (1982). "Wind-loading underestimate in transmission line design." *Transmission and Distribution*, December, 40–46.

Twisdale, L. A., and Dunn, W. L. (1983). "Probabilistic analysis of tornado wind risks." *J. Struct. Eng.*, 109(2), 468–488.

U.S. Forest Service (USFS). (1994). "Telecommunications handbook, R3 supplement 6609.14-94-2." *Forest Service Handbook*, USFS, FSH6609, 14, Washington, D.C.

Vellozzi, J. W., and Cohen, E. (1968). "Gust response factors." *J. Struct. Div.*, 94(ST6), 1295–1313.

Vickery, P. J., and Twisdale, L. A. (1995). "Prediction of hurricane wind speeds in the United States." *J. Struct. Eng.*. ASCE, New York, N.Y., 121(11), 1691–1699.

Walmsley, J. L., Taylor, P. A., and Keith, T. (1986). "A simple model of neutrally stratified boundary-layer flow over complex terrain with surface roughness modulations." *Boundary-Layer Meteorology*, 36, 157–186.

Wang, Q. J. (1991). "The POT model described by the generalized Pareto distribution with Poisson arrival rate." *J. Hydrol.*, 129, 263–280.

Wardlaw, R. L. (1967). "Wind-excited vibrations of slender beams with angle cross-sections." *Proc., Int. Research Seminar—Wind Effects on Buildings and Structures*, IAWE, Ottawa, Canada.

Watson, L. T. (1955). "Drag of bare stranded cables." Technical Memorandum 114, Australian Aeronautical Research Laboratories Aerodynamics, Melbourne.

Western Area Power Administration (WAPA). (1992). *Engineering fall protection committee report*. WAPA, Lakewood, Colo.

Wen, Y-K., and Chu, S-L. (1973). "Tornado risk and design windspeed." *J. Struct. Div.*, 99(5T12) 2409–2421.

Whapham, R. (1982). *Field research for control of galloping with air flow spoilers*. Preformed Line Products, Cleveland, Ohio.

Whitbread, R. S. (1979). "The influence of shielding on the wind forces experienced by arrays of lattice frames," J. E. Cermak, ed., *Proc., Fifth Int. Conference on Wind Engineering.*, Pergamon Press, New York, N.Y., 1, 405–420.

White, H. B. (1979). "Some destructive mechanisms activated by galloping conductors." Report No. A79 106-6. IEEE PES WPM, New York, N.Y.

White, H. B. (1985). "A practical approach to reliability design." *IEEE Trans. on Power Apparatus and Systems*. PAS-104(10), 2739–2742.

White, H. B. (1999). "Galloping of ice covered wires of a transmission line." *Proc., ASCE Cold Regions Conference*, August, 790–798.

Wieringa, J. (1973). "Gust factors over open water and built-up country." *Boundary-Layer Meteorology*, 3, 424–441.

Wood, C. J. (1983). "A simplified calculation method for gust factors." *J. Wind Eng. Ind. Aerod*. 12, 385–387.

Yip, T. C., and Mitten, P. (1991). *Comparisons between different ice accretion models*. Canadian Electrical Association, Transmission Line Design Section, Engineering and Operating Division, Ottawa, Ont.

Yip, T. C. (1993). "Estimating icing amounts caused by freezing precipitation in Canada." *Proc., Sixth Int. Workshop on Atmospheric Icing of Structures*. Budapest, Hungary.

Young, W. R. (1978). "Freezing precipitation in the southeastern United States." M.S. dissertation, Texas A&M University, Department of Atmospheric Sciences, College Station, Tex.

INDEX